ESTIMATION OF TOTAL RED SNAPPER ABUNDANCE IN LOUISIANA AND ADJACENT FEDERAL WATERS

Final Report

For

LDWF Purchase Order No. 2000461788

Attn: Andrew Fischer, Contract Monitoring and Liaison Representative
Louisiana Department of Wildlife and Fisheries
P.O. Box 98000 Baton Rouge, LA 70898

By

LGL Ecological Research Associates, Inc.

4103 South Texas Ave, Suite 211
Bryan, TX 77802

25 March 2022

TABLE OF CONTENTS

1.0 Introduction

There are numerous studies that have described Red Snapper *Lutjanus campechanus* distribution based on presence/absence, relative abundance, density, and catch rate data across a range of habitat types in the northern Gulf of Mexico (GoM) (e.g., Shipp and Bortone 2009, Gallaway et al. 2009, Karnauskas et al. 2017, Streich et al. 2017, Reynolds et al. 2018, Dance and Rooker 2019, Bolser et al. 2020, Gallaway et al. 2021). While such information is useful for understanding how the species is distributed and the relative value of different habitats to Red Snapper, such studies do not provide an indication of the overall stock abundance. Stock abundance is essential for determining the overfishing/overfished status, harvest limits, and the amount of allocation among fishing sectors. Assessing stock abundance has traditionally relied upon modeling spawning rates, fecundity, growth rates, age at maturity, natural mortality rates, fishing mortality, and emigration/immigration. Yet no published study has estimated the absolute total abundance of this species through directed surveys across the myriad of habitats that Red Snapper occupy. The logistical complications for such an effort appear daunting, but with available sampling technologies and advanced statistical procedures, estimating total abundance, though ambitious, is feasible. Here we present a first such attempt to estimate the total abundance of Red Snapper existing within the State of Louisiana's entire management area for Red Snapper.

On 1 November 2019, the Louisiana Department of Wildlife and Fisheries (LDWF) entered into a Contract (Purchase Order No. 2000461788) with LGL Ecological Research Associates, Inc. (LGL) with the overarching goal to estimate the total Red Snapper abundance in Louisiana and adjacent federal waters in the GoM. Specific objectives of the contract were to:

- Determine finfish species composition at 106 sampling sites at predetermined locations per approved sampling methodology.
- Conduct hydroacoustic, Submersible Rotating Video (SRV), and composition sampling for finfish at the 106 sampling sites.
- Conduct water column surveys at the 106 sampling sites.
- Conduct a Red Snapper mark/recapture study at a subset of six sites (1 platform and 1 artificial reef site in each of three regions).

Of importance, the study was required to be compatible with the "Great Red Snapper Count" (Stunz et al. 2021). As acknowledged by Stunz et al. (2021), unusual complications prevented their initial scope of sampling for Louisiana to be accomplished. Therefore, a Louisiana-specific study was necessary and accomplished over the period 1 November 2019 - 30 June 2021.

Prior to initiation of the formal Red Snapper survey, a Proof-of-Concept Study was conducted, primarily to 1) test the utility of using trammel nets as a non-size-selective sampling device, and 2) finalize all field sampling protocols. The results (LGL 2020)

suggested trammel nets would not be practical for this purpose. A longline sampling program was developed as an alternative method for sampling widely-dispersed Red Snapper over uncharacterized bottom (UCB). The final methods for field sampling used hydroacoustic methods to count fish. Submersible rotating video cameras (SRVs) at discrete sites and towed video (TV) cameras over UCB were used to apportion hydroacoustic counts into individual species or taxa. Hook-and-line (vertical lines and longlines) methods were used to collect fish for quantifying selected biological attributes (e.g., length, weight, sex, age).

We first describe our Study Area (the Louisiana State Red Snapper Management Area), provide a characterization of the major types of habitats represented within the area, and how 106 the sites were apportioned across habitats. Next, we describe our field sampling strategies for each habitat. Sampling design and our basis for inference is covered under the Data and Statistical Analyses section. Results of our study are then described and discussed.

2.0 Description of Study Area and Site Selection

Our study area was restricted to the Louisiana Red Snapper Management Area, which was divided into three regions (West, Central and East) and then four depth zones (Shallow=10-25 m; Mid=25-45 m; Deep=45-100 m; and Shelf=100-150 m). Note that the Deep and Shelf depth zones were ultimately combined as one Deep zone. Five habitat types were targeted: (1) uncharacterized bottom or UCB, (2) natural banks, (3) artificial reefs, (4) pipeline crossings, and (5) standing oil and gas platforms (Figure 1).

2.1 Estimation of the Sampling Universe

Areal coverage of all habitats within each region and depth zone was determined using GIS. We used an Albers Conic Projection with North American Datum of 1983 (NAD83). This projection reduces distortion when calculating areal coverage of bottom habitats and is centered at 91.5° W, 28.0° N on the area offshore of Western Louisiana encompassing the study area.

Uncharacterized bottom and natural banks were considered natural habitats and quantified using the same databases. The extent of UCB habitat was estimated from the usSEABED bottom sediment database (Buczkowski, 2006). This is a gridded database that estimates percent coverage of rock, mud, sand, and gravel within each grid cell (2.22 km by 1.96 km). We considered UCB as being those grid cells that had less than 66% rock (Table 1). Natural bank habitat was estimated using a dataset obtained from Gulf States Marine Fishery Commission (Jeff Rester, pers. comm.). Aerial extent of natural bank habitat was calculated by combining the natural bank coverage with those areas from the usSEABED dataset with 66% or greater rock coverage (Table 2).

The number of manmade habitats (Table 3) was estimated from several sources. Locations of standing oil and gas platforms (fixed leg, well protectors and caissons) were

obtained from the Bureau of Ocean Energy Management (BOEM 2021, accessed March 2021). This database includes all historical installations of offshore structures and was filtered to remove those platforms that had a removal date prior to January 1, 2020 in its attribute table. The remaining structures are considered standing structures. Artificial reef locations were obtained from the Louisiana Department of Wildlife and Fisheries (LDWF 2021). Pipeline locations were obtained from the Bureau of Ocean Energy Management (BOEM 2018) and were filtered to identify and quantify the intersections of pipelines 20 inches in diameter or greater. Wrecks and obstructions were accessed from the National Oceanic and Atmospheric Administration Office of Coast Survey (NOAA OCS 2021).

Each of the datasets was clipped to show spatial coverage within the defined study area. Spatial joins were utilized to calculate the number of discrete structures within each regional depth zone. Geometry for aerial extent was calculated for UCB habitat within each region-depth zone combination after removal of rock habitat defined previously. We followed the same methodology to calculate the aerial coverage of natural banks.

2.2 Allocation of Sampling Sites

The number of sites sampled for each habitat was chosen to balance the need for representative sampling across multiple habitats and geographic regions within specified cost constraints. As such, sampling designs varied among habitat types and are described in the Data and Statistical Analyses section. For now, we simply describe where samples were allocated across longitudinal regions, depth zones, and habitat types. Of the 106 total sampling sites, 37 were located in the West Region, 33 were in the Central Region and 36 were in the East Region (Figure 1; see Appendix 1 for more detail). Of these, 55 were discrete sites (standing platforms, natural banks, artificial reefs, and pipeline crossings,) whereas 51 were UCB sites. In addition to these habitats, there were 132 obstructions and 56 wrecks that have been documented to occur within the study area (Figure 2). However, these habitat types were not sampled as part of this program.

UCB - UCB (sometimes referred to as “open bottom”) habitat (49,000 km^2) dominates most of the study area and is comprised mainly of mud substrate, although sandy areas are well represented in the western shallow region, and some rock/gravel patches occur at greater depths (Figure 3, Panel A). The UCB surveys included 39 unique sites; 12 more UCB sites were paired with 12 pipeline crossing sites (Figure 3, Panel B). These 12 sites where were taken at the same substrate with and without pipeline crossings present and included site numbers 41 and 42 (West Shallow), 46 and 47 (West Mid), 52 and 53 (West Deep), 56 and 57 (West Deep), 61 and 62 (Central Shallow), 64 and 65 (Central Mid), 66 and 67 (Central Deep), 70 and 71 (Central Deep), 73 and 74 (East Shallow), 82 and 83 (East Mid), 85 and 86 (East Deep) and 88 and 89 (East Deep). It should be noted that UCB hydroacoustic surveys were conducted by Auburn University. Alternative site numbers (1-39) were assigned by Auburn for internal tracking purposes. A key for relating the Auburn site numbers to the original LDWF site number locations is included in Appendix 1. Our samples for UCB habitat did not include any taken from the deepest

shelf zone. The shelf zone constituted about 8% of the total sampled area, and our sampling covered 0.37% of the total remaining area.

Natural Banks - Natural bank habitat is much smaller in total area (724 km^2) than UCB (49,000 km^2) and occurs almost exclusively in the shelf depth zone (Figure 4). Fifteen sites were located over natural banks representing a sampling area of 2.4 km^2, which constituted 0.33% of the total natural bank sampling universe (Table 2).

Standing Platforms - A total of 821 petroleum platforms and well protectors (henceforth referred to as "standing platforms" or just "platforms") were present in the study area as of January 1, 2020 of which 11 were sampled during this study; 37 additional platforms were sampled during 2017 and 2018 were included from the Gallaway et al. (2021) study (Figure 5). In all, 5.8% of the standing platform universe was sampled (Table 3). There were 147 single-pipe caissons standing in 2020 but were not sampled as part of our study.

Artificial Reefs - In summer/fall of 2020 there were on the order of 442 reefed platforms (termed "artificial reefs" for this study) in the Louisiana Artificial Reef Program; 16 (3.6%) were sampled during 2020 (Figure 6; Table 3).

Pipeline Crossings – There were 514 oil and gas pipeline crossings where each of the pipes were greater than 20" in diameter (Figure 7; Table 3). Twelve crossings (2.3%) of these were sampled during 2020.

Table 1. Total area of UCB and area sampled for this habitat.

Name	Zone_ID	Area_km^2	Num Sites Uncharacterized Bottom	Area sampled _km^2	Percent sampled
West Shallow	1	10,267.60	3	12.94	0.13
West Mid	2	5,297.20	6	25.87	0.49
West Deep	3	5,892.60	6	25.87	0.44
Central Shallow	5	4,407.10	2	8.62	0.20
Central Mid	6	3,760.00	2	8.62	0.23
Central Deep	7	6,043.10	4	17.25	0.29
East Shallow	9	3,058.40	7	30.18	0.99
East Mid	10	2,326.70	3	12.94	0.56
East Deep	11	3,853.00	6	25.87	0.67
West Shelf	4	1,269.70	0	0.00	0
Central Shelf	8	1,468.30	0	0.00	0
East Shelf	12	1,359.50	0	0.00	0
Total - Shallow, Mid,Deep		**44,905.70**	**39**	**168.17**	**0.3745%**

Table 2. Total and sampled area (in parentheses) of natural bank habitats in the study area.

Natural Bank Area (km^2)	
Natural Bank Region	**Total**
West Mid/Deep (Sonnier)	45.85 (0.48)
West Shelf/Deep (Bright)	133.97 (0.48)
Central East Deep/Shelf	544.42 (1.44)
Total	**724.25 (2.4)**
% Sampled = 0.33	

Table 3. Numbers of artificial reefs present, and the number of each reef type sampled. For standing platforms (A), the first number in parentheses represents the number of sites sampled in the present study, the second number represents the additional BOEM sites from a previous study, and the third is the total number of samples (see text).

A) Standing Platforms			
Depthzone	**West**	**Central**	**East**
Shallow	62 (1+3=4)	118 (1+3=4)	182 (1+4=5)
Mid	25 (1+5=6)	133 (1+9=10)	58 (1+2=3)
Deep	45 (2+2=4)	107 (2+8=10)	55 (1+1=2)
Shelf	7 (0)	10 (0)	19 (0)
Region Total	139 (14)	368 (24)	314 (10)
Total			**821 (48)**
			% Sampled= 5.8

B) Pipeline Crossings			
Depthzone	**West**	**Central**	**East**
Shallow	24 (1)	93 (1)	18 (1)
Mid	28 (1)	70 (1)	49 (1)
Deep	61 (2)	50 (2)	61 (3)
Shelf	2 (0)	50 (0)	8 (0)
Region Total	115 (4)	263 (4)	136 (5)
Total			**514**
			% Sampled=2.3

C) Artificial Reefs			
Depthzone	**West**	**Central**	**East**
Shallow	0 (0)	0 (0)	0 (0)
Mid	5 (1)	35 (1)	57 (3)
Deep	117 (3)	129 (6)	59 (2)
Shelf	4 (0)	31 (0)	5 (0)
Region Total	126 (4)	195 (7)	121 (5)
Total			**442**
			% Sampled=3.6

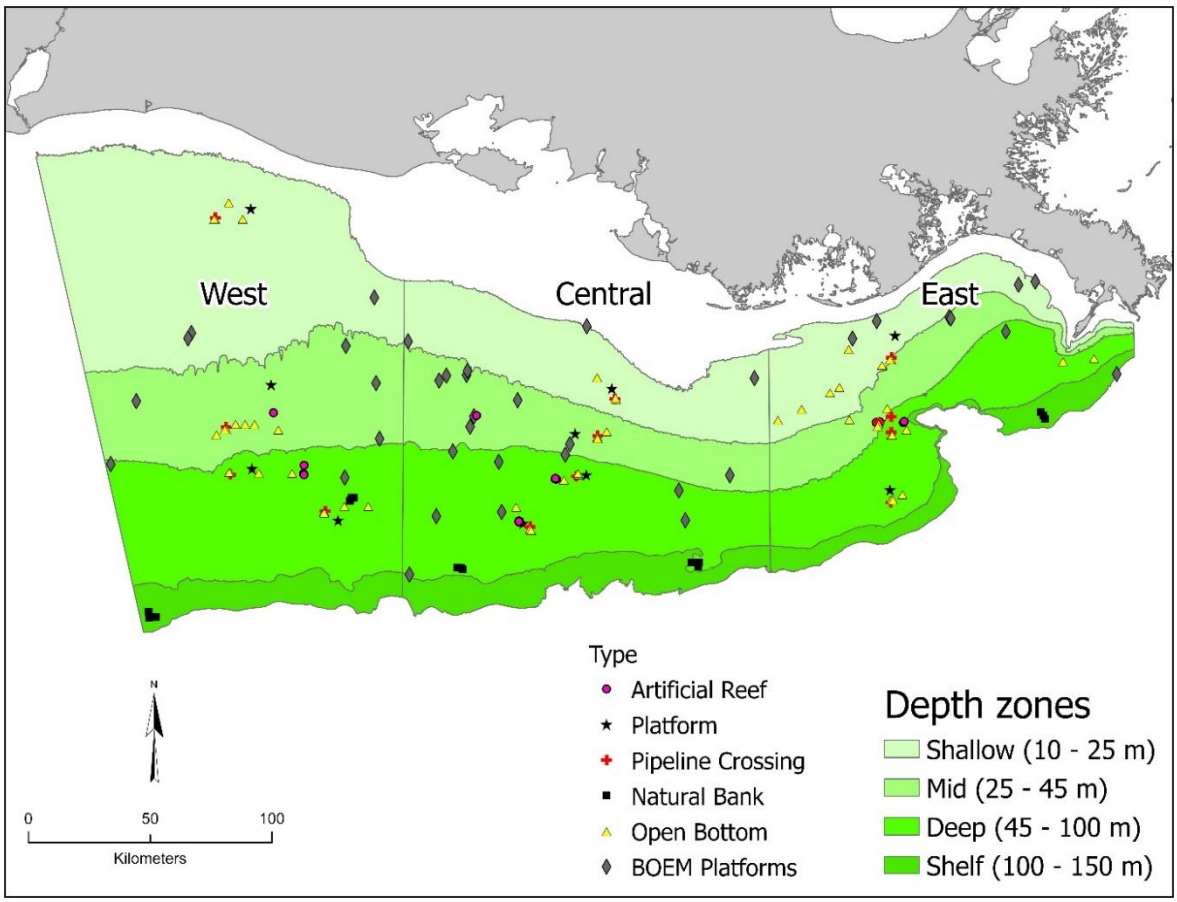

Figure 1. The Louisiana study area stratified by longitudinal regions and depth zones. Superimposed are the 106 sites parsed by habitat type sampled during 2020. An additional 37 platform sites sampled during 2017 and 2018 (Gallaway et al. 2021) are also shown.

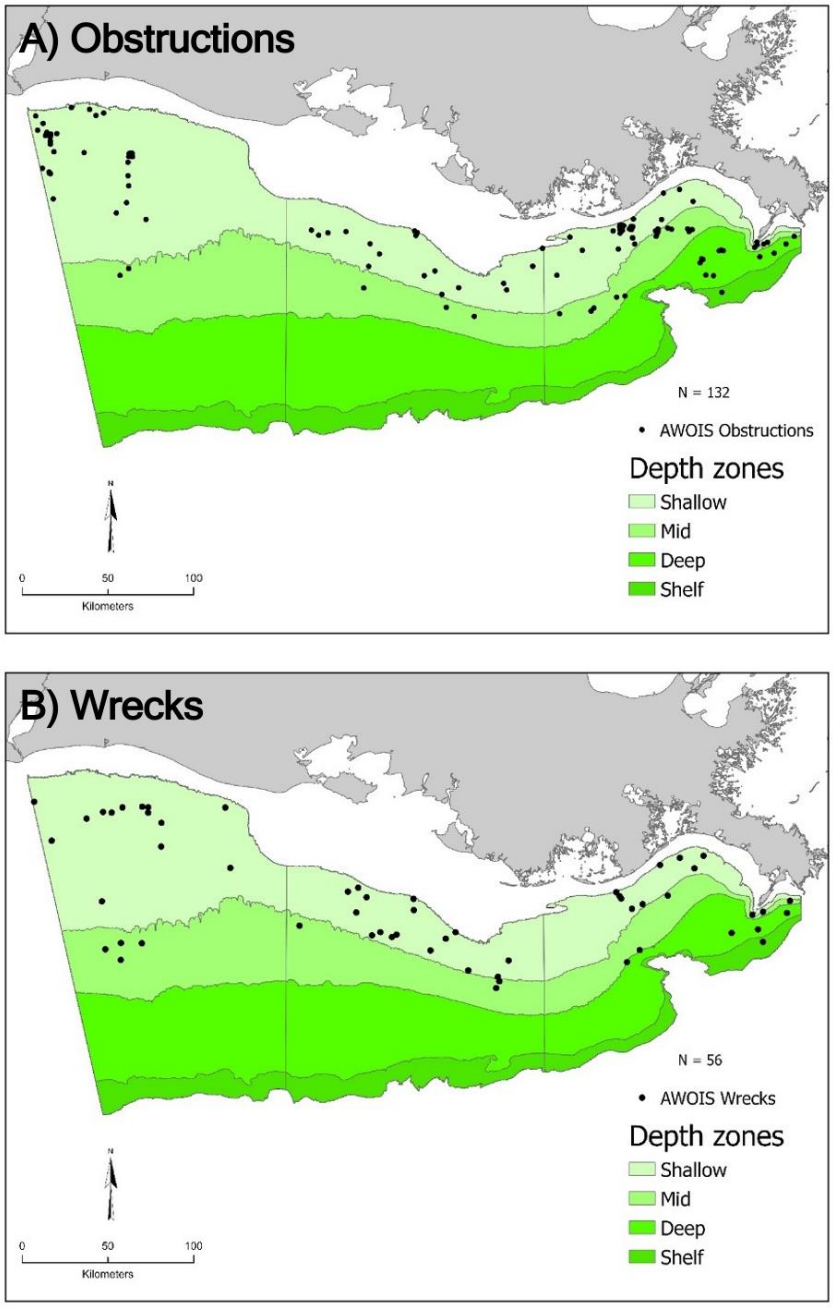

Figure 2. Number and location of documented (A) obstructions (filled circles) and (B) wrecks (filled circles) in the study area. These habitats were not sampled during this study.

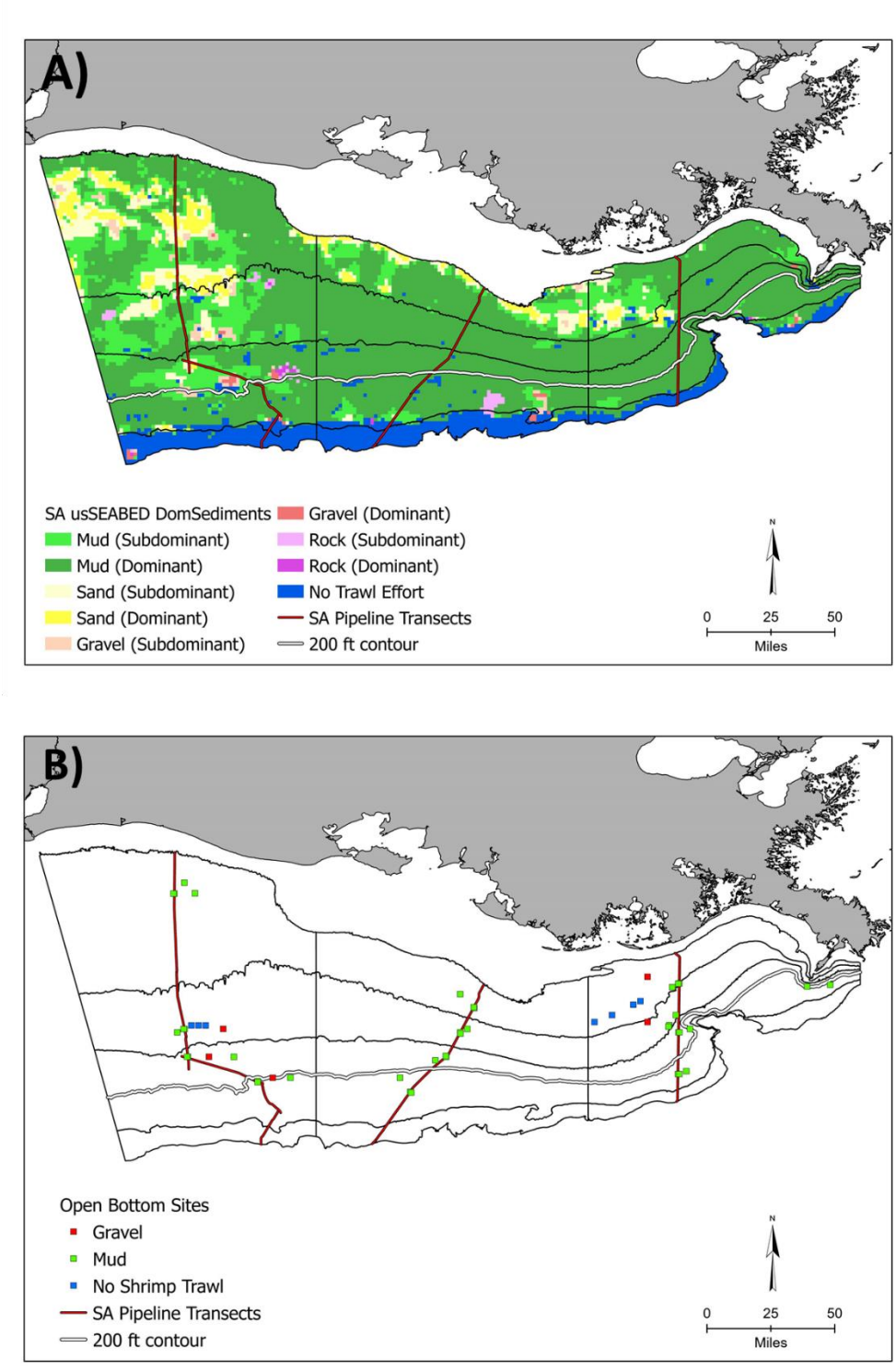

Figure 3. Distribution and special extent of (A) uncharacterized bottom habitat (shown as areas shaded in color) and (B) sampling sites therein. Sampling occurred during 2020.

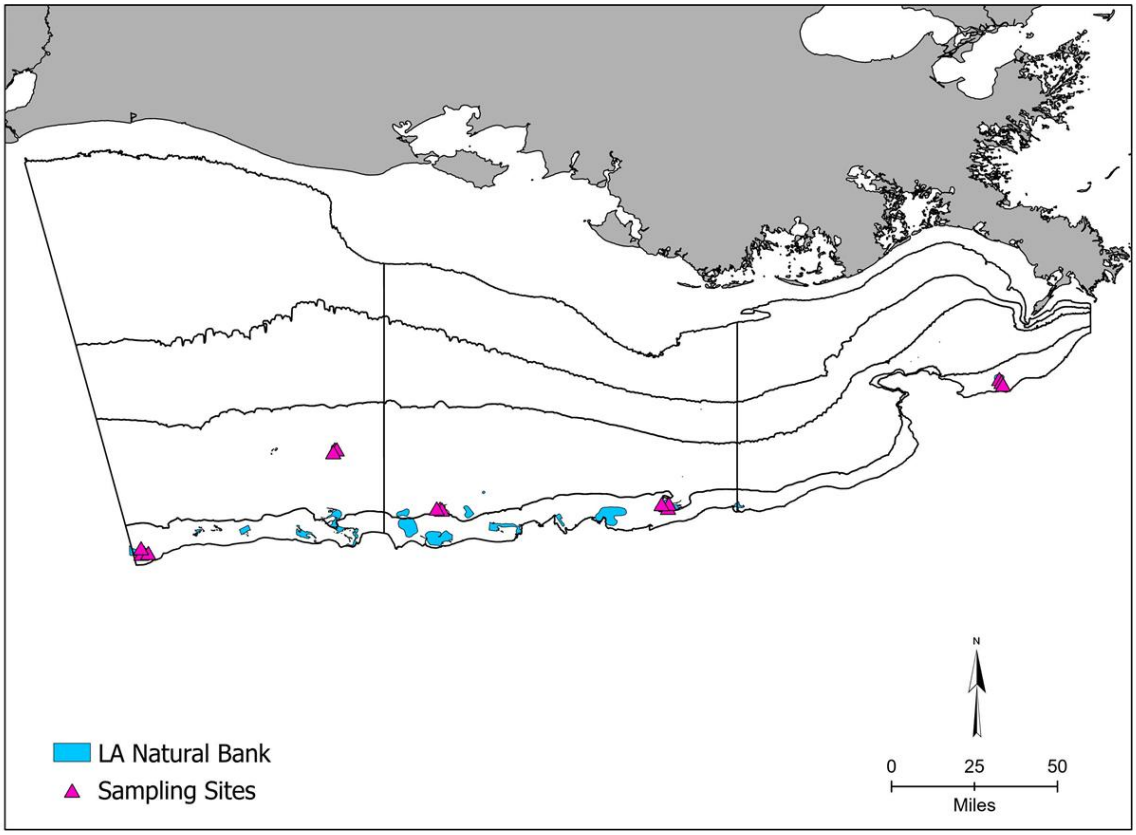

Figure 4. Sampled natural banks and the sampling universe from which they were selected. Sampling occurred during 2020.

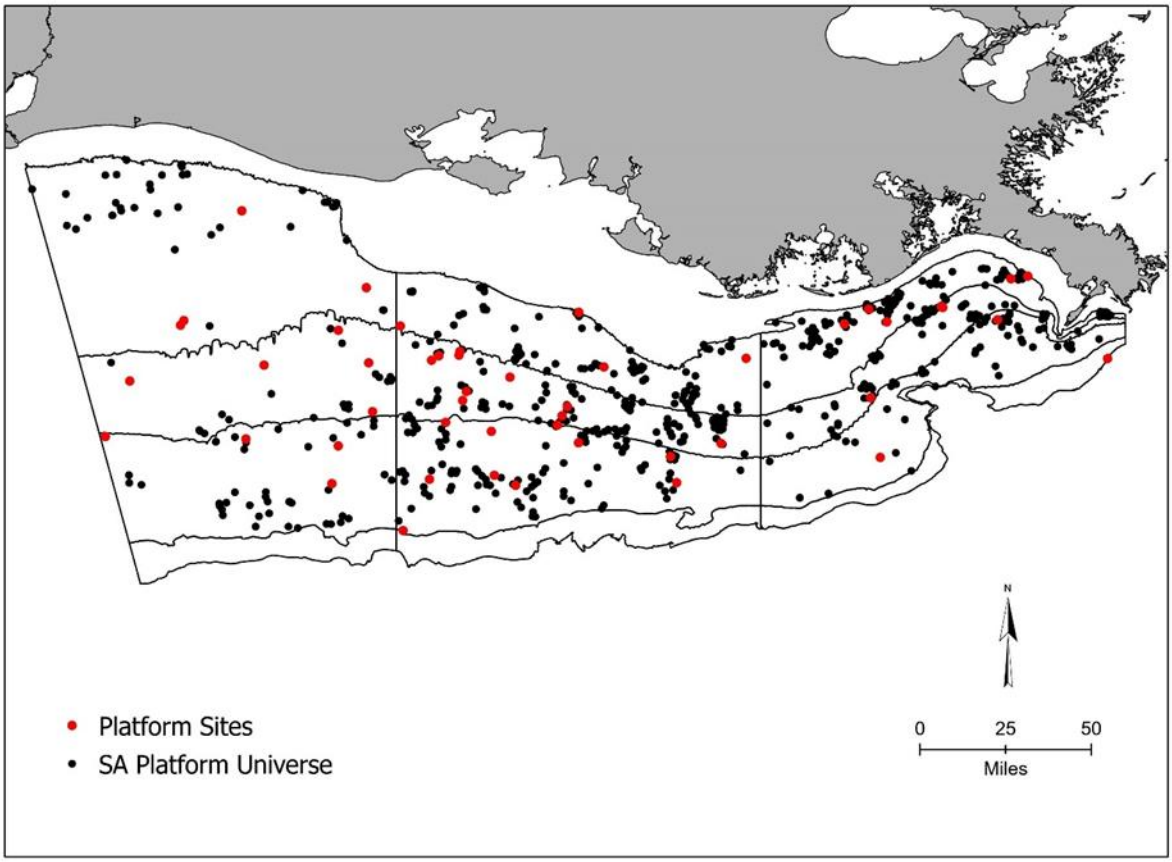

Figure 5. Sampled standing platform sites and the sampling universe from which they were selected. Sampling occurred during 2017, 2018, and 2020.

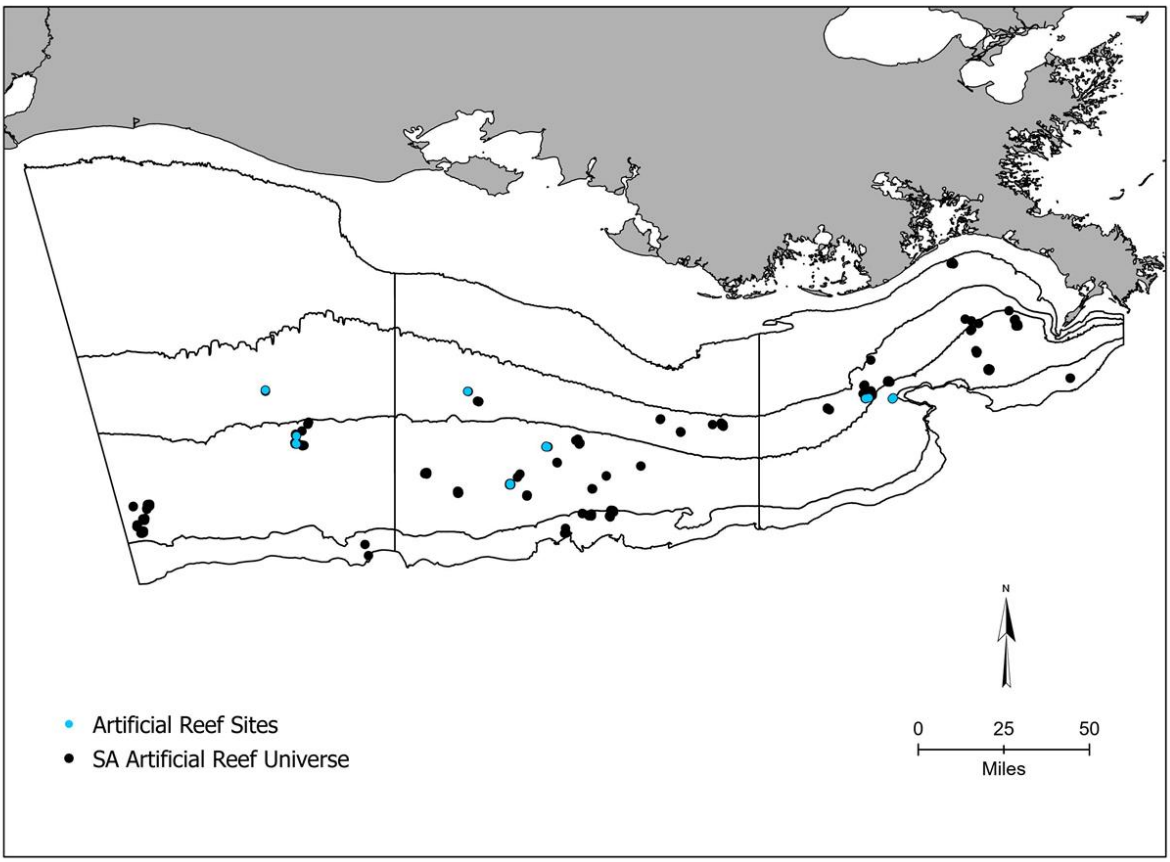

Figure 6. Sampled artificial reef sites and the sampling universe from which they were selected. Sampling occurred during 2020.

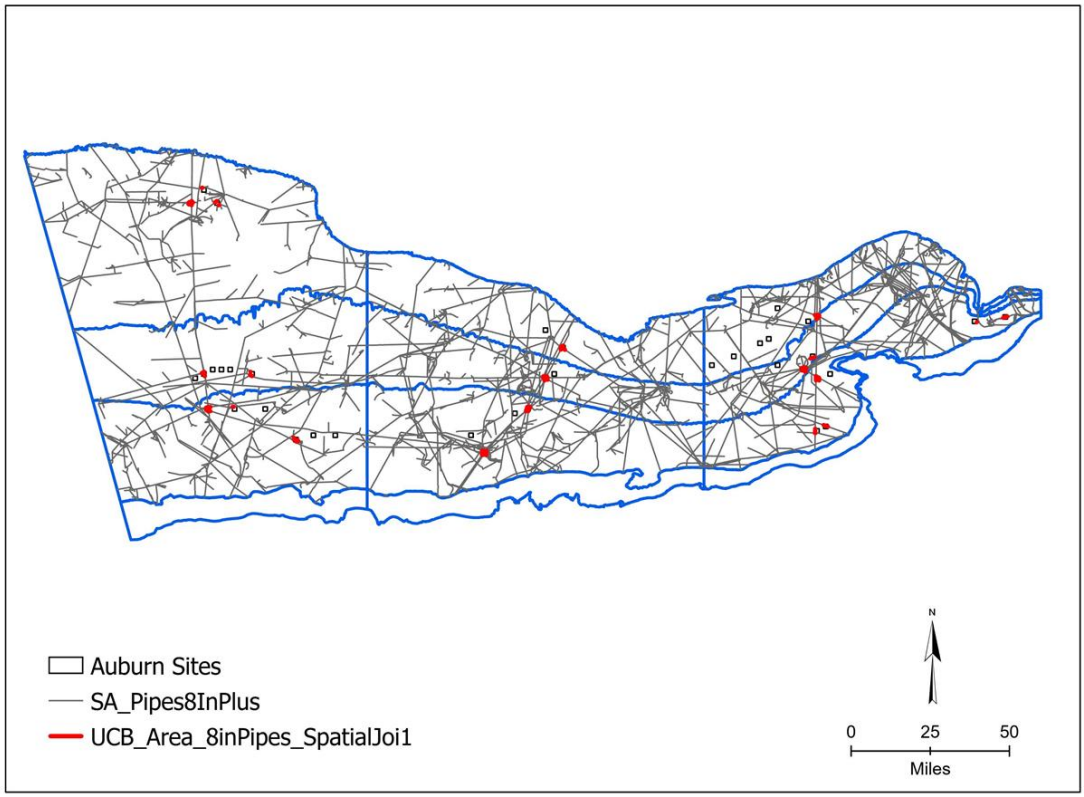

Figure 7. Sampled pipeline crossings and the sampling universe from which they were selected. Sampling occurred during 2020.

3.0 Field Surveys and Sample Processing

Our field surveys included hydroacoustic sampling to enumerate the fish associated with each of the defined habitat categories, camera surveys to estimate species composition of the fish communities represented at a site, and hook-and-line sampling to determine length, weight, sex and age of Red Snapper in the resident community.

Prior to departing the dock, Field Team Leaders were required to file a Float Plan (Appendix 2), with the Project manager, the Field Coordinator, and specified office staff designated as safety contacts. The Float Plan described the locations and activities to be performed. The Field Team Leader then conducted a pre-trip meeting with the vessel captain, the deckhand(s) and scientific staff, covering sampling objectives for the day as well as an overview on the location of safety equipment aboard the vessel. The Field Team Leader notified the designated safety contact of departure and successful return to dock. A copy of the Letter of Authorization (LOA) from NOAA was present during all field activities (Appendix 3).

3.1 Sampling Environmental Variables

Water column measurements were taken in conjunction with each type of sampling using a YSI EXO3 CTD which measured dissolved oxygen saturation (ODO %), dissolved oxygen concentration (ODO mg/L), specific conductance (SpCond µS/cm), conductivity (µS/cm), salinity (psu), total dissolved solids (TDS mg/L), turbidity (FNU), total suspended solids (TSS mg/L), and temperature (°C). All data were downloaded to a notebook computer, converted to .csv files and backed up on an external hard drive on board, immediately after being recorded. These data were used for the calibration of the echosounders applied in the hydroacoustic analyses and for the statistical model of Red Snapper abundance, as described below.

Surface conditions were measured using the vessel's instruments at each sampling station. We recorded air temperature (°F), wind speed (kts) and direction, atmospheric pressure (mbar), and water depth (ft). In addition, wave height (ft), current speed (kts) and direction were estimated by the captain of the vessel and recorded. CTD data were restricted to just the data for the downward drop. Prior to binning the data into 10 m increments, the top 3 meters and the bottom 1 meter of the water column were excluded to correspond to hydroacoustic exclusion zones. The 1-m depth-interval data were then binned to 10 m increments and averaged for each depth bin.

3.2 Hydroacoustic Field Surveys and Initial Data Processing

Hydroacoustics has been used in the Gulf of Mexico for the assessment of fishes around platforms for many years (e.g., Stanley and Wilson 1996, Boswell et al. 2010, Reynolds et al. 2018, Gallaway et al. 2021).

Hydroacoustic surveys were conducted using a multi-frequency series of three BioSonics DT-X split beam transducers - 38 kHz (10-degree beam angle), 70 kHz (5.0 degree beam angle), and 120 kHz (7.8 degree beam angle). Echosounder transducers were pole mounted over the side of the survey vessel using a customized bracket, with the transducer faces located approximately 1 m under the surface of the water aimed directly downwards (Figure 8). Prior to each survey event, each transducer was calibrated using standard methods (Foote et al. 1987). Any offsets between the actual and expected acoustic response from the calibration sphere were applied during data processing. The specified ping rate was set to "max," depending on site water depth, and pulse duration was set to 0.2 ms. More detail is provided below.

In hydroacoustic fish surveys, adequate coverage of the survey area is needed to achieve a reliable estimate of fish abundance. Degree of coverage (Λ) is defined as: $\Lambda = D/\sqrt{A}$, where D is the cruise track length, and A is the size of the survey area. Empirical data from Aglen (1989) showed the ratio needs to be 6:1 or greater. This was planned and achieved at all survey sites (Table 4).

The hydroacoustic surveys at all sites were conducted in a parallel transect pattern, covering different total areas depending on habitat type (Table 4). Discrete artificial structure sites were centered on the central point of the structure itself, and additional spiral transects were conducted around standing platforms in order to maneuver around above-water structures and capture fish present in these proximal locations. A sample area of 250 m by 250 m (eleven transects, 250 m long) was chosen for discrete artificial sites, resulting in a radius of at least 100 m around the structure. This was chosen to ensure the entire reef-associated fish community was captured, as previous studies have found that fish densities further than 50 to 80 m from platforms were comparable to background levels (Stanley and Wilson 1996, 1997, 2000, Szedlmayer et al. 2019)). Discrete natural bank sampling transects were expanded to 500 m by 500 m (eleven transects, 500 m long) to encompass greater variability of rugosity and fish assemblages found in this habitat type. UCB sites were based on 2.22 km by 1.96 km usSEABED database cell sizes (Buckowski et al. 2006), and surveys sampled an approximate 2 km by 2 km area over these sites (nine transects, 2 km long).

3.3 Hydroacoustic Data Processing Methods

Our approach in the hydroacoustic surveys utilized the process of 'decibel differencing,' using data from the three transducers of differing frequencies; 38kHz, 70kHz and 120kHz. This approach has gained momentum in recent years with the major benefit being able to separate acoustic signals of swimbladdered fish from those organisms without swimbladders (both fish and plankton) (Madureira et al., 1993; Mosteiro et al. 2004; Korneliussen et al., 2009, De Robertis et al., 2010), as different types of organisms produce different strengths of acoustic return at different frequencies (Reynolds et al., 2018). Our focus in this study was placed on the swimbladdered Red Snapper, and the decibel differencing approach greatly assisted with 'cleaning' the data to leave only fish of interest (primarily mixed reef fish assemblages), reducing the risk of inflated values from non-target species.

The decibel differencing methodology was combined with "echo integration," a technique that divides the total energy reflected from fish (proportional to fish biomass (Boswell et al. 2007)), called "Sv" (in this case from those fish with swimbladders) by the known amount of energy reflected by a single fish (Target Strength (TS)), in order to calculate fish density (MacLennan and Simmonds, 1992). This method (as opposed to "echo counting") is necessary when fish are not adequately dispersed enough to count individuals. TS is known for various fish species of different sizes through established TS to Length (L) equations in the published literature, so it can be applied via the size distributions resulting from catch data. This method (*ex situ* TS) works well with single species stocks but is problematic in mixed species communities. The use of *ex situ* TS is difficult in situations such as this, where TS-L equations are unknown for most of the species present, and while species composition could be estimated over a site as a whole, the species community present in any one acoustic cell is practically impossible to determine.

TS and Sv are also known to vary considerably with aspects of fish behavior such as tilt angle and condition (Love, 1971). Therefore, our approach was to use mean *in situ* TS to calculate density within each acoustic cell. This approach follows Rudstam et al. (2009) and has been used in studies and environments similar to this (e.g., Stanley and Wilson, 1996, 1997, 2000, Boswell et al. 2007; Zenone et al. 2019, Egerton et al. 2021). This approach is, however, also subject to biases if valid mean TS cannot be extracted from the data within an acoustic cell, such as in situations where fish occur in dense schools (see below). Due to the challenging nature of deriving fish density in mixed species communities such as this (Gastauer et al., 2017), final abundance estimates should be considered as estimates.

As an overview the following approach was taken: System calibration → Data cleaning and noise removal → Decibel differencing to extract Sv of swimbladdered fish → valid TS from swimbladdered fish extracted→ Echo integration (Sv/TS) → Data exported to spreadsheet in units of fish per m^3→ multiply by acoustic cell thickness (data converted to fish per m^2) → GIS →mean fish per m^2 value multiplied by area of grid cell → final abundance of swimbladdered fish.

Calibration - Before every survey event the echosounders were calibrated following standard methods (Foote et al. 1987). The 38kHz and 70kHz transducers were calibrated using a 38.1 mm tungsten carbide sphere, and the 120kHz transducer was calibrated with a 33.2 mm tungsten carbide sphere. These offsets were applied in the data processing in addition to the mean temperature and salinity measurements taken at each site with a YSI EXO3 sonde. Temperature and salinity are necessary to calculate the speed of sound through the water column.

Data processing - Data were analyzed in 20 m x 20 m horizontal, and 10 m deep cells, chosen as a balance between suitable spatial resolution and the number of valid Single Targets (ST) available for valid *in situ* target strength (TS) measurements (see below). In each of these cells, fish density (in units of fish per m^3) was calculated via echo integration (Sv/TS scaling). To deal with the absorption of sound through water, a Time Varied Gain

(TVG) correction of 40log(R) for TS values and 20log(R) for Sv values was applied. The bottom was detected via the Echoview algorithm and checked by eye to ensure that the algorithm correctly detected the seabed. A bottom exclusion line of 1 m was also applied to ensure echoes from the seabed were not included in the analysis and to avoid sampling in the "acoustic dead zone" (Ona and Mitson, 1996). If individual fish could clearly be seen within this exclusion zone with 'a visibly distinct gap' between the fish and the bottom, they were also included in the analyses. Any other remaining noise visible in the echogram, such as surface bubbles and leaking gas plumes, was removed by eye. At the platform and artificial reef sites, the structures were identified by eye and blanked out in the echograms (set to "no data"). A dataflow of all processing steps was constructed in Echoview (ver. 11.1) to process the raw data (Figure 9).

Noise removal - Prior to the decibel differencing, data at all frequencies were cleaned to remove any noise that can come from a variety of sources. In order to do this the following steps were taken:

1. The impulse noise (IN) removal filter removes sound spikes that may be resultant from other sound sources such as an unsynchronized echosounder (Ryan et al., 2015). This operator identifies and adjusts sample values that are significantly higher than those of surrounding samples at the same depth. Within this filter, a threshold of -170 dB was used, with a vertical window size of 3 samples and a horizontal window size of 3 pings for the smoothing. Samples with a 20 dB threshold difference from the adjacent samples were removed and a mean value from these adjacent samples was used instead.

2. After the IN filter, transient noise (TN) removal was applied following Ryan et al, (2015). This operator identifies and adjusts sample values that are significantly higher than those of surrounding samples. Within this filter, data was thresholded at -170dB, the context window was 3 pings by 3 samples. Sample values had a threshold of 20 dB, and when identified, these mean values were taken from the context window.

3. Finally, a Background noise (BN) filter was used, which estimates the background-noise level and subtracts it from the value of each sample. Within this, Sv values that were below the defined Signal to Noise Ratio (SNR) level were set to -999dB re 1 m^2 (Ryan et al., 2015), with a maximum noise value of -125dB and a minimum SNR of 10. Averaging parameters set within the filter used a horizontal extent of 3 pings and a vertical extent of 1 m. Smoothing does not affect the noise removal but reduces the variance among ping by ping measurements (De Robertis and Higginbottom, 2007). This smoothing of the data occurred above and below the bottom exclusion line separately, so that the seabed signal is not combined with near-bottom data above the Signal to Noise Ratio SNR (De Robertis and Higginbottom, 2007).

4. In the last step the 'processed data' variable was applied to remove all data below the bottom exclusion line at 1 m and above the surface exclusion line at 3 m depth. The data at each frequency were then smoothed using the XxY Echoview operator (5x5 pings). This is needed to average the acoustic measurements to reduce natural

stochastic variations in the data (Korneliussen et al. 2009, Lezama-Ochoa et al. 2011). The data from the different frequencies were then matched in terms of ping times and geometry to ensure accurate comparison.

Decibel differencing - Next decibel differencing techniques were used to mask all but the data related to swimbladdered fishes. To achieve this, 70 kHz echogram data were subtracted from 120 kHz echogram data. Data resulting in a difference in dB ranging between -15 and 1 were classified as fish with swimbladders, whereas results ranging from 2 to 25 were classified as organisms lacking swimbladders (Reynolds et al. 2018; Simonsen 2013). Additionally, 38kHz Sv data subtracted from 120kHz Sv data were also used to classify swimbladdered fish (Ballon et al. 2011; Lezama-Ochoa et al. 2011). Here a criterion of Sv 120kHz-38kHz resulting in a <3dB difference was used to apportion swimbladdered fish. These two decibel differencing categories were used to create Boolean (True/False) masks, which were used to only allow valid data to persist for subsequent analyses. In order to avoid masking valid fish data, data were acceptable that satisfied either decibel differencing criteria (Sv 120-38 <3dB or Sv 120-70 <2dB). (Initially the plan was for the data to have to satisfy Sv 120-38 <3dB AND Sv 120-70<2dB; however, this was seen to be too conservative and some valid data were masked. Scrutiny of the data showed Sv 120-38 <3dB OR Sv 120-70<2dB to be more appropriate.)

In addition to the decibel differencing criteria described above, the data also had to satisfy the criteria of 120kHz+70kHz+38kHz<-170dB, the value of which was determined by scrutinizing the resulting data in the echograms. This summation assists in determining fishes of interest, as it retains only those that exist on all frequencies (Fernades 2009, Ballon et al. 2011). This criterion was also used to create a Boolean True/false mask which was applied to the data at 120kHz for subsequent processing. The 120kHz data was chosen for the main analyses in order to facilitate incorporation of data from the BOEM study platform surveys that also used this frequency.

Following the application of these masks, it could be seen that there were occasionally gaps in the acoustic record within fish schools that did not satisfy the criteria, i.e., valid fish data was on occasion also masked. Therefore, following Ballon et al. (2011) and Lezama-Ochoa et al. (2011), the resultant fish data were smoothed with the XxY operator on a 3x3 basis to fill these gaps. This resulted in the creation of an expanded fish echogram, which was used as a mask on the original (noise removed) 120kHz data. This final mask was also applied to the single targets data so that only targets from swimbladdered fish were used in the echo integration process. Following the masking process, data were thresholded at an Sv of -50dB, with a minimum threshold TS of -50dB also applied in order to further assist in the removal of any remaining non-swimbladdered fish scatterers.

Determining valid TS from single targets - Single echoes were detected and accepted using the split beam single targets detection algorithm in Echoview, with a TS threshold of -50 dB, pulse length determination level of 6dB, minimum normalized pulse length of 0.7, maximum normalized pulse length of 1.5, and a maximum standard deviation of 0.6 degrees for the minor-axis and major-axis angles. To ensure that the TS of the single

echoes was not artificially inflated by the issue of multiple echoes, following Sawada et al. (1993), the Nv index and the M% of multiple echoes criteria were employed to mask cells that compromised the criteria of Nv < 0.1 and M < 70% (Parker-Stetter et al. 2009; Kocovsky et al. 2013). This was important because, if not accounted for, these 'multiple echoes' cause TS to be overestimated, resulting in an underestimation of fish density (Kocovsky et al. 2013).

Following the removal of multiple echoes as described above, TS data were taken from the valid *in situ* Single Targets (ST). In echo integration, the objective was to use the TS of valid ST within the same cell as the Sv data being scaled. If this was not available, TS data was taken from ST from adjacent cells through the use of the "XxY" variable in Echoview with values of 3 by 3 cells. If there were none available in adjacent cells, a mean TS from within the same depth layer was used (1 by 999 cells), and finally if not available within the layer, a site mean (10 by 999 cells) had to be used.

Fish Density Calculations - Final density values were obtained by dividing Sv by the best available *in situ* TS. These values were extracted in units of numbers of fish /m^3 within the 20 m x 20 m horizontal by 10 m deep cells to a spreadsheet. Within the spreadsheet, the numbers of fish were converted to fish number/m2 within a depth layer by multiplying the fish number/m^3 value by the thickness of the layer (normally 10 m, except in the layer closest to the bottom which was sometimes less). These fish number/m^2 values were then exported to GIS for subsequent analyses. In areas of the echogram where there were no data, for example within the matrix of a platform, then the mean value of horizontally adjacent cells was used.

Geographic Information System (GIS) Analyses - The fish number/m^2 values were imported to a Geographic Information System (GIS) (QGIS ver 3.14) for each acoustic cell within a site. A grid was placed over these cell values to obtain averages and abundance data (absolute number of fish per site). Three different sizes of grids were used:

- Discrete Artificial sites – 250 m x 250 m block comprising 25 50 m x 50 m grid cells.
- Natural Bank sites – 500 m x 500 m block, comprising 25 100 m x 100 m grid cells.
- Uncharacterized bottom sites – 2000 m x 2000 m block, comprising 25 400 m x 400 m grid cells.

A spatial join was then performed in the software, so that the point cell data within each grid cell were extracted.

Table 4. Hydroacoustic site numbers and survey areas and methods.

Site Type	Habitat Type	Number of Hydroacoustic Sites	Number of Transects	Sampling Area Dimensions	Area Sampled (m^2)	Aglen Ratio (>6)	Analysis Grid Applied	Analysis Grid Cell Size
Discrete	Platform	11 + 37 (BOEM)	11*	250m x 250m	62,500	11	5x5	50m x 50m
	Artificial Reef	16	11	250m x 250m	62,500	11	5x5	50m x 50m
	Pipeline Crossing	13	11	250m x 250m	62,500	11	5x5	50m x 50m
	Natural Bank	15	11	500m x 500m	250,000	11	5x5	100m x 100m
UCB	Uncharacterized Bottom	39	9	2000m x 2000m	4,000,000	10	5x5	400m x 400m

*Additional spiral transects conducted in order to maneuver around standing structures.

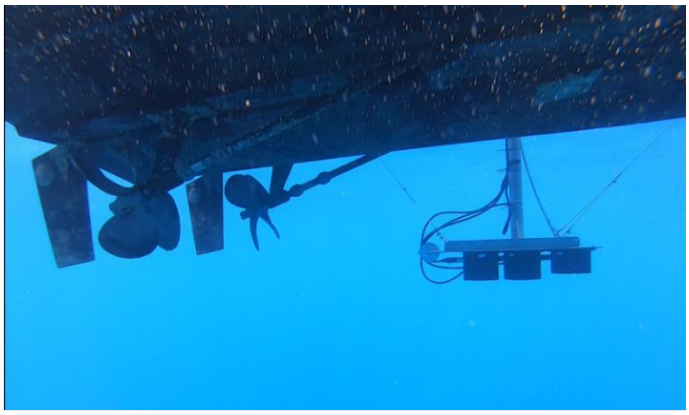

Figure 8. Echosounder transducers pole mounted over the side of a survey vessel, 1 m under the surface of the water.

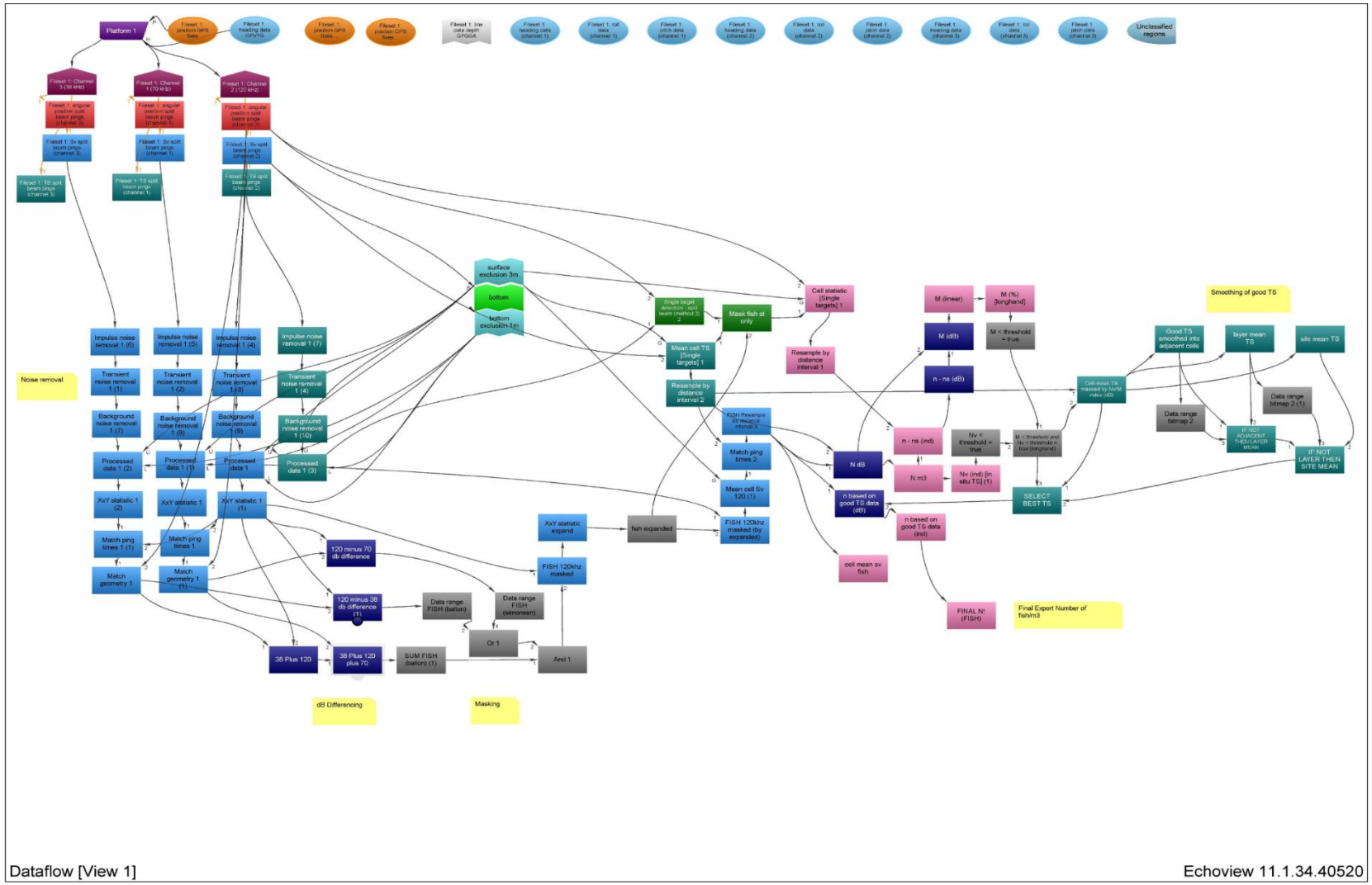

Figure 9. Hydroacoustic post-processing dataflow in Echoview (version 11.1).

3.4 Camera Surveys

As noted above, SRV surveys were taken at discrete habitats and opportunistically at UCB habitats, and TV surveys were taken only over UCB habitat. The purpose of these surveys was to allocate the total fish counts to individual fish species or taxa occurring at a site.

SRV Surveys - Design of the SRV was patterned to be consistent with Koenig and Stallings (2015). The SRV consisted of a waterproof canister housing that encased a gear motor run by a rechargeable battery (Figure 10). The motor shaft extended through the top of the canister and was attached to a round platform that served as the mounting point for a GoPro (Hero 7 Black) digital HD camera in an appropriately rated dive housing. GoPros were set to record at 60 frames per second (fps), "Hypersmooth" video stabilization, 4:3 Aspect Ratio, 1920 x 1444 resolution, wide field of view (FOV), and zoom = 0%. A 360° view of fish fauna was captured as the camera rotated, completing two 360° rotations ever minute. The 30 second rotation simulates the stationary visual point count method, the most commonly used method to count reef fish (Bohnsack and Bannerot 1986), where each rotation can serve as a subsample or replicate count for repeated measures of the fish density at the site, if desired.

The SRV was deployed at each discrete site at a stationary point as close to the targeted fish assemblage as possible without risking entanglement of gear. The camera was lowered in 10 m intervals, corresponding to hydroacoustic analysis layers, in order to obtain accurate species proportions used to partition hydroacoustic abundance data. A minimum of 5 minutes of footage was recorded at each depth layer. This time was selected based on the exponential decay curve of new species detected over survey time in similar temperate reef systems (Koenig and Stallings 2015). We expected to capture all non-cryptic taxa including Red Snapper and other important federally-managed species, as well as their relative distribution by depth.

The SRV was additionally deployed in UCB sites immediately after conducting hydroacoustic transects. If fish aggregations were observed during hydroacoustic surveys, a location was marked on the vessel's GPS and was subsequently surveyed with a targeted SRV drop, using the methodology described above. This allowed visual census data to be captured on significant fish assemblages and "patch reef" habitats in an otherwise relatively low-density environment. Data were recorded in the field on mini-SD cards then returned to the laboratory for analysis, backup, and archiving. All videos were examined on a high-resolution monitor with multiple reviewers. All fish species were identified to the lowest possible taxon and enumerated in ten 360° revolutions at each depth interval using MaxN, defined as the maximum number of a taxon seen in a single frame. The MaxN method is a commonly used relative abundance metric which provides a conservative estimate that avoids double counting fish (Schobernd et al. 2014, Bacheler et al. 2013, Campbell et al. 2015). These relative abundance data were used to calculate species percentage compositions at each depth layer and subsequently to apportion hydroacoustic abundances to species. Species that were considered cryptic or that did

not have swimbladders were excluded from hydroacoustic apportionment, due to the acoustic dead zone and decibel differencing hydroacoustic methodologies.

Towed Video Transects - For each of the designated "UCB" sites (n=51), we deployed a towed video camera (GoPro Hero 7 Black) in either a standard GoPro dive housing in waters less than 60 m, or an Isotta housing, rated to 200 m (Figure 11). The cameras were all set to record at 60 frames per second (fps), "Hypersmooth" video stabilization, 4:3 Aspect Ratio, 1920 x 1444 resolution, wide field of view (FOV), and zoom = 0%. These settings correspond with directional FOV angles as follows: Vertical FOV 94.4°, Horizontal FOV 122.6° and Diagonal FOV of 149.2°.

The towed video sled was custom built by LGL Animal Care Products. The sled frame was constructed from 1/2" aluminum 6061 T6511 rod and the vein from 0.080" aluminum 5052 H32 Sheet and fitted with a ¼" x 2" stainless steel eyebolt for attachment. The sled was designed to be towed from the surface to record video in straight, near-bottom transects while avoiding bottom snags and turbidity within 1 m of the bottom, where visibility was assumed to negligible and hydroacoustic methods were unable to distinguish fishes from the bottom (Figure 12). The video camera angle was gradually adjusted to account for deployment depth whereby the camera was near forward-looking in shallower waters and near downward-looking in deeper waters (Figure 12). All videos were downloaded to a computer and backed up to an external hard drive onboard the vessel, immediately after recording.

All videos were analyzed in full using a VLC video player on an ASUS notebook computer with an external 27" Apple thunderbolt flat panel display with a resolution of 2560 × 1440 pixels. The videos were generally reviewed at 1x speed. When possible images of fish came into view, the video was carefully reviewed at 0.25x speed. The maximum number of fish of each species observed in each video was derived using MaxN by enumerating every observed fish with time stamps. All fish were subsequently identified to the level of species or the lowest taxonomic level possible or, if unknown, recorded as unidentified. Still images of most fish detected were extracted and saved to confirm identifications. One viewer analyzed all videos and two additional observers analyzed three of the videos independently for verification. Finally, all species identifications were confirmed by three biologists.

Visibility varied among sampling sites and at times was reduced to zero, e.g., in those sites nearest to the outfall of the Mississippi River. It was assumed that catchability (i.e., visual detectability) was constant within each transect and among all species. We assumed that there was no bias for either avoidance or attraction to the sampling gear for any species. Visually derived fish counts were not used to estimate the total numbers of fish in each transect. Instead, the data were used to apportion abundance detected using hydroacoustic methods as the proportion of Red Snapper to the total number of fish detected, as described in SRV methodology. Therefore, while visibility varied among transects, it was relatively constant within transects and the relative apportioning was unaffected.

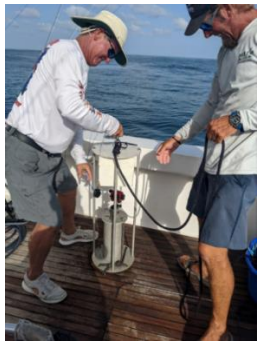

Figure 10. Deployment of Submersible Rotating Video (SRV) System.

Figure 11. Towed video camera sled made of ½" aluminum rod and plate, with 25 pounds of lead bolted to the bottom, a current vane at the back, and a GoPro Hero 7 Black (set at 1440, 120 fps, 4x3 wide) in an Isotta housing rated to 200m. The camera is mounted upside down but can be angled between straight forward and 45o down.

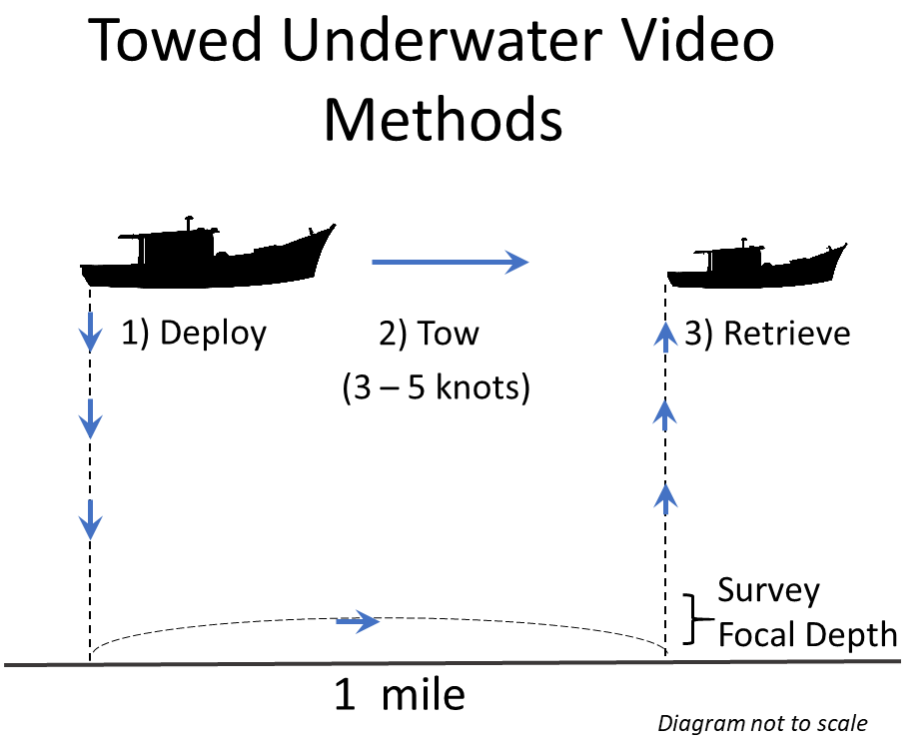

Figure 12. (A) Towed video cameras were deployed by (1) lowering the camera sled straight to the bottom from a stationary vessel, (2) towing the sled along the 1 mile transact at speeds of 3-5 knots without adding additional scope to the tow line, (3) allowing the sled to touch bottom at the end the transect and retrieving vertically. (B) The field of view captured the survey focal depth in shallow waters by angling the GoPro straight ahead and in deeper waters by angling the camera downwards at ~ 45°.

3.5 Hook and Line Surveys

Vertical hook-and-line sampling was conducted at discrete sites and longlines were fished on UCB habitats.

Vertical Hook-and-Line Effort - This method was used at discrete sites (platforms, artificial reefs, pipeline crossings and natural banks) and used 2 hook sizes. The first was a Mustad 6/0, Model # 39948NP-BN, 2X strength, and the second, was a Mustad 11/0, Model # 39965-DT, 2X strength. Bait types consisted of squid and menhaden, with squid size cut to match menhaden size. Each bait type was fished on each hook size giving 4 combinations of hook and bait type. Only one bait-hook combination was fished on an individual pole, and each bait-hook combination was fished an equal number of drops at each site. As fish were brought on board, they were placed into 1 of 4 shrimp baskets specific to hook and bait combination (Figure 13).

To indicate the hook and bait combination used to catch an individual fish, holes were punched in the operculum for processing dockside (Figure 14). To maintain consistency

throughout the field season, hole punches specific to hook and bait combinations were as follows:

- Combination 1 - 6/0 - Squid – No hole
- Combination 2 - 11/0 - Squid – 1 hole
- Combination 3 - 6/0 - Menhaden – 2 holes
- Combination 4 - 11/0 - Menhaden – 3 holes

Start and end times for composition sampling were recorded on a catch data sheet. Composition sampling lasted for 1.5 hours or ended whenever 40 Red Snapper were caught on a given site. When multiple sampling sites were visited during a day, fish from different sites were marked to site and separated in the ice hold for dockside processing. Upon completion of on-water field sampling activities, vessel and crew returned to port for dockside workups that evening. Once at dock, specimens were unloaded by site, iced down, and prepared for workups. All specimens had bait-hook combination of capture recorded and whole weight measured to the nearest 0.001 kg using an Adam's 165 lb. warrior wash-down scale. Fork and total lengths were measured to the nearest millimeter using a Wildco measuring board, Model # 118-B30. Sex was recorded for every specimen. Red Snapper otoliths were then extracted, cleaned, dried, and stored in a labeled coin envelope specific to each individual and site for age determination (Figure 15). Gutted, whole fish were iced and donated to charity.

Longline Effort - We deployed bottom longlines from the F/V Hull Raiser at 51 UCB sites in the study area (Figure 1). Longlines were deployed using a hydraulic winch mounted on the bow of the vessel. The main line was made of 1,400 lb. test monofilament with 74 hooks per set; 80 lb. test monofilament gangions, 3 feet in length with Mustad circle hooks alternating between 6/0 and 11/0 (Figures 16 and 17). All hooks were baited with squid. Longlines were deployed by three persons, one driving the vessel, one baiting the hooks and one attaching gangions to the main line as it was fed out. The longlines were set using standard methods with one buoy on each end, with weights (20-40 lbs. depending on current) below the buoys and one mile (1.6 km) of line between them (Figure 17). The mainline was cut after attaching the second buoy so the gear was detached from the vessel during the set. Longlines were set parallel to latitude or longitude lines, N-S or E-W, through the center point of each pre-designated 2 km^2 sampling site. Set direction was selected by the captain based on his assessment of currents, winds, depth, obstructions and other factors. We deployed a total of 51 miles of longline, with a total of 60 hours of soak time during the course of the study.

Longlines were soaked for approximately one hour from the start of the deployment to the time the entire line was back on deck. Deployment times ranged from 9 – 21 minutes with a mean of 13 minutes (n=51). Total soak times ranged between 30 and 107 minutes, with a mean of 70 minutes (n=51) and a total soak for all samples of 60 hours. The longline was retrieved with the hydraulic winch in the same direction that it was deployed to standardize the amount of time each hook on the line was fished. The line was "peeled" off the bottom by backing the vessel towards the line to avoid dragging the line along the

bottom. As the line was retrieved, all gangions were unhooked from the main line and all fishes were removed from the hooks.

All captured fish were retained and marked at sea to distinguish site and hook size. Fish were marked with a leather punch by punching holes through the gill plate of those fish captured on 11/0 hooks. All fish were stored on ice until the vessel reached port. At dockside, all fish were sexed, measured (FL and TL in mm) and weighed to the nearest 0.001 kg following methods described above. Sagittal otoliths were extracted from all Red Snapper, cleaned, dried and stored in a labeled coin envelope for aging purposes.

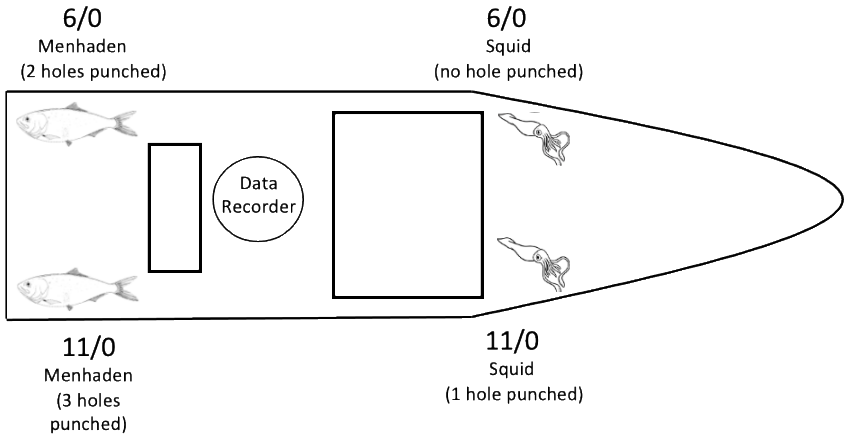

Figure 13. Diagram of vessel setup for sampling at discrete sampling sites.

Figure 14. Hole punching a Red Snapper to indicate bait-hook combination utilized for capture.

Figure 15. Dockside sampling after field sampling activities for the day.

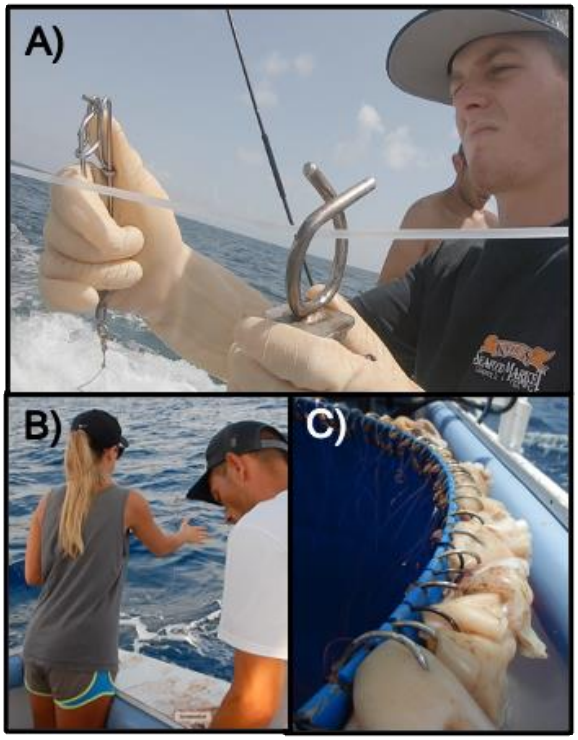

Figure 16. Longline deployment. A. Attaching gangions to the mainline, B. Feeding out the mainline, 3. Hooks, alternating 6/0 and 11/0, baited with squid.

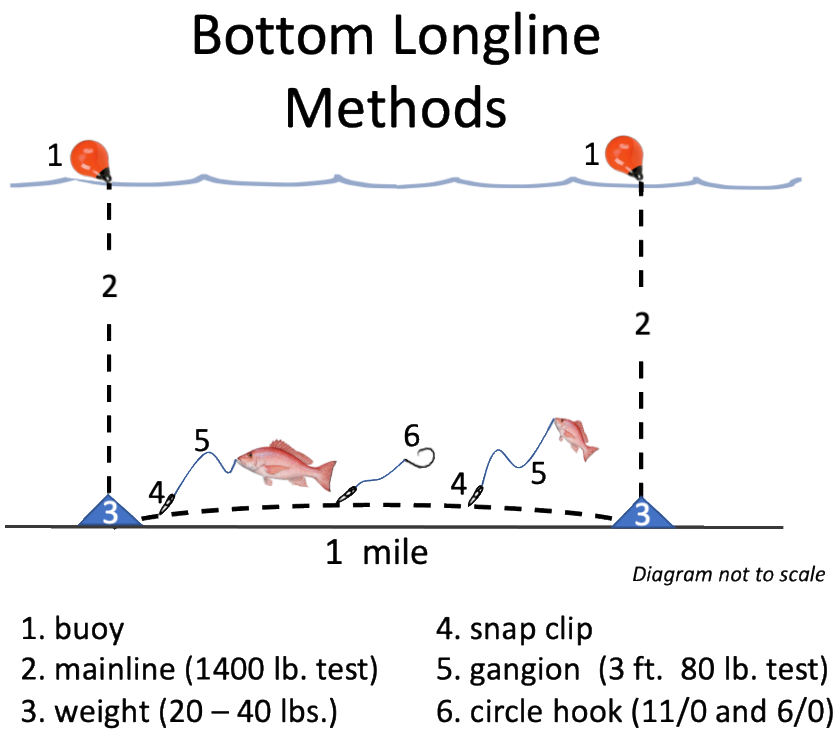

Figure 17. Bottom longline deployment for composition sampling over uncharacterized bottom.

3.6 Mark/Recapture Studies

As an independent assessment of Red Snapper abundance, a mark/recapture study was conducted at 3 of the 11 of standing platforms and 3 of the 16 artificial reefs sampled during this study. Each of the 3 platforms and 3 artificial reefs were located in the mid-depth zone of each region. In addition, 6 mark/recapture estimates at standing platforms made during 2017 and 2018 are reported from the Gallaway et al. (2020) study.

Red Snapper were captured by hook and line and then anesthetized with tricaine methanesulfonate (MS-222, 150 mg L^{-1} seawater for 90 sec.). The length (mm) and weight (0.1 kg) of each fish was recorded before being doubled tagged dorsally with Hallprint PDAT 135 mm dart tags. Before release, the fish were held in a 110 L container until they showed substantial recovery, that is, active fin and gill movements. Active fish were then transferred to a release cage and lowered to the bottom. Contact with the bottom caused a door to open so that the fish could exit the cage on their own initiative.

Recapture sampling was also conducted using hook-and-line. All fish caught were measured and, if not a recapture, were released at the surface. Recaptures were weighed, measured and the otoliths removed for aging in the laboratory. A photographic depiction of the mark-recapture process is provided in (Figure 18).

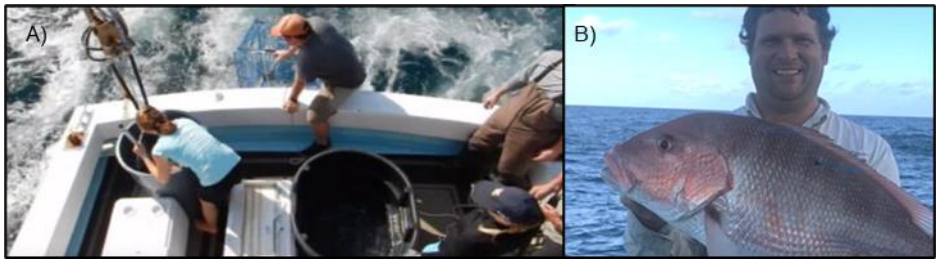

Figure 18. Photographic depiction of the mark-recapture process showing (A) the release of tagged fish and (B) recapture of a doubled tagged Red Snapper.

3.7 Age Determinations

Otoliths provided from field sampling were mounted in the laboratory and thin sectioned in a transverse plane with a Pace Technologies, Pico 155 sectioning machine outfitted with 2, 4" diamond embedded wafering blades with a 0.75 mm spacer between the blades. Sections were polished on 2,000 grit wet-dry sandpaper. Otoliths sections were submerged in water in a clear dish and read under transmitted light using a dissecting microscope outfitted with a Tucsen Bioimager camera. This method allowed us to read the annuli along the dorsal margin of the sulcus acousticus from the core to the proximal edge (GSMFC 2009). Edge condition was documented as having an opaque margin or a translucent margin, and depending on width of the margin and time of year at capture compared to the next expected annulus deposition period, an edge code of either 0 (opaque margin present or annulus deposition already completed that year) or 1 (annulus deposition yet to be completed) was assigned. Ages were advanced by one year for an assigned edge code of 1 to standardize ages among fish at different stages of annulus deposition during the year. Two independent readers counted annuli and assigned edge codes without knowledge of morphometric data. Instances of disagreement in initial counts resulted in a second count by both readers and consensus was reached.

4.0 Statistical Analyses

4.1 Choosing an Inferential Framework for Survey Data

Before we describe our sampling design and modeling approach, we review the two general frameworks for inferring population parameters from estimates based on survey samples—design-based versus model-based inference. The distinction between the two and how sampling design is related to the model specification is routinely omitted by researchers across a range of disciplines. Sterba (2009) reviews these frameworks for the field of psychology; Williams and Brown (2019) expound upon this discussion and tailor it to the field of ecology noting the advantages and disadvantages of each, the consequences of ignoring the distinction, and describe conditions under which sampling design can be safely ignored.

If samples are collected at random from the population's universe of units with all possible units having an equal probability of being sampled, then a simple random sample has been obtained. Any statistic derived from this sample, such as an average, is said to be design-unbiased. Values of the sampled units themselves are held to be fixed, and the variance around any statistic based on these samples comes from randomness in the selection process. Sampling probabilities can vary across units when more complex designs are employed—for example stratified random, systematic, or cluster sampling designs—yet the statistics and associated variances they render are still design-unbiased as long as the selection process controlling these probabilities is accounted for. Thus, the sampling design must be clearly defined and accounted for to ensure unbiased design-based inference (Thompson 2002). The researcher is unconcerned with the conditions causing unit values to vary from one to the next. As long as the sample was random, then the conditions controlling their values were observed randomly, and are therefore representative of what the population experienced.

Not all survey designs are random. This situation can arise when samples are selected for convenience to minimize costs (opportunistic sampling) or intentionally selected from a specific set of conditions to ensure their inclusion for comparison purposes (purposive sampling). Design-unbiased inference is dubious for these datasets as the conditions controlling the unit values are not known to be representative of what the entire population experienced. Nevertheless, model-based inference is still possible if a statistical model can be parameterized to capture the important structural features of the ecological system that control the unit values and of the selection process when it deviates substantially from simple random sampling (Thompson 2002; Sterba 2009; Williams and Brown 2019). If so, then predictions from this model (inference) will represent the infinite population (i.e., be model-unbiased) if they are conditioned on these features. Thus, identifying the relevant conditioning variables and specifying them correctly in the statistical model becomes crucial. Under the model-based framework sample selection is held to be fixed while values of the sample units themselves are not, and their randomness comes from a stochastic process, which is assumed to be defined by a parametric distribution (e.g., normal, lognormal, Poisson, binomial, etc.) chosen for the statistical model (Thompson 2002; Sterba 2009; Williams and Brown 2019).

The design-based framework was advocated by prominent statisticians J. Neyman and E. Pearson starting in the 1930s, who wanted to avoid the subjectivity that comes with assuming a distribution for the response, appropriate specification of a model, and correct conditioning on all selection and design variables (Sterba 2009). Conditioning often swallows degrees of freedom and can be prone to error if relevant selection and auxiliary variables are unknowingly omitted. In addition to avoiding these issues, design-based inference should be more accepted by stakeholders with differing interests that can influence model specification, which often has an infinite complexity of alternatives (Thompson 2002; Williams and Brown 2019). However, empirical random sampling is not always possible and causal hypotheses about important auxiliary variables and their interactions cannot be addressed with design-based inference (Williams and Brown 2019).

Given this, another famous statistician, R. A. Fisher, promoted model-based inference throughout the 1950s, which was widely accepted by sociologists and economists and involves three steps (Sterba 2009). Step one was to formulate a statistical model with terms for all important variables and their interactions that are thought to influence the dependent variable. Step two was to assume a parametric distribution from which the error term was randomly generated, which in turn renders a random dependent variable. Step three involves meeting Fisher's "conditionality principle" that can be compromised under three circumstances (Sterba 2009).

Under these circumstances, aspects of the selection mechanism must be included in the model specification. First, if sampling units were stratified before selection, then terms for these strata should be included in the model. Second, units are sometimes clustered into groups that are each sampled multiple times. Multiple observations at a given site or repeated observations on a given subject leads to non-independent samples and were dubbed forms of pseudoreplication by Hurlbert (1984). Not accounting for this within-subject/site-effect causes variance estimates to be biased low, and therefore confidence and prediction intervals to be too narrow (Stroup 2013). Davies and Gray (2015) argue that the concept of pseudoreplication in ecology is applied too dogmatically, blocking publication of studies where the issue has been dealt with appropriately, which in turn slows the pace of ecological research. Pseudoreplication in the fisheries literature has received less attention than in the general ecology literature; nevertheless, modern statistical procedures afford a way of handling multiple observations per site or subject with the inclusion of random effect terms (Millar and Anderson 2004; Davies and Gray 2015; Williams and Brown 2019). The final circumstance that compromises the conditionality principle is when the selection of sampling units is influenced by the unit values. Williams and Brown (2019) refer to this as informative sampling. An example would be if samples were selected because they were known to exhibit high or low unit values. Even in the absence of stratification and clustering (circumstances one and two above), these samples would not be representative of the population, and any prediction produced by a model based on these samples would be biased. We expound upon why we think these circumstances were avoided/corrected within our study under the Statistical Model Specification section.

4.2 Sampling Designs

The primary objective of the sample selection process used for this study was to choose samples representative of the population while reducing the cost of their collection to fall within budgetary constraints. In so doing, random sample selection was sacrificed for several habitat types that were surveyed. Regardless, the data collected still resulted in a model-unbiased estimate of Red Snapper abundance given that, within our study, the conditionality principle was met.

The study area was divided into three longitudinal regions (West, Central, and East; see Figure 1) and then four depth zones (10-25 m; 25-45 m; 45-100 m; and 100-150 m).

Upon final site selection, only two platform sites occurred in the deepest zone; therefore, the deepest two zones were combined before analysis (45-150 m) ultimately resulting in three zones. These depth zones were selected to capture major shifts in Red Snapper abundance along the bottom depth gradient based on previous studies (Gallaway 1981; Gallaway and Lewbel 1982; Dance and Rooker 2019; Gallaway et al. 2021).

Initially, five habitat types were targeted: (1) standing platforms, (2) natural banks, (3) pipeline crossings, (4) artificial reefs, and (5) uncharacterized bottom or UCB. Platform sites were selected according to a random sampling design stratified by region and depth zone with sampling probability proportional to the number of platforms present in each stratum (Figure 5). Natural banks only occurred in the 45-150 m depth zone. Two banks were selected at random in the western zone, two in the central zone, and one in the eastern zone. Within each bank, three sites were then selected at random (Figure 4). Pipeline crossings were sampled as a distinct habitat. Owing to limited differences between open-bottom habitat and pipeline (discussed in more detail, below) the data from pipeline crossing were eventually dropped from the analysis. Nonetheless, there selection influenced the selection of both artificial reef and UCB sites. Three pipelines were chosen that approximately ran through the center of each region and traversed all of the depth zones. Subsequently, crossing sites were randomly selected along these pipelines within each depth zone (Figure 7). Artificial reef and UCB sites were chosen opportunistically based on their proximity to the selected pipeline crossing sites to facilitate sampling logistics and reduce costs (Figure 6 and Figure 3). Furthermore, UCB sites were purposively positioned to represent the various substrate types (mud, sand, and gravel) and areas where shrimp trawling was historically limited.

Finally, subsequent to sampling we noticed that some sites were close enough together such that independence among samples may have been compromised. Thus, we had to decide on a distance at which species assemblages could be considered independent. Scott et al. (2015) studied the effective range to which offshore artificial reefs influence neighboring fish assemblages (total abundance and composition) in the surrounding pelagic environment and report this association to deteriorate beyond 30 m for all but one species and beyond 100 m for all species near Sydney Harbor, Australia. Another study in New South Wales, Australia recommend a minimum reef proximity distance of 200 m, but preferably 400 m to ensure independence among sites (Schultz et al. 2012). Thus, we pooled all sites of the same Habitat Type that were less than 400 m apart. These included five artificial reef sites in the central-deep stratum. Sites 18 and 20 were 276 m apart and thus combined into a single site. Sites 21 and 23 were separated by 336 m and Sites 23 and 22 by 257 m; thus, all three Sites were pooled together. Regarding distances between sites differing in habitat type, Site 8 (standing platform) and Site 25 (artificial reef) were separated by 196 m. As our sample size for standing platforms was greater than artificial reefs, we chose to drop Site 8 from our analysis.

4.3 Statistical Model Specifications

The abundance estimation approach combining hydroacoustic and SRV data had to be carefully evaluated. For example, at a given site an estimation of Red Snapper abundance could be accomplished by combining total fish abundance estimated from the hydroacoustic survey with species relative abundances estimated concurrently with an SRV. This abundance estimate would be wrong if either the total fish abundance or the proportion attributed to Red Snapper was in error. For instance, the hydroacoustic density estimate may have accurately estimated a total abundance of 2,000 fish and was unknowingly comprised of 1,000 Atlantic Bumper *Chloroscombrus chrysurus* and 1,000 Red Snapper. However, if the SRV sample only recorded 10 fish because of poor visibility, nine of which were Atlantic Bumper and only one was a Red Snapper, then the Red Snapper abundance estimate would be biased low (i.e., 200 instead of 1,000). Thus, at a given site error in the species apportionment would be magnified by the respective estimated total abundance. Averaging across site-specific estimates could then result in a biased overall estimate if an especially egregious apportionment error were unduly weighted by a large total abundance estimate for one of the sites.

For this reason, site-specific estimates were not estimated. Instead, we modeled the average proportion of the assemblage structure comprised of Red Snapper for a given habitat type, region, depth zone, and vertical depth band given average environmental variables. Then, we used this output to apportion the corresponding model output of average total fish abundance. In so doing, random errors in species apportionment (i.e., proportion that were Red Snapper) had a greater chance of canceling each other across sites before being multiplied by the total abundance estimates. The same was true for site-specific errors in the total abundance estimates. This same approach was used by Gallaway et al. (2021) to estimate various species abundances on platforms in the northern GoM.

Below we describe how relative abundance of Red Snapper and total fish abundance were modeled separately. For each habitat type-region-depth zone-vertical depth band combination, predictions from both models were combined to provide Red Snapper abundance estimates with confidence intervals.

Independent Variables - The categorical variable Habitat Type included the following levels: artificial reef, natural bank, uncharacterized bottom, pipeline crossing, and standing platform. Originally, pipeline crossings were thought of as a discrete habitat type that justified targeted sampling similar to standing platforms. However, upon sampling it became clear that the BOEM (2018) database (see Figure 7 for the rendered sampling universe coverage) was unable delineate whether a pipeline crossing was buried or exposed above the substrate. Therefore, the degree of useable pipeline habitat was unknowable. Based on the hydroacoustic surveys, a paired t-test of the twelve pipeline crossing sites and corresponding UCB sites yielded little statistical difference with respect to total fish density (two-tailed p-value = 0.2714). Furthermore, results from the SRV surveys of these sites were ambiguous. Fish were observed at both open bottom and pipeline crossing drops at only three of the twelve paired sites. The proportion of fish

being Red Snapper was statistically greater ($\alpha = 0.05$) for the open bottom than the corresponding pipeline crossings for two of the pairs (two-tailed p-values = 0.0009 and <0.0001) and nonsignificant (two-tailed p-values = 0.923) at the other. Therefore, we decided to not use the hydroacoustic and SRV data collected at the pipeline crossing sites. Instead, we estimated two pipeline metrics from the BOEM (2018) database for all of the sites, regardless of habitat type—number of pipeline crossings per km^2 and meters of pipe per km^2. The rationale was that sites with greater densities of pipelines and/or pipeline crossings might hold more Red Snapper; however, these variables proved to be uninformative (likely due to the issue of being unable to know whether crossings were buried or exposed) and were dropped from consideration.

Likewise, other variables were deemed to be too intractable for consideration. For standing platforms, variables quantifying the number of legs descending from the surface and categorizing a given platform as manned/unmanned were considered but were not used in the final model. The number of legs did not capture the number of total pipes descending to the ocean floor nor the complexity of cross structures beneath the surface. We reasoned that the fish assemblage on a manned platform would be exposed more to fishing pressure. However, during field activities, crew boats were sometimes observed tied to and actively fishing platforms designated as "unmanned" in the BOEM database. For these reasons, these variables were considered poor descriptors and were ultimately dismissed as misleading.

Variables quantifying the percent coverage of bottom sediment (rock, mud, sand, and gravel) within each grid cell (2.22 km by 1.96 km) were estimated from the usSEABED bottom sediment database (Buczkowski, 2006). These data were compositional by nature in that their values summed to a standard simplex of one, which by definition causes collinearity (if one increases, the others must decrease to maintain unity). We attempted to remedy this problem with center log ratio transformation and leaving out one variable, but ultimately none were useful descriptors of total fish abundance or percent Red Snapper. Collinearity aside, we suspect the real culprit to be that the resolution of the grid cells (4,351,200 m^2) was too coarse to accurately reflect the substrate at each of our sites.

Ultimately, three factors and three covariates were used as fixed effects; *Site* was used as a random effect term (henceforth, model terms will be capitalized and italisized). Excluding pipeline crossings, all other levels of the factor Habitat Type (*HabType*) were used. In addition, the factors *Region* (East, Central, and West) and Depth Zone (*DZ*; 10-25 m, 25-45 m, and 45-150 m) were used; again, the original two deepest zones (45-100 m and 100-150 m) were combined to define the 45-150 m zone.

Available covariates were meters from the bottom (*MFB* = meters from the bottom to the center of each vertical depth band), *Salinity*, water temperature, and dissolved oxygen (*DO*); physicochemical variables were averaged within each depth band. Correlation among covariates was assessed as per Dormann et. al. (2013), who found that avoiding the simple threshold of Pearson's $|r| > 0.7$ between two variables, and the use of ecological understanding to determine which variables to exclude when this threshold

was reached was enough to thwart problems of collinearity. The correlation between temperature and salinity breeched this threshold for both the hydroacoustic and SRV datasets (r = -0.71 and -0.72, respectively). We reasoned that salinity would capture stratification events at sites more influenced by freshwater from the Mississippi River better than temperature. Moreover, *Salinity* was less correlated with the *DO* and *MFB* covariates; thus, temperature was discarded.

Modeling Proportion Red Snapper from SRV Surveys - At each site, a survey of the assemblage structure was available from the SRV MaxN count observations for each vertical depth band. From these data, the relative abundance of Red Snapper (PropRS) was estimated as its MaxN count divided by the sum of the MaxN counts for all species in the sample. This binomial response was modeled using the logit link function. Hence, we modeled the log odds of a fish in the assemblage structure being a Red Snapper rather than being something else. Our final model specification formed a generalized additive mixed model (GAMM) for which we estimated parameters using the gam function in the mgcv Package Version 1.8-39 (Wood 2022) for the R statistical programming language implemented with RStudio (RStudio Team 2022); the R code for this model was as follows:

```
TFD <- gam(RS/Total ~ Region + DZ + HabType +
                s(DO, k=5, bs="tp", m=1) + s(Salinity, k=5, bs="tp", m=1) +
                    s(MFB, by=HabType, bs="tp", k=5, m=1) +
                    s(Site, bs="re"),
                family = binomial(link="logit"), weights=Total, method="REML",
                optimizer=c("outer","newton"), data=SRVdata)
```

where, *RS/Total* = the proportion fish for a given sample's total that were Red Snapper (i.e., *PropRS*), and s() represents a smooth function whose basis was a thin plate regression spline basis as indicated by the bs = "tp" syntax for *DO*, *Salinity* and *MFB*. *Site* was entered as a random effect with the bs = "re" syntax. The k = 5 syntax held the upper limit for the degrees of freedom associated with the smooth to four (k-1), which helped to prevent overparameterization; others have also used this approach (Pedersen et al. 2019, Bolser et a. 2020, Dance and Rooker 2019, and Egerton et al. 2021). The maximum degrees of freedom for each smooth were automatically penalized by minimizing the restricted maximum likelihood (REML; recommended by Wood 2022), which results in effective degrees of freedom (the number of coefficients to be estimated). We chose to penalize the squared first derivative for each smooth function as indicated by the syntax m=1. The default is to penalize the second squared derivative (m=2), but low order penalties are recommended when the response can be zero over large areas of covariate space and avoids extreme estimation when the data are uninformative (Wood 2022). Lower order penalties also help to reduce concurvity (similar to collinearity in linear regression models) among smooth functions (Pedersen et al. 2019). Further to this point, we only included the factor and factor-smooth interaction terms for *HabType* and *MFB*. Not including a global smoother for the *MFB* term by itself helps to avoid concurvity issues with factor-level smoothers (Pedersen et al. 2019).

Modeling Total Fish Density from Hydroacoustic Surveys - The hydroacoustic surveys provided observations of total fish density (*TFD*; fish per m^3) for each *Site*-depth band combination. This response was assumed to be from a Tweedie distribution, which uses the log link function. The same fixed effects variables were considered as was described above for modeling *PropRS* in addition to the random effect of *Site* to form a GAMM with the same specification of terms:

```
TFD <- gam(TFD ~ Region + DZ + HabType +
                 s(DO, k=5, bs="tp", m=1) + s(Salinity, k=5, bs="tp", m=1) +
                       s(MFB, by=HabType, bs="tp", k=5, m=1) +
                       s(Site, bs="re"),
                 family=tw(a=1.01, b=1.99, link="log"), method="REML",
                 optimizer=c("outer","newton"), data=HydroData)
```

Meeting Fisher's Conditionality Principle - As discussed above, the accuracy of our estimates based on the survey data collected in this study is predicated on correctly specifying the statistical models and appropriately conditioning their predictions to meet Fisher's Conditionality Principle. One of the drawbacks of model-based inference is the seemingly limitless ways in which a model can be specified (Thompson 2002; Williams and Brown 2019). "There is a bewildering array of different types of spline" (Simpson 2018).

Generalized linear models (GLMs) and generalized additive models (GAMs) are common statistical approaches used to generate population indices from survey data (Potts and Rose 2018). As many ecological patterns are nonlinear, more researchers are gravitating towards relaxing the linearity assumption (Oddi et al. 2019). Potts and Rose (2018) show that GAMs outperformed GLMs for estimating indices from fishery independent surveys. Furthermore, random effects are increasingly being added to these models to account for nonindependence among samples (Harrison et al. 2018, Pedersen et al. 2019). Thus, we chose to use GAMMs, but the routine use of these models is relatively new to ecology (Pedersen et al. 2019); these authors refer to them as hierarchical GAMs [HGAMs]) and updates on best practices regarding model specification are rampant in the current literature. Our choices regarding smooth terms, automation of smoothness selection, basis functions, penalties, and overall model specification were strongly influenced by the recommendations of Simpson (2018), Pedersen (2019), Harrison et al. (2018), and Wood (2022).

We considered only a fraction of the potential model specifications that were possible based on what made sense ecologically—a practice that is routinely and strongly recommended (Burnham and Anderson 2002, Harrison et al. 2018, Pedersen et al. 2019). Of the independent variables that were considered, their various combinations and specifications were compared based on several criteria to assess model fit and adequacy. First, the MuMIn Package Version 1.43.17 (Barton 2020) was used to estimate and tally the sample size adjusted Akaike Information Criterion (AICc), as this adjustment is recommended when the sample size (n) to parameter (K) ratio $n/K < 40$ (Burnham and

Anderson 2002). During this process, maximum likelihood (ML) was used instead of REML as recommended for comparing AICs when fixed effects differ among models (Wood 2022); although REML was used once the final model was chosen. Second, Harrison et al. (2018) recommend fitting the most complex mixed model that the data will allow, but overfitting (i.e., including too many parameters for the data to accurately estimate) can either result in failed convergence or spurious inference. To prevent overfitting, the minimum n/K ratio should be ≥3 (Crawley 2013). This recommendation varies widely in the literature, but as a rule of thumb type I errors increase dramatically below this threshold (Forstmeier and Schielzeth 2011). Model variations whose n/K ratio was <3 were discarded. Overspecification, was also checked with the concurvity function available in the mgcv Package (Wood 2022), which yields indices of the extent to which a smooth term could be approximated by one or more of the other smooth terms.

Finally, residual diagnostics were used to compare model behavior. Residuals can be difficult to interpret if not misleading for non-Gaussian generalized mixed models even when Pearson or deviance residuals are used (Hartig 2022). Fortunately, recent advances in residual analysis offer a remedy by way of simulation (Harrison et al. 2018). Models were assessed with scaled (quantile) residuals via the DHARMa Package Version 0.4.5, which extends this tool to models parameterized with the mgcv Package (Hartig 2022).

When the conditionality principle is met, sampling design can be ignored and model-unbiased inference regarding the population can be achieved (Thompson 2002, Sterba 2009, Williams and Brown 2019). We argue that such was the case for our survey of Red Snapper in Louisiana and adjacent federal waters even though a variety of sampling designs were used across the range of habitat types. First, pertinent strata utilized to parse sampling units prior to selection were included in the final model specifications, which exhibited adequate model diagnostics (see Appendices 6 and 7). Second, the non-independence of multiple observations at each *Site* were accounted for with the inclusion of a random effect term that allowed the intercepts to vary randomly across *Sites*. Furthermore, the *MFB* fixed effect smooth term in the final GAMMs quantified nonlinear changes in the responses among samples collected along the vertical depth gradient. GAMs have less residual correlation than GLMs when the model itself includes smooth terms that account for correlation among adjacent samples (Segurado et al. 2006, Potts and Rose 2018). Third, none of the *Sites* chosen were influenced by our presumption of Red Snapper densities; thus, our sample selection was noninformative.

Predicting Red Snapper Abundance and Associated Variance Propagation - For each Region-DZ-HabType-vertical depth band combination, the PropRS and TFD were predicted from their respective models described above based on the average observed covariates within each stratum combination. These predictions were conditioned on the random effect of Site being centered (i.e., the random intercept was set to zero) thus allowing our estimates to be applicable to the entire population and not just the Sites that were sampled. Conditioning estimated responses on null random effects versus integrating across random effects is recommended when broad inference to the entire

population is desired (Lee and Nelder 2004; Muff et al. 2016). This practice is termed "broad conditional inference" by Stroup (2013) and yields predictions that are medians of the marginal distribution.

Density of Red Snapper (per m^3) was then predicted as the product of their *PropRS* predictions from the binomial model output based on SRV data and the *TFD* predictions from the Tweedie model output based on hydroacoustic data. The arithmetic variance of *TFD* was given by the method of moments estimator:

$$Var[TFD] = e^{2\mu+\sigma^2}\left(e^{\sigma^2} - 1\right) \quad (1)$$

where, μ and σ were the respective prediction and its associated standard error (SE) in log space (i.e., on the link scale). Variances from *TFD* and *PropRS* were then combined using Goodman's (1960) variance of products estimator:

$$Var[PropRS * TFD] =$$

$$PropRS^2 Var[TFD] + TFD^2 Var[PropRS] - Var[TFD] * ar[PropRS] \quad (2)$$

Interpretation of the standard errors output from our models is atypical as described by Simpson (2018) and Wood (2022). The confidence intervals output from the GAMMs and the standard errors on which they are based would normally be considered pointwise from a traditional frequentist interpretation. For a typical regression model, that means that the expected coverage probability would only apply to the single points observed along the trend. However, because the standard errors were derived from the Bayesian posterior covariance matrix for the estimated model parameters, the traditional frequentist interpretation does not apply. Instead, the intervals produced are Bayesian credible intervals that have good "across-the-function" coverage. As Simpson (2018) and Wood (2022) describes it, this means that when averaged across the range of the function, interval coverage comes close to what is expected. However, this coverage may be more or less than the expected coverage for some parts of the function.

Red Snapper per m^3 was converted to per m^2 via multiplication by the average width of each vertical depth band for each stratum combination and summed across bands with the variances expanded and summed accordingly. Then, total Red Snapper abundance for each *HabType* was estimated by extrapolation based on the total area or number of structures within each *Region-DZ* combination. For natural banks and UCB, the total areas of these habitats were used as multipliers. For platforms and artificial reefs the respective total number of structures were the multiplied by the predicted number of Red Snapper per respective structure. Red Snapper per structure was estimated by assuming the average area covered at a sampling site subsumed all Red Snapper present at a typical *Site*. These areas were 62,500 m^2 for artificial reefs and 42,000 m^2 for platforms (equates to a sampling radius of about 115 m from the center). Again, variance estimates for Red Snapper abundance were propagated through all extrapolations.

4.4 Mark/Recapture Population Estimates

The purpose of the mark/recapture studies was to obtain an independent evaluation of the population estimates for Red Snapper that were derived from hydroacoustic and camera surveys. The mark-recapture population estimates for each site were made using the sequential Bayes algorithm described by Gazey and Staley (1986). We selected this method rather than the traditional Petersen approach as modified by Chapman (1951) and Bailey (1951). While the traditional methodologies perform well if large samples are obtained relative to the population level, they have difficulty when the sample size is small (see Corwack 1968). Ricker (1975) and others have pointed out that a pronounced negative bias will occur if the combination of the number of animals marked, and the total number later examined for marks falls too low.

Gazey and Staley (1986) addressed the problems associated with small sample sizes using a sequential Bayes algorithm. While the approach is intensive in computation, the advent of cheap, universally-available computing power has made the algorithm both tractable and convenient. The method requires that one first sets the smallest feasible population size (must be at least equal to the number of animals marked); then provide a feasible upper bound to the population which can be finitely large; and lastly, establish K (the number of discrete population levels to be considered within the range of possible population sizes). The Gazey and Staley (1986) Bayes' method can be applied to both single-census type estimates (e.g., Petersen method) as well as to multiple-census type estimates without replacement (e.g., Schnable-type estimates as described by Ricker 1975).

The only known data are M (the marked animals at large), C (the total number of individuals caught in the recapture event) and R (number of recaptures in sample C). Equation 2 of Gazey and Staley (1986) allows calculation of the probability of observing all the R's given some population level N (the sampling distribution); and their Equation 3 calculates a "noninformative" discrete uniform distribution called the prior distribution. The sampling and prior distributions are combined to form the posterior distributions (probability of each N given the data) by using the Bayes' algorithm (Equation 4 from Gazey and Staley 1986). Gazey and Staley (1986) also provide a simple algorithm for computation of the posterior distribution and statistics of interest.

Growth and Condition

Growth was modeled for observed TL (cm) with the 3-parameter Von Bertalanffy growth equation:

$$TL_t = L_\infty (1-e^{-K(t- t_\theta)}) \qquad (3)$$

where, TL_t = TL at age t, L_∞ = TL asymptote, K = growth coefficient, t = age in years, t_θ = age at length = 0. Individual weight (*Wt* in kg) for Red Snapper was related to total length (*TL* in mm) as per Anderson and Neumann (1996) using the power function ($Wt=aTL^b$) to assess condition.

5.0 Results

All *Sites* were successfully sampled as planned (Appendix 4) and analysis of all hydroacoustic, SRV, TV, age and mark/recapture samples was completed by the end of April 2021 (Appendix 5). Following the removal of pipeline crossing *Sites*, the removal of a single platform *Site* that was too close to artificial reef *Sites*, the pooling of other *Sites* of like *HabType* that were <400 m apart, and the addition of platform *Sites* from the BOEM study (Gallaway et al. 2021) the final number of *Sites* used for statistical modeling of *TFD* was 113; multiple depth bands at most *Sites* rendered 533 total observations. After the same data restructuring, modeling the *PropRS* included 283 observations across 78 sites for which 37,885 fish were observed (1,935 were Red Snapper) with the SRV sampling.

5.1 PropRS and TFD Model Diagnostics and Verification with Mark/Recapture Estimates

The final parameterized GAMMs used to predict the *PropRS* and *TFD* included all factors defining the strata (*Region*, *DZ*, and *HabType*), smooths for the covariates *Salinity* and *DO*, and smooth-factor interactions between *MFB* and *HabType*. In addition, the intercepts were allowed to vary randomly across *Sites*. The partial effects of these terms with 95% credible intervals can be found in Appendix Figures A6.6 and A7.6. Model diagnostics indicate no major cause for concern that could have arose from improperly assumed distributions, link functions, overdispersion, zero inflation, term misspecifications, or over-parameterization (Appendices 6 and 7).

Including data from Gallaway et. al. (2021), 11 mark/recapture *Sites* were available for comparison with our *PropRS-TFD* model predictions (Table 5) in the mid *DZ* (25-45 m). The differences between the two estimation approaches were biologically negligible and relatively small against the background of their collective uncertainties. In pairwise comparisons between M/R estimates and the corresponding *PropRS-TFD* model predictions by *Region*, 95% CIs always overlapped for both platforms and artificial reefs. The maximum of the two estimates divided by the minimum ranged from about one to three, well within an order of magnitude of each other. Overall, these comparisons combined with the model diagnostic results demonstrate that the *PropRS-TFD* model predictions from this study are a good first approximation of Red Snapper total abundance for Louisiana and adjacent federal waters.

5.2 Predicted Red Snapper Abundance

Subsequent to combining model outputs, predicted Red Snapper densities per 100 m^2 are shown as a function of all combinations of fixed effect terms in Figure 19. While the magnitudes and shapes of their vertical gradients fluctuate to some extent among strata, these results generally show Red Snapper densities to decline exponentially towards the surface from a peak at about 5-15 m from the bottom.

The overall estimate of total Red Snapper abundance came to about 8.4 million, with the 95% credible limits ranging from about 6.4 to 11.0 million (Table 6). The exact estimate (8,377,591) had a SE of 1,179,981 and a corresponding CV of 14%. We report Red Snapper density per 100 m^2 across all strata so that relative densities can be compared. While standing platforms and artificial reefs yielded greater densities, the distribution of total abundance is quite different once extrapolated by their respective structure counts (platforms and artificial reefs) or areas (km^2 for natural banks and uncharacterized bottom). Most of this abundance occurred over uncharacterized bottom (89%), followed by standing platforms (9%), natural banks (1%), and artificial reefs (1%). Within *HabType*, densities were more or less evenly distributed across *Regions* for natural banks and artificial reefs; UCB exhibited higher densities in the east, while lower densities occurred in the east for platforms. Across most *Regions* and *HabTypes*, densities were greater in the mid Depth Zone (25-45 m); exceptions were the east *Region* for platforms and the central *Region* for UCB.

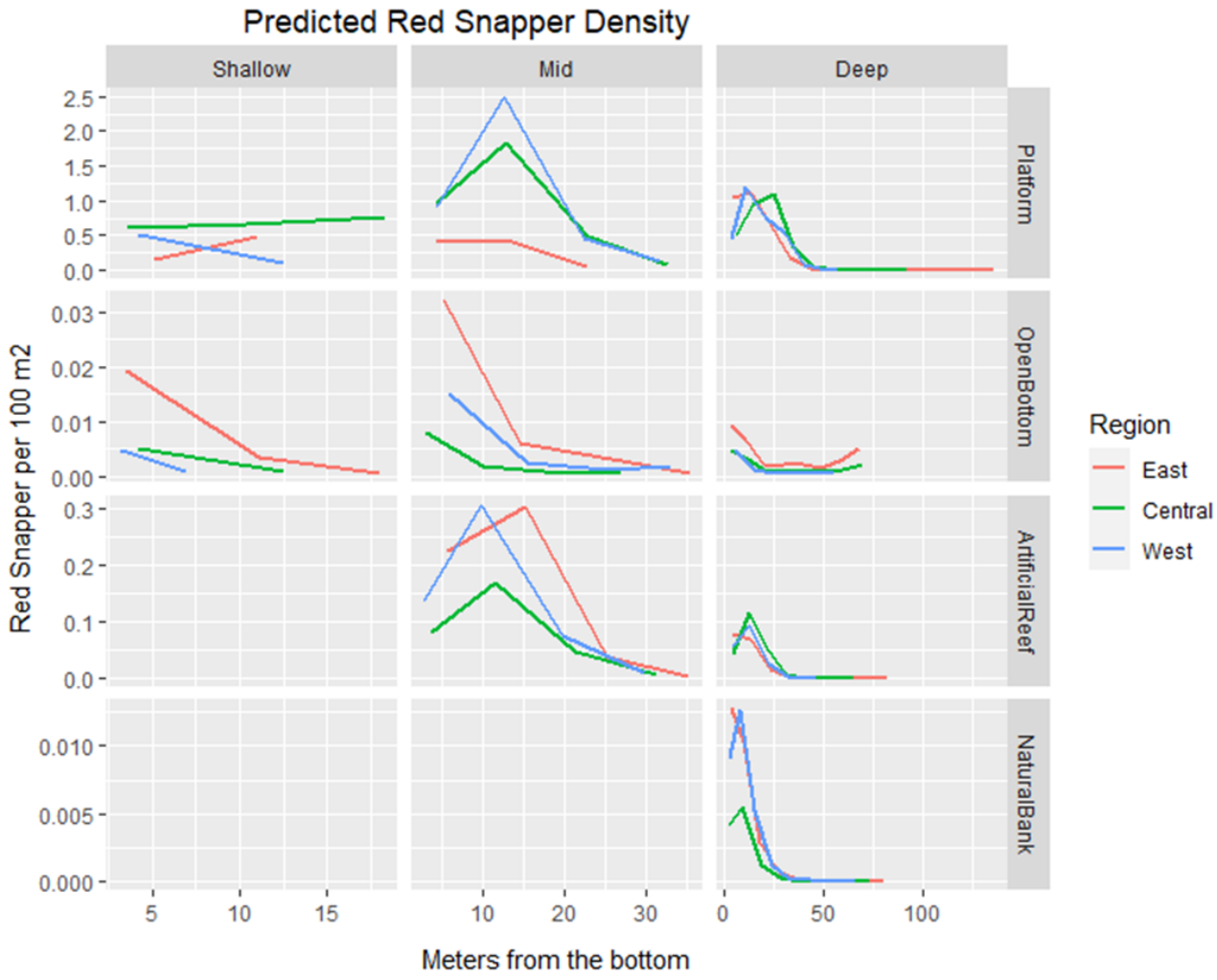

Figure 19. Predicted Red Snapper density for all combinations of fixed effects included in the combined GAMMs for the responses *PropRS* and *TFD*. The continuous variables *Salinity* and *DO* were held at the observed averages for each factor combination. Predictions were conditioned on the random intercept term for *Site* fixed at zero.

Table 5. Red Snapper population estimates and corresponding information based on mark/recapture studies (M/R; left of the thick vertical lines) and modeled output from hydroacoustic-submerged rotating video surveys (hydro-SRV; right of the thick vertical lines). M, C, and R represent the number of fish marked, checked for marks, and recaptured, respectively. Sites were pooled across years but separated by Habitat Type and Region for the hydro-SRV estimates. M/R geometric means by Habitat Type-Region combinations, as well as the max est./min est. ratio for each M/R Site are provided to facilitate comparison between the two approaches. All sites occurred in the mid Depth Zone (25-45 m).

				Mark-recapture information											Hydro-SRV information				
Habitat type	Region	Year	Site	Tagging date	Recapture date	Days between sampling	M	C	R	M/R estimate	M/R 95% CI	Geometric mean across M/R estimates	Max est./ min est.	Hydro-SRV estimate	Hydro-SRV 95% CI	Number of sites sampled with hydro-SRV	Earliest hydro-SRV survey month	Latest hydro-SRV survey month
Platform	West	2017	B7	21-Jul	16-Aug	26	30	57	2	854	448-8,695	1,219	1.98	1,689	800-3,565	5	2-Jul	25-Jul
		2020	S3	29-May	14-Jun	16	30	117	2	1740	616-8,818		1.03					
	Central	2017	B9	15-May	18-Jul	64	30	55	2	824	430-8,655	830	1.73	1,423	748-2,705	10	26-Jun	31-Jul
			B11	20-Jul	31-Jul	11	64	77	11	412	249-785		3.45					
			B13	17-Jul	14-Aug	28	101	95	18	534	383-926		2.66					
		2018	B47	9-May	2-Aug	85	33	107	3	1,177	631-7,957		1.21					
			B49	8-May	3-Aug	87	67	75	2	2,514	1,216-9,519		1.77					
		2020	S7	28-May	16-Jun	19	28	89	4	609	223-2,894		2.34					
	East	2020	S8	21-May	17-Jun	29	4	35	0	-	-	-		373	128-1,089	2	4-Sep	4-Sep
Artificial reef	West	2020	S13	8-May	3-Aug	16	45	45	3	827	269-5,491	827	2.03	408	238-698	1	29-May	29-May
	Central	2020	S17	28-May	16-Jun	19	31	81	4	608	221-2,891	608	2.61	233	134-404	1	2-Jul	2-Jul
	East	2020	S26	21-May	18-Jun	28	16	58	1	902	244-9,051	902	2.05	440	236-819	2	4-Sep	4-Sep

Table 6. Predicted Red Snapper densities and total abundances by habitat type, region, and depth zone (shallow=10-25 m, mid=25-45 m, and deep=45-150 m). Horizontal bars indicate relative magnitude within each habitat type.

Habitat type	Region	Depth zone	Red Snapper per 100 m^2 Mean	LCL	UCL	Red Snapper per km^2 (*) or per structure (**)	LCL	UCL	Area km^2 (*) or structure count (**)	Total abundance	Subtotal (% of overall)	LCL	UCL
Natural Banks*	West	Deep	0.03	0.01	0.06	291	134	634	180	52,393	118,647	66,390	212,036
	Central		0.01	0.00	0.03	115	47	279	521	59,923	(1%)		
	East		0.03	0.01	0.08	272	95	783	23	6,331			
Platforms**	West	Shallow	0.61	0.19	1.92	257	81	811	62	15,911	727,210	545,780	968,953
		Mid	4.00	1.89	8.44	1,689	800	3,565	25	42,226	(9%)		
		Deep	3.07	1.81	5.23	1,299	763	2,210	52	67,528			
	Central	Shallow	2.04	0.88	4.74	861	370	2,002	118	101,624			
		Mid	3.37	1.77	6.40	1,423	748	2,705	133	189,220			
		Deep	2.95	1.76	4.94	1,247	744	2,088	117	145,852			
	East	Shallow	0.64	0.17	2.38	268	72	1,005	182	48,854			
		Mid	0.88	0.30	2.58	373	128	1,089	58	21,615			
		Deep	3.02	1.38	6.60	1,275	583	2,790	74	94,381			
Artificial reefs**	West	Mid	0.53	0.21	1.36	408	238	698	5	2,038	86,954	67,068	112,737
		Deep	0.18	0.08	0.39	135	85	213	121	16,329	(1%)		
	Central	Mid	0.30	0.11	0.79	233	134	404	35	8,144			
		Deep	0.22	0.10	0.50	170	108	269	160	27,279			
	East	Mid	0.57	0.19	1.68	440	236	819	57	25,056			
		Deep	0.16	0.06	0.42	127	74	218	64	8,109			
UCB*	West	Shallow	0.01	0.00	0.02	56	15	218	10,268	579,014	7,444,780	5,440,478	10,187,477
		Mid	0.02	0.01	0.05	207	90	479	5,297	1,096,405	(89%)		
		Deep	0.01	0.00	0.02	84	46	153	7,162	599,056			
	Central	Shallow	0.01	0.00	0.03	62	14	267	4,407	271,732			
		Mid	0.01	0.00	0.03	112	40	314	3,760	420,083			
		Deep	0.01	0.01	0.03	149	85	261	7,511	1,120,980			
	East	Shallow	0.02	0.01	0.08	234	69	799	3,058	716,409			
		Mid	0.04	0.02	0.11	420	156	1,130	2,327	978,324			
		Deep	0.03	0.02	0.05	319	185	550	5,213	1,662,776			
											8,377,591	6,365,225	11,026,166

5.3 Length, Age, Growth, and Condition

In all, 1,152 fish were aged from otolith cross sections and used in the growth model after removal of outliers. Red Snapper at natural banks typically included large fish with a mostly uniform distribution between 475 mm and 690 mm TL; ages were unimodal ranging from 4 to 9 years with a mode at age 8 (Figure 20). On platforms, Red Snapper exhibited a wide length range, 270 mm TL to 770 mm TL, and most of these fish were 3 and 8 years in age (Figure 21). Likewise, a broad range of sizes were observed at artificial reefs (300-740 mm), but were less uniformly distributed with a distinct mode at about 450 mm. The age range at artificial reefs was similar to that of platforms but less uniform with a modal age of 4 years (Figure 22). Of all habitat types, the largest and oldest distributions of Red Snapper were observed for UCB. Most fish were between 600 and 800 mm (mode ≈ 725 mm), and while ages 4-8 years were the most frequent, UCB had more fish ages 10–16 years than any other habitat type (Figure 23). Hydroacoustic and SRV data were not used from the pipeline crossing sites; however, we report the length and age data because of the interesting distribution (Figure 24). The length distribution was bimodal (modes = 425 mm and 650 mm) and appears similar to a distribution that would result from combining those from platforms, artificial reefs, and UCB. The age distribution was mostly 3 to 8 years, similar to platforms and artificial reefs but with a few more fish age-10 and older.

Our Von Bertalanffy growth curve (Figure 25) across all sites was lower than that reported in SEDAR 52 (2018), while the weight-length relationships were indistinguishable (Figure 26). There were no apparent biologically significant differences in weight-length relationships across regions (Figure 27), habitat types (Figures 28 and 29), or regions for UCB (Figure 30).

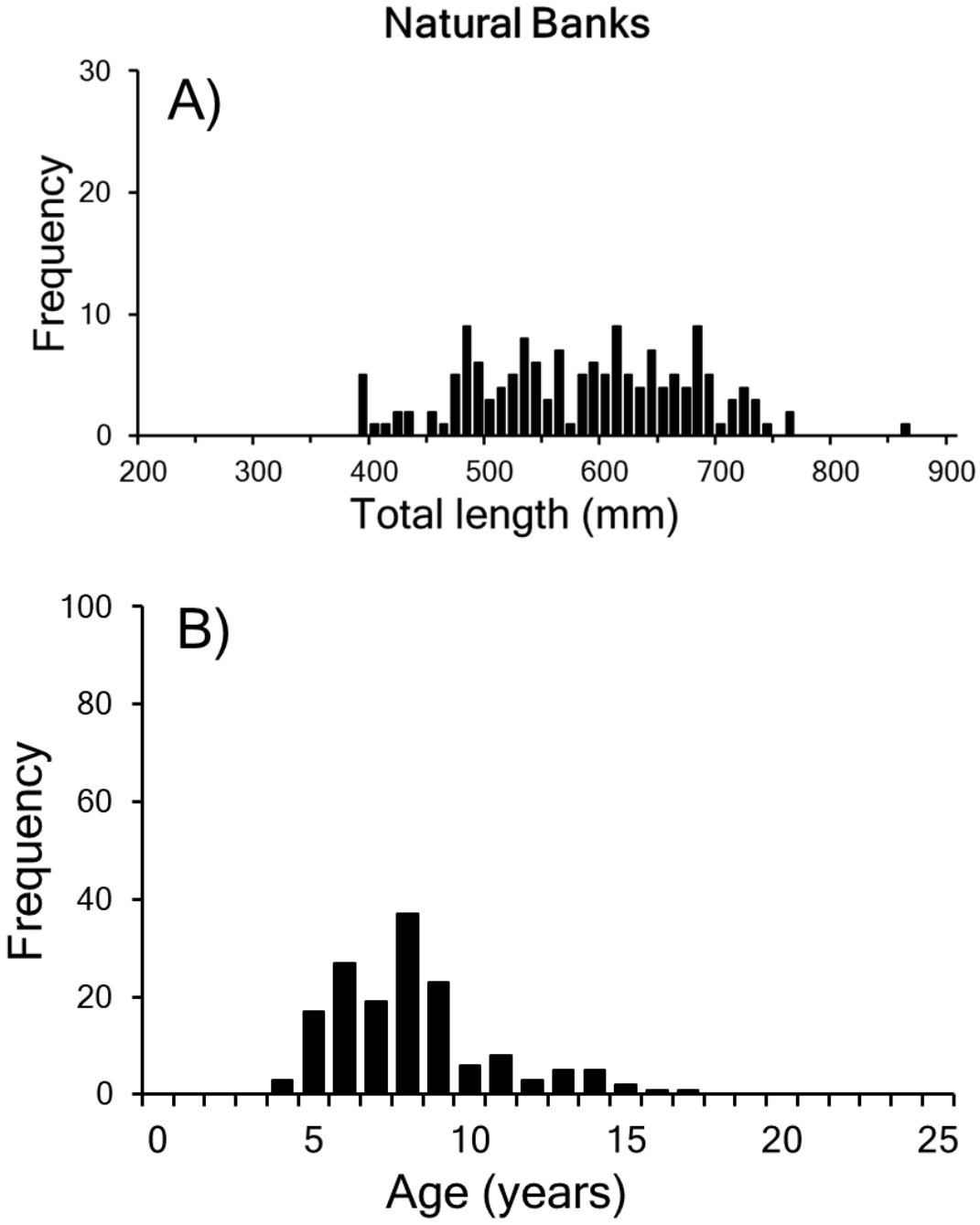

Figure 20. (A) Length and (B) age frequency of Red Snapper on natural banks within the study area 2020.

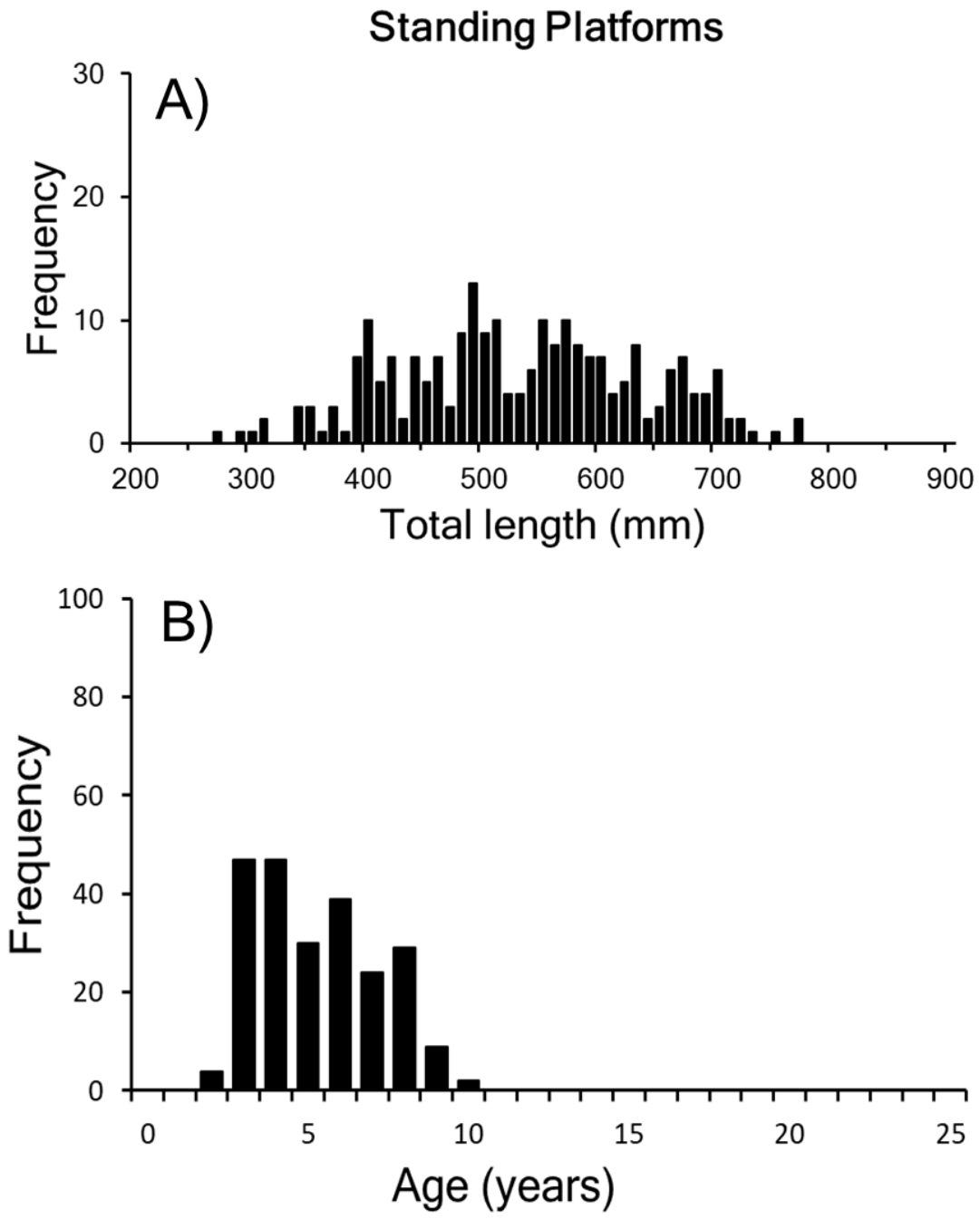

Figure 21. (A) Length and (B) age frequency of Red Snapper on offshore oil and gas platforms within the study area 2020.

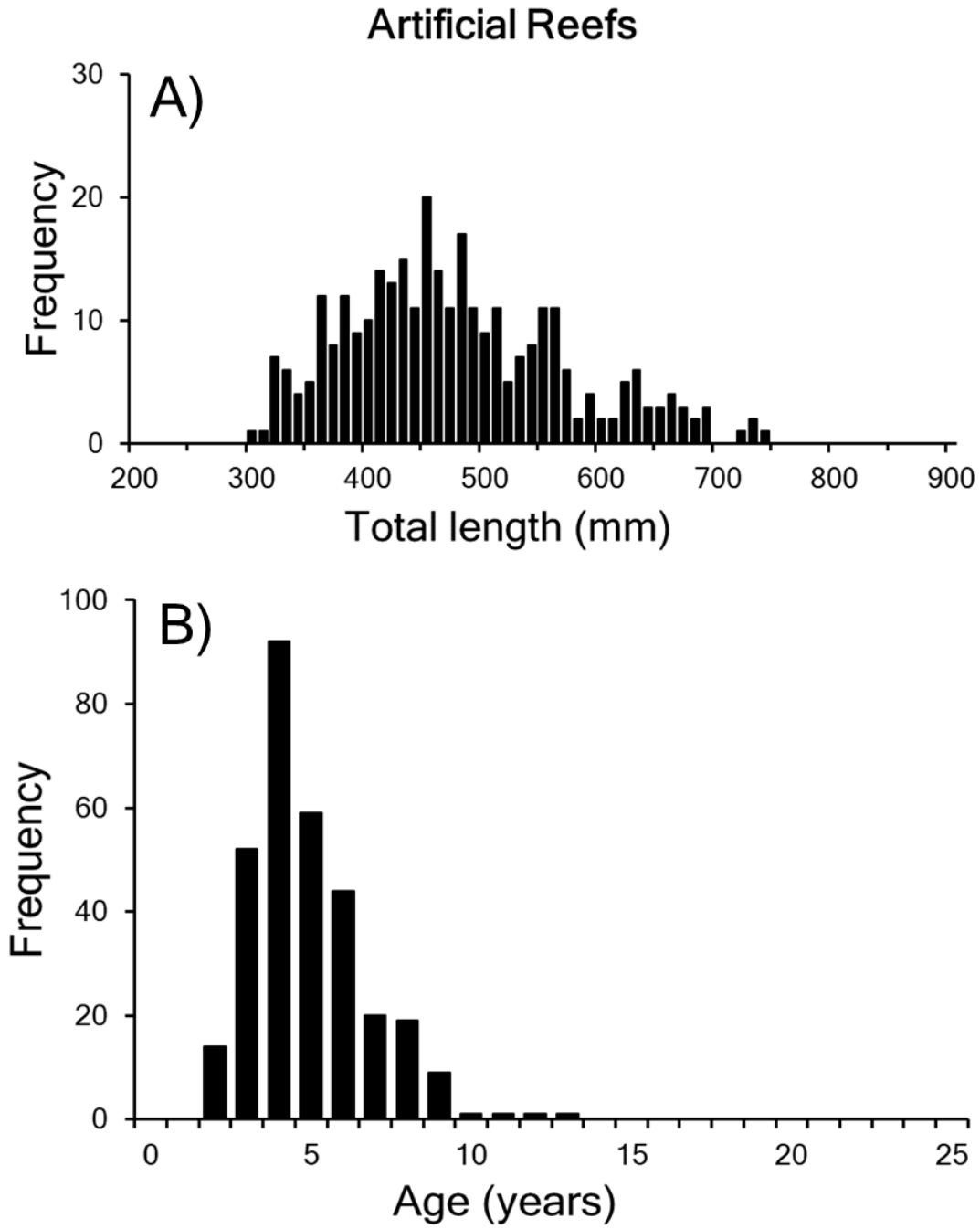

Figure 22. (A) Length and (B) age Frequency of Red Snapper on artificial reefs within the study area 2020.

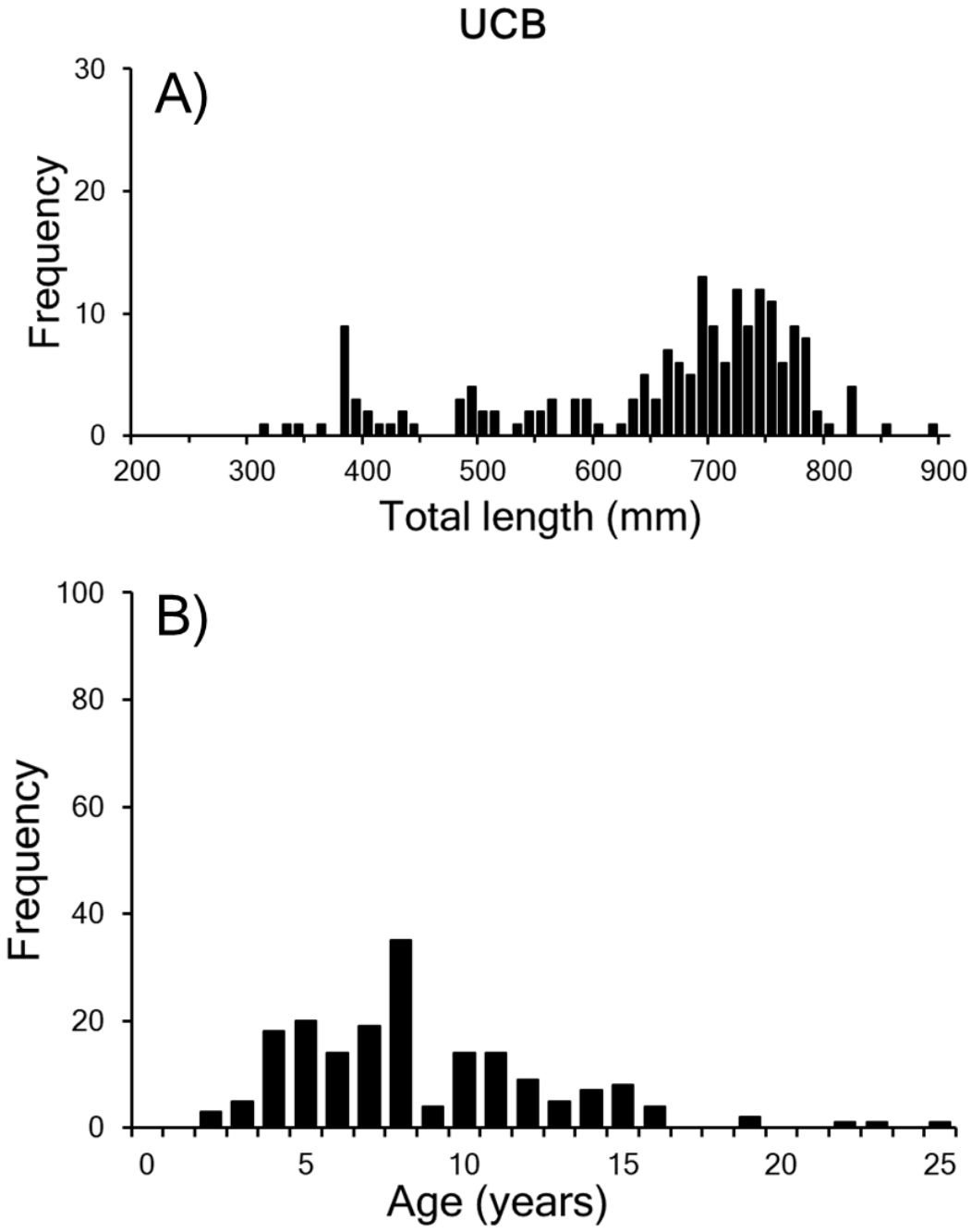

Figure 23. (A) Length and (B) age frequency of Red Snapper on UCB within the study area 2020.

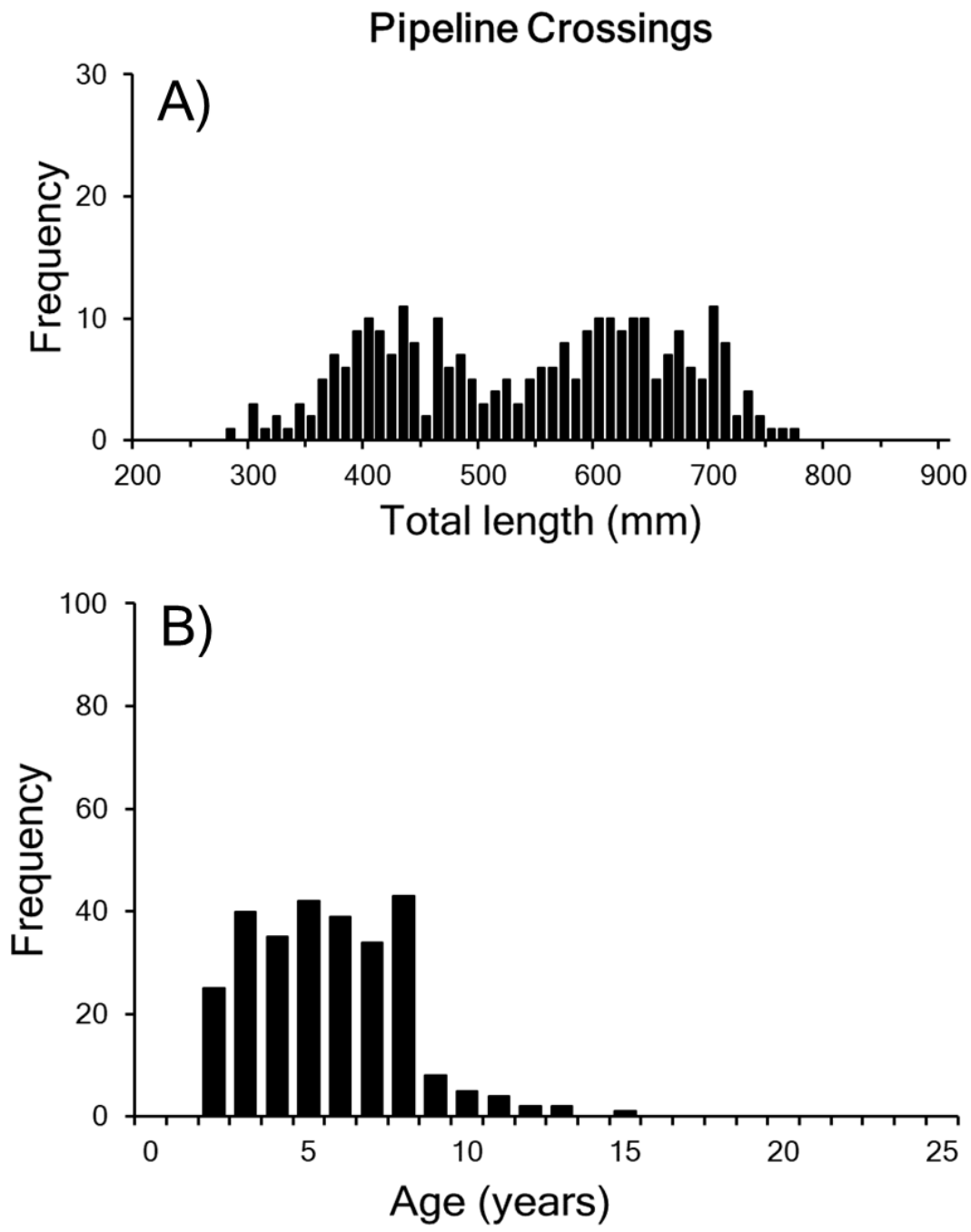

Figure 24. (A) Length and (B) age frequency of Red Snapper on pipeline crossings, within the study area 2020.

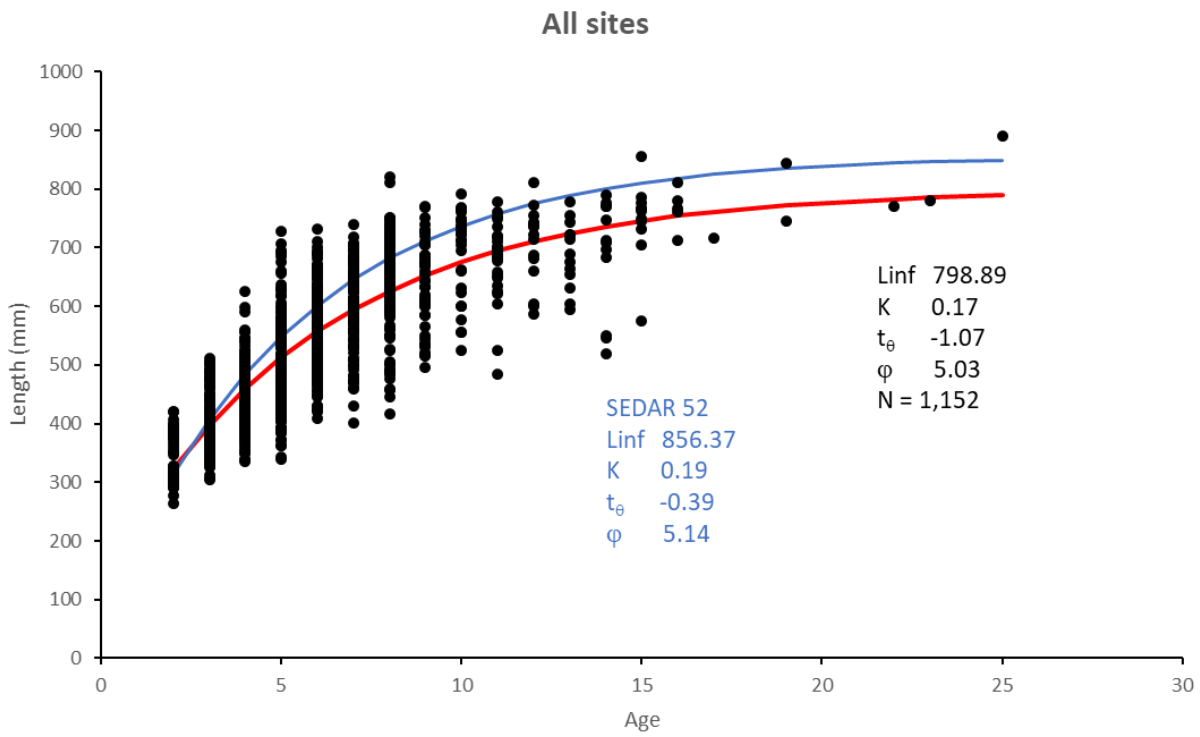

Figure 25. Von Bertalanffy growth curves for all sites within the study area (3 outliers removed, red line) and the most recent stock assessment, SEDAR 52 (blue curve).

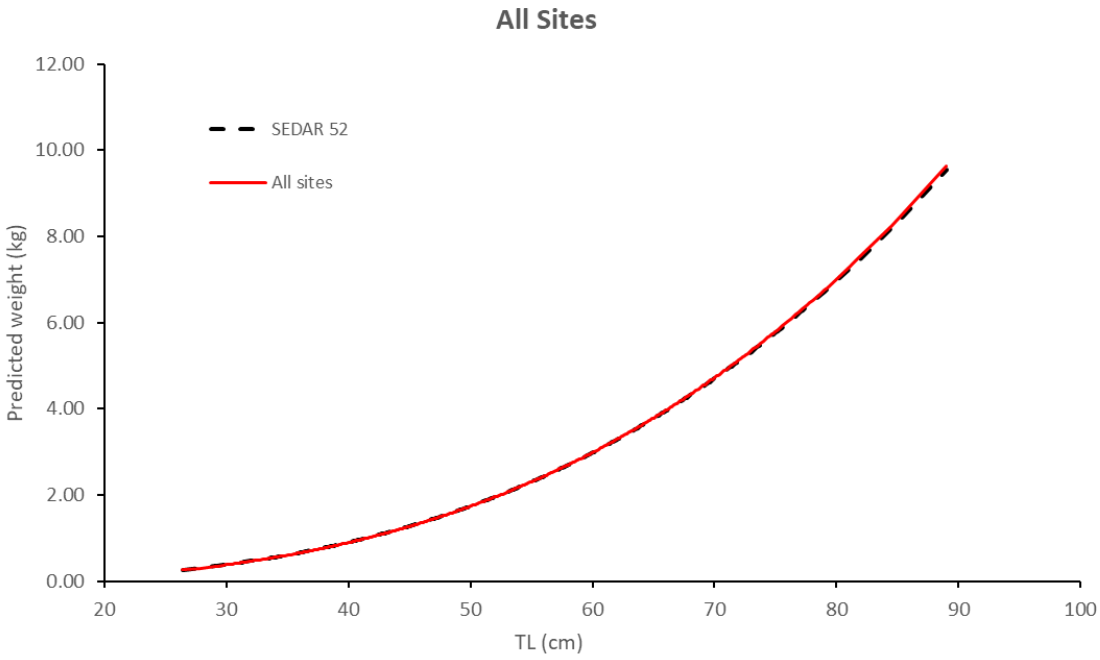

Figure 26. Predicted mean weight (kg) as a function of TL (cm) for all sites between the current study and SEDAR 52.

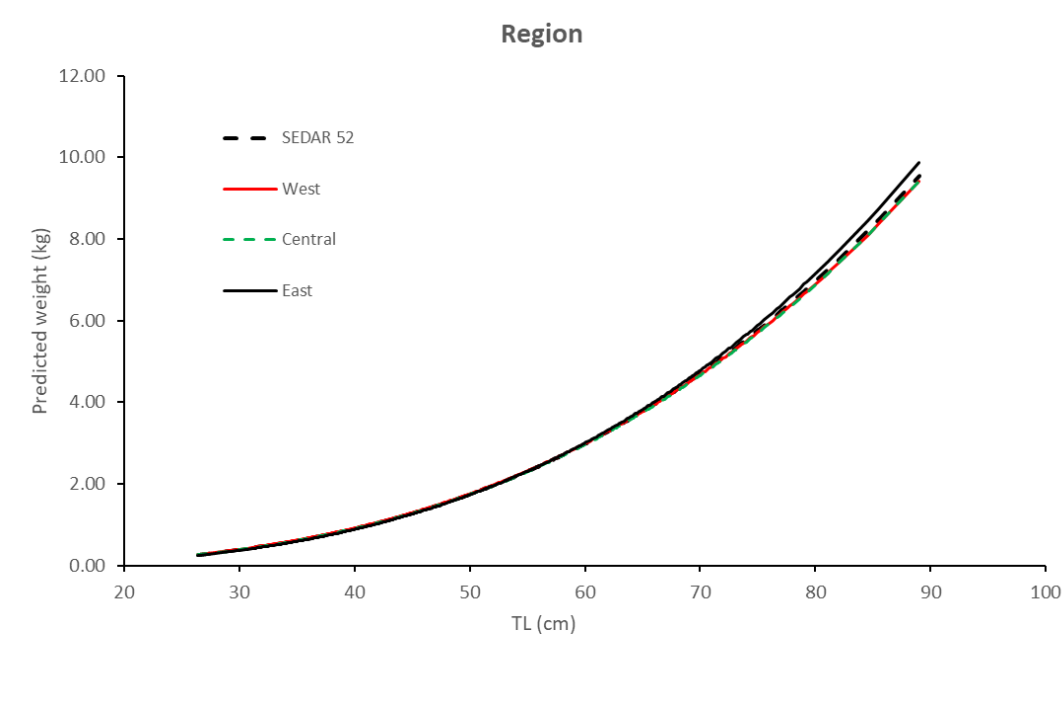

Figure 27. Predicted mean weight (kg) as a function of TL (cm) by geographic region between the current study and SEDAR 52.

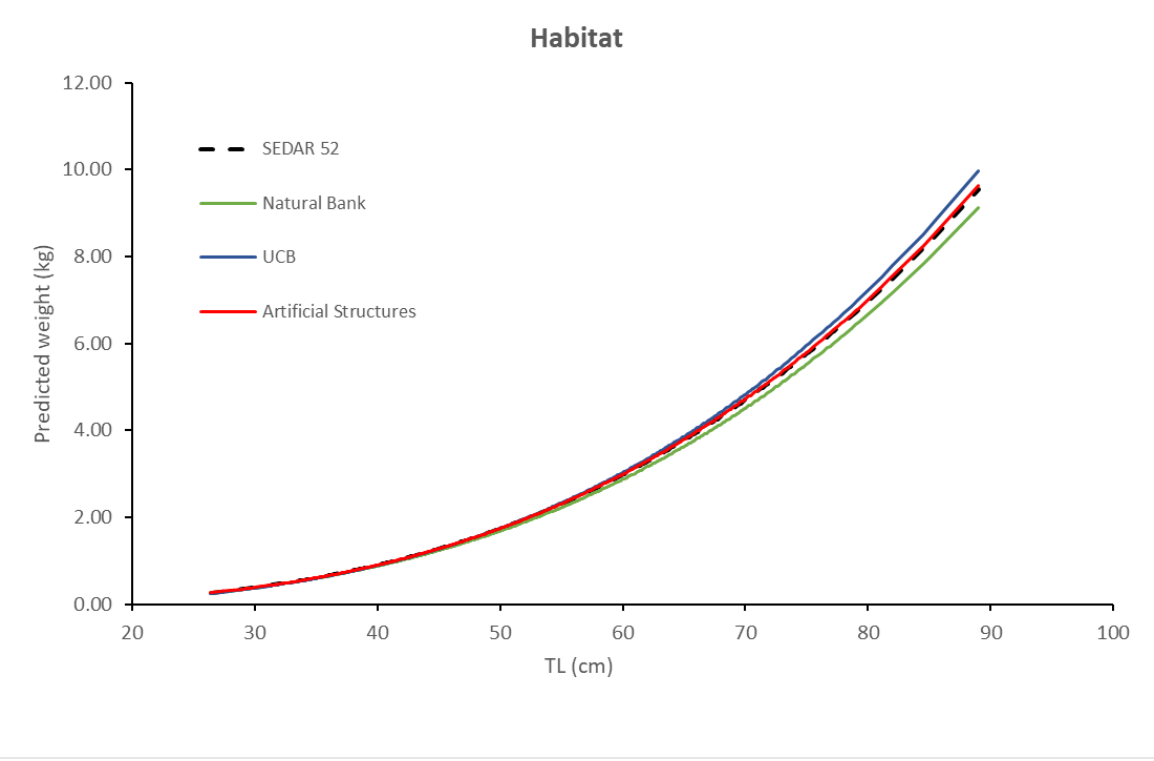

Figure 28. Predicted mean weight (kg) as a function of TL (cm) by habitat (natural banks = green, UCB = blue, artificial structures = red). Data from SEDAR 52 (dashed black line) are plotted for reference.

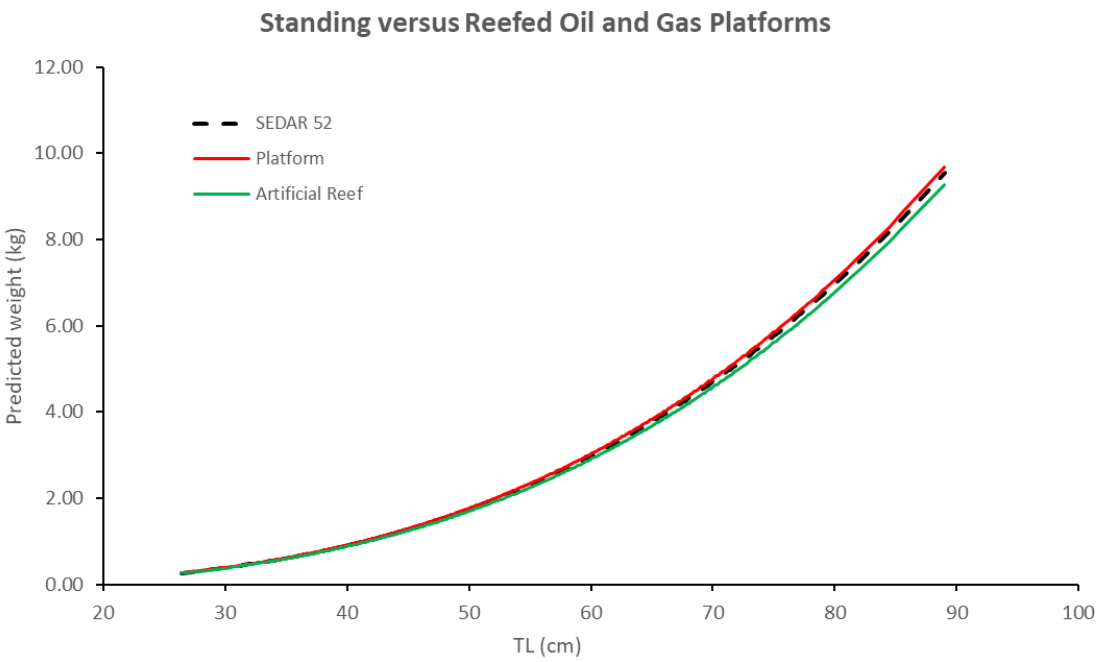

Figure 29. Predicted mean weight (kg) as a function of TL (cm) for standing platforms (red), reefed platforms (green) and SEDAR 52 (dashed black).

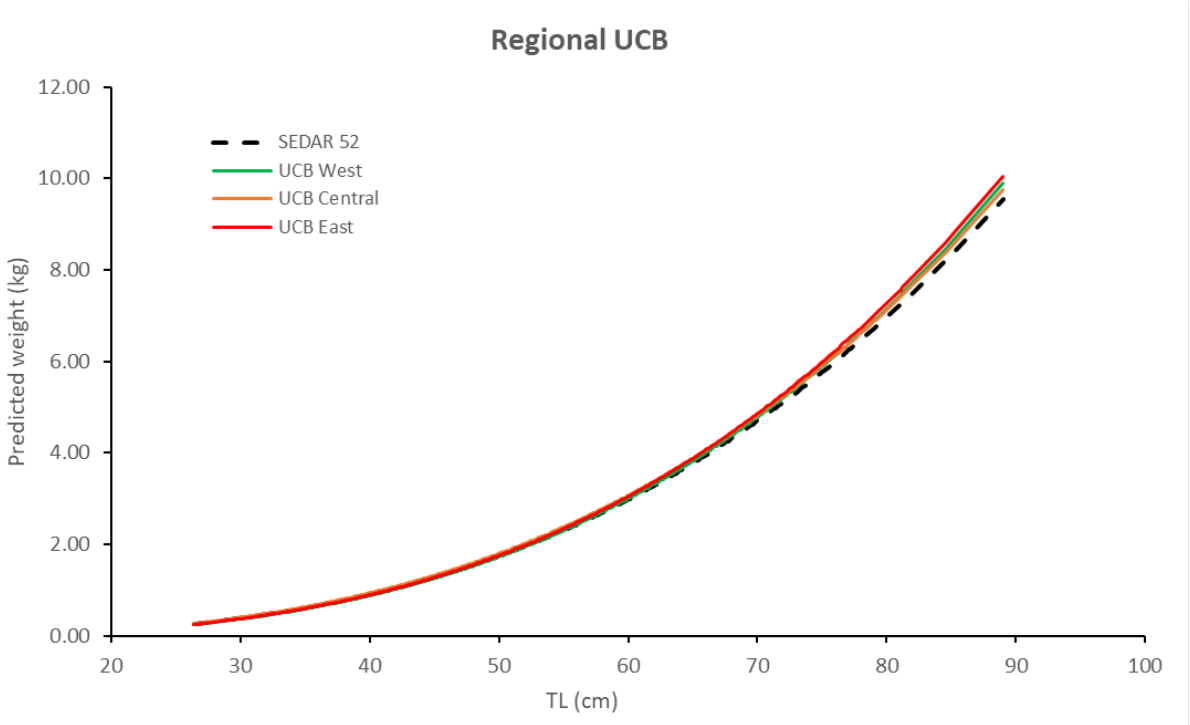

Figure 30. Predicted mean weight (kg) as a function of TL (cm) for UCB by geographic region (green = West, orange = Central, red = East) and SEDAR 52 (black dashed).

6.0 Discussion

As described above, the results of the comprehensive statistical modeling assessment shows that an estimated 8.4 million (95% CI=6.4–11.0 million; SE=1,2 million; CV=13.8%) Red Snapper occupy the Louisiana State Red Snapper Management Area. Numerous different specifications of the statistical model resulted in estimates that ranged between about 4.5 to 10 million Red Snapper; however, the models producing the extremes of this range failed model diagnostics in some way. More reasonable parameterizations fell between 6 and 8 million. These results imply our most defensible estimate of 8.4 million that passed diagnostic scrutiny is robust. Furthermore, the mark/recapture effort was an independent approach that produced comparable stratum specific estimates providing partial verification of our results.

The Stunz et al. (2021b) estimate of ≈18 million is roughly 2.1 times greater than that of the current study; however, their results were extrapolated based on data obtained from eastern Texas because of circumstances that prevented their completion of the originally planned field-sampling for Louisiana. The results of this study were derived from model-based inference of survey data actually collected in Louisiana. The old adage "Essentially all models are wrong, but some are useful" was coined by the statistician George Box. Certainly, some inaccuracies exist in our estimates, as in all studies, but given the preamble of the previous paragraph we argue that our models are useful and provide the best first approximation of Red Snapper total abundance in Louisiana waters.

In Table 7 we isolate the discrepancies between the two studies. The amount of habitat types (areas or structure counts) were similar with the Stunz et al. (2021b) estimates being 1.1 to 1.4 times the LGL estimates. In contrast, the catch rates of Stunz et al. (2021b) were from 1.0 to 20.8 times higher than the corresponding LGL catch rates. Total abundance estimates ranged from 2.1 to 32.5 times higher than the LGL estimates. These differences could be attributed to a number of factors (see Appendix 7 for a comparison of hydroacoustic methods), but as one of the peer reviewers of our initial submission stated: "However, since the Louisiana estimates in LGL are based solely on sampling in Louisiana and adjacent Federal Waters, whereas Stunz et al. used extrapolated samples from outside that area, this provides some *prima facie* support for using the LGL results in support of management."

Table 7. A comparison of the differences between Red Snapper estimates in Louisiana from Stunz et al. (2021b) verses this study. LGL pooled estimates of habitat quantities and mean catch rates are reported to facilitate component comparisons to Stunz et al. (2021b) and to illustrate why the total abundance estimates differ; however, the LGL stratified estimates reflect what the model predictions actually produced.

Habitat type		Area km^2 (*) or structure count (**)	Stunz/LGL ratio	Mean catch rate	Stunz/LGL ratio	Total abundance (millions)	Stunz/LGL ratio
Natural banks*	Stunz et. al. (2021b)	821	1.1	4,693 /km^2	20.8	3.9	32.5
	LGL pooled	724		226 /km^2			
	LGL stratified					0.1	
Standing platforms & artificial reefs**	Stunz et. al. (2021b)	1,771	1.4	2,174 /structure	3.2	3.9	4.7
	LGL pooled	1,263		680 /structure			
	LGL stratified					0.8	
UCB*	Stunz et. al. (2021b)	53,052	1.1	183 /km^2	1.0	9.7	1.3
	LGL pooled	49,003		183 /km^2			
	LGL stratified					7.4	
Overall	Stunz					17.4	2.1
	LGL pooled						
	LGL stratified					8.4	

6.1 Pertinent Fishery Metrics

Average total length (inches), individual weight (lbs.), and age are reported by factor levels in Table 8 to make size metrics more relatable for stakeholders and to facilitate extrapolation of total abundance into total biomass for comparisons to fishery reference points. Overall, fish averaged a total length of 21.2 inches, weighed 5.6 lbs. and had an average age of 6.2 years. The largest average sizes were found on UCB habitats (25.6 inches and 9.4 lbs.) and the smallest on artificial reefs (18.5 inches and 3.6 lbs.)

We estimated that Red Snapper abundance on natural banks was 118,647 that constituted a biomass of 716,625 lbs. (Table 9). Abundance and biomass estimates for the 821 platforms remaining in 2020 were 727,210 and 3,686,957 lbs. (5% of the total biomass). These estimates for the 442 artificial reefs were 86,954 and 312,166 lbs.

Of most interest, we estimated that UCB held 7,444,780 of the largest Red Snapper with a combined biomass of 70,055,377 lbs. (94%). Many of these UCB fish were observed to have had fully developed gonads and many showed signs of imminent spawning (Figure 31). Fish in these habitats may represent an unexploited breeding stock. Because the fish are widely dispersed over this area, they are largely unavailable to the vertical line fisheries. The UCB may functionally serve as a large marine protected area for source population of Red Snapper offshore.

The Red Snapper population within the study area was characterized by a wide size and age range, with older, larger fish being common. As a result, the total biomass of Red Snapper within the study area was estimated to be large (74,771,125 lbs.; Table 9). For

reference purposes, the Overfishing Limit (OFL) for Red Snapper for the entire Gulf of Mexico during the period 2016 through 2021 was 15.5 million pounds, roughly 21% of the biomass estimated to occur offshore Louisiana alone (NMFS 2021).

Table 8. Length and weight summary for Louisiana Red Snapper by region, depth and habitat.

Habitat	Avg Length (in)	Avg Weight (lbs)	Avg Age
Overall	21.24	5.58	6.16
West	22.58	6.31	7.22
Central	20.58	5.09	5.52
East	20.01	5.03	5.30
Shallow	19.86	4.83	4.14
Mid	19.94	4.87	5.17
Deep	21.99	6.11	6.74
Shelf	21.87	5.27	8.40
Artificial Reef	18.52	3.59	4.89
Platform	20.71	5.07	5.29
Pipeline Crossing	21.03	5.47	5.60
Natural Bank	22.69	6.04	8.13
UCB	25.57	9.41	8.60

Table 9. Summary of Red Snapper modeled abundance and biomass in Louisiana, 2020.

Habitat type	Mean individual weight (lbs.)	Total abundance	Total biomass (lbs.)
Natural banks	6.04	118,647	716,625
Platforms	5.07	727,210	3,686,957
Artificial reefs	3.59	86,954	312,166
UCB	9.41	7,444,780	70,055,377
	Overall total	8,377,591	74,771,125

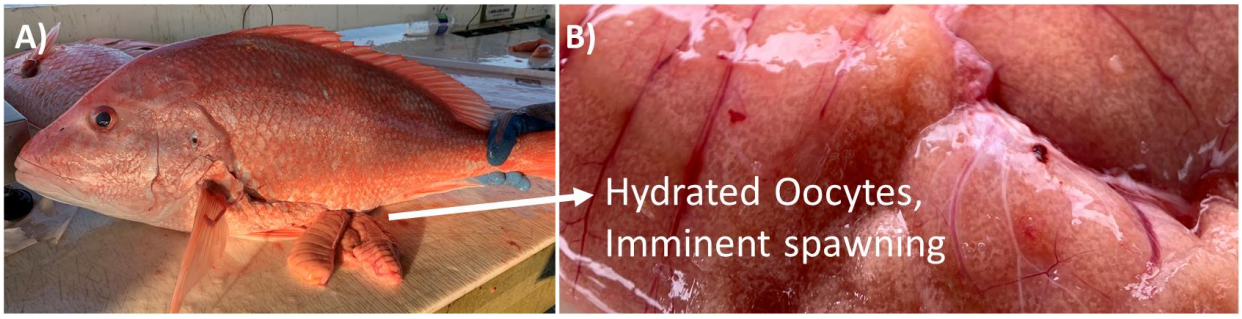

Figure 31. (A) A female Red Snapper collected from the mid-depth area of the East Region. (B) A magnified view of hydrated oocytes of this Red Snapper, indicative that this individual was in spawning condition.

6.2 Impact on stock status

The Stunz et al. (2021b) estimate of the absolute abundance of Red Snapper in the Gulf of Mexico was estimated to have been about 118 million fish in 2019 as compared to about 37 million fish estimated to be present by the SEDAR 52 Stock Assessment (SEDAR 2018). SEDAR 52 estimated that 24 million age 2+ Red Snapper were present in the Western Gulf (Texas and Louisiana) as compared to 39 million estimated to be present in the Western Gulf by Stunz et al. (2021b)—about 1.6 times higher. For the East Gulf, Stunz et al. (2021b) estimated 78 Red Snapper were present—6.0 times as many as estimated for the Eastern Gulf by SEDAR 52 (13 million). A graphic comparison of the respective estimates is shown by Figure 32. However, if our Louisiana estimates are combined with the Texas estimates from Stunz et al. (2021), the overall estimate of 30 million Red Snapper in the Western Gulf is closer to the SEDAR 52 estimate of 24 million.

The size differences for Red Snapper in the Eastern Gulf differ greatly from the Western Gulf. In Florida, most of the Red Snapper are small; 62% of the fish appear to be below the legal-size limit of 16 in. In Louisiana, a wide size range was evident in 2020 with 87% of the fish being above the legal-size limit (Figure 33).

The size/age distributions for Red Snapper observed in Louisiana suggest that approximately 8.4 million age 2+ Red Snapper are present in the Louisiana Recreational Red Snapper Management Area and have a very high biomass, on the order of 74.8 million lbs. To put this in perspective, the most recent recreational Red Snapper fishery quota for Louisiana was 784,332 lbs., which is about 1.0% of the biomass in 2020 estimated from this study. Platforms alone, the most heavily fished habitat in Louisiana, were estimated to harbor about 3.7 million pounds of Red Snapper. Further, 70.0 million pounds of Red Snapper were estimated to occur over UCB habitats, and these fish appear largely unexploited.

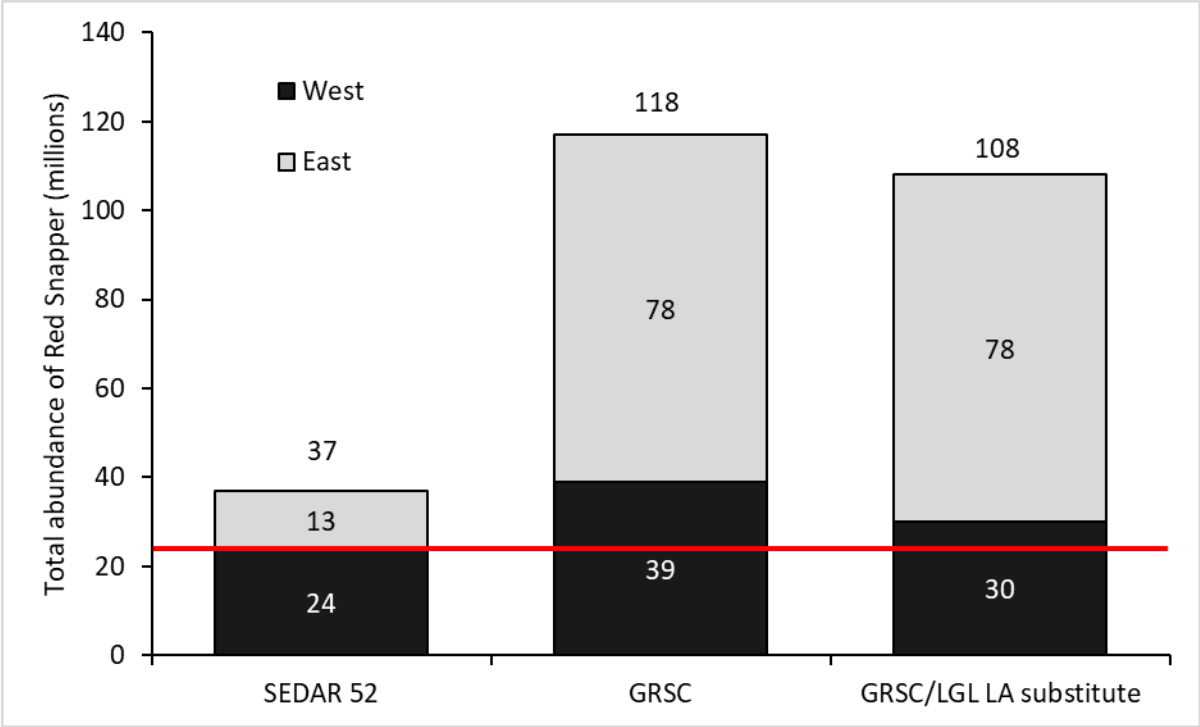

Figure 32. Population estimates for Red Snapper in the Gulf of Mexico based on the SEDAR 52 stock assessment, Stunz et al. (2021b), and this study. Total abundance values for each study are given at the top of each column; regional values are centered within each series. The horizontal red line is shown to facilitate comparison with the SEDAR 52 estimate for the West region.

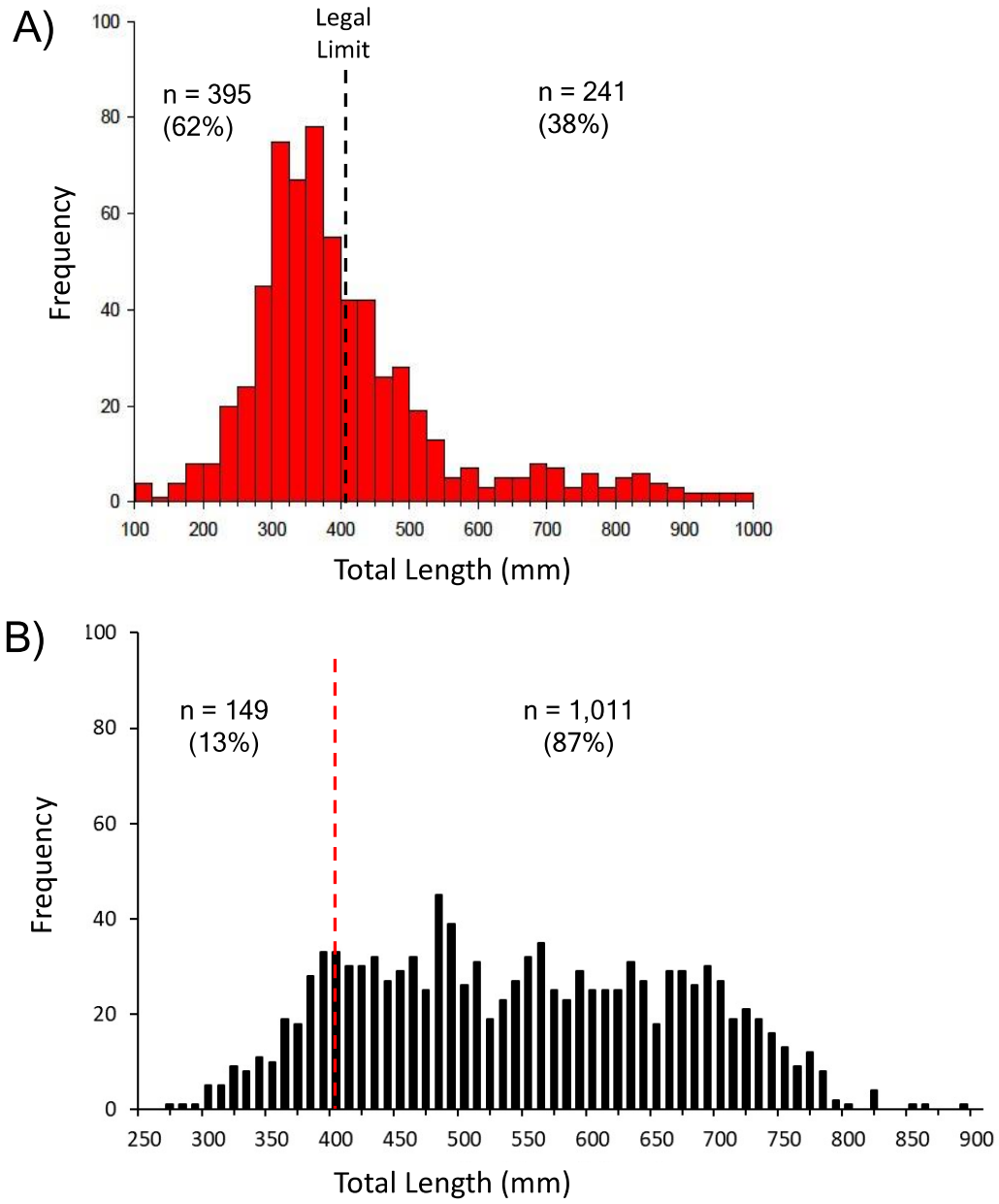

Figure 33. Red Snapper in the Louisiana study area had a higher percentage of legal sized fish than those from Florida. (A) Red Snapper from Florida sampling sites (n = 637) illustrates that only 38% were of legal size (16 inches) (adapted from Figure 6 in Stunz et al. 2021). (B) Length frequency of all Red Snapper from Louisiana measured directly in this study (n = 1160) showing that 87% were above the legal size.

7.0 Acknowledgments

Funding for this study was provided by Louisiana Department of Wildlife and Fisheries (LDWF) through Contract with LGL Ecological Research Associates, Inc. (LGL) (Purchase Order No. 2000461788). We especially acknowledge Dr. Steve Szedlmayer and Dr. Pete Mudrak, Auburn University for completing hydroacoustic surveys on uncharacterized bottom and for mark/recapture work on reefed and standing platforms.

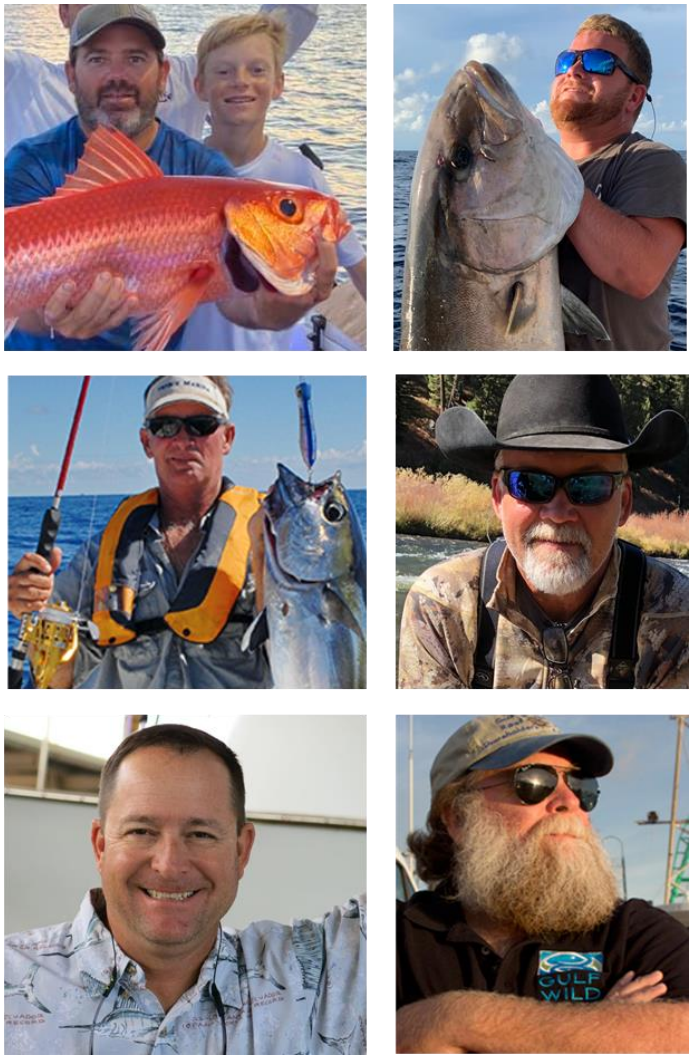

The results of this study are based on data gathered at 100% of the 106 intended sampling sites during summer 2020, despite a historic hurricane season and various restrictions from COVID-19. Our success is due in large part to our trusted captains (clockwise from top left): Jamie Gaspard, Hans Guindon, Mike Jennings, Buddy Guindon, Scott Hickman, and Bill Butler.

8.0 Literature Cited

Algen, A. 1989. Empirical results on precision-effort relationships for acoustic surveys. International Council for the Exploration of the Sea. C.M. 1989/B:30. 28 p.

Algorithm for the Identification of Sandeel School Echotraces. ICES CM2004/R:12, pp. 1-13. http://www.ices.dk/sites/pub/CM%20Doccuments/2004/R/R1204.pdf.

Bacheler, N.M. and K.W. Shertzer. 2014. Estimating relative abundance and species richness from video surveys of reef fishes. Fish. Bull. 113(1):15-26. doi: 10.7755/fb.113.1.2.

Bacheler, N.M., C. Schobernd, Z. Schobernd, W.A. Mitchell, D. Berrane, G.T. Kellison, and M.J.M. Reichert. 2013. Comparison of trap and underwater video gears for indexing reef fish presence and abundance in the southeast United States. Fish. Res. 143:81-88. Doi: 10.1016/j.fishres.2013.01.013.

Bailey, N.J.J. 1951. On estimating the size of mobile populations from recapture data. Biometrika 38: 293-306.

Ballón, M., A. Bertrand, A. Lebourges-Dhaussy, M. Gutiérrez, P. Ayón, D. Grados, and F. Gerlotto. 2011. Is there enough zooplankton to feed forage fish populations off Peru? An acoustic (positive) answer. Progress in Oceanography, 91(4), pp.360-381.

Barton, K. 2020. MuMin: Multi-Model Inference. R package version 1.43.17. https://CRAN.R-project.org/package=MuMin.

Bohnsack, J.A., and S.P. Bannerot. 1986. A stationary visual census technique for quantitatively assessing community structure of coral reef fishes. Department of Commerce, National Marine Fisheries Service. NOAA Tech. Rep. NMFS 41. iii + 15 p.

Bolser, D., J. Egerton, A. Grüss, T. Loughran, T. Beyea, K. McCain, B. Erisman. 2020. Environmental and Structural Drivers of Fish Distributions among Petroleum Platforms across the U.S. Gulf of Mexico. Marine and Coastal Fisheries Dynamics Management and Ecosystem Science. 12. 142-163. 10.1002/mcf2.10116.

Boswell, K. M., M. P. Wilson, and C. A. Wilson. 2007. Hydroacoustics as a tool for assessing fish biomass and size distribution associated with discrete shallow-water estuarine habitats in Louisiana. Estuaries and Coasts 30:607-617.

Boswell, K.M., Wells, R.J.D., Cowan Jr., J.H., Wilson, C.A., 2010. Biomass, density, and size distributions of fishes associated with a large-scale artificial reef complex in the Gulf of Mexico. Bull. Mar. Sci. 86, 879-889. http://dx.doi.org/10.5343/bms.2010.1026

Buczkowski, B.J., J.A. Reid, C.J. Jenkins, J.M. Reid, S.J. Williams, and J.G. Flocks. 2006. usSEABED: Gulf of Mexico and Caribbean (Puerto Rico and U.S. Virgin Islands)

offshore surficial sediment data release. U.S. Geological Survey, Data Series 146, version 1.0, Reston, Virginia. Available: http://pubs.usgs.gov/ds/2006/146/

Bureau of Ocean Energy Management. 2018. Geographic Mapping Data in Digital Format [online spatial repository]. Bureau of Ocean Energy Management, Washington, D.C. Available: https://www.data.boem.gov/Main/Mapping.aspx.

Bureau of Ocean Energy Management. 2021. Platform structures online query [onlinedatabase]. Bureau of Ocean Energy Management, Washington, D.C. Available: http://www.data.boem.gov/Platform/PlatformStructures/Default.aspx.

Burnam. K. P., and D. R. Anderson. 2002. Model selection and multimodel inference: a practical information-theoretic approach, 2nd edition. Spinger-Verlag, New York.

Chapman, B.G. 1951. Some Properties of the hypergeometric distribution with applications to zoological sample censuses. University of California Publications in Statistics: 131-160.

Corwack, R.M. 1968. The statistics of capture-recapture methods. Oceanography and Marine Biology. An Annual Review 6: 455-506.

Crawley, M. 2013. The R Book. 2nd edition. Chichester: Wiley.

Dance MA, Rooker JR (2019) Cross-shelf habitat shifts by red snapper (Lutjanus campechanus) in the Gulf of Mexico. PLoS ONE 14(3): e0213506. https://doi.org/10.1371/journal.pone.0213506.

Davies, G. M. and A. Gray. 2015. Don't let spurious accusations of pseudoreplication limitour ability to learn from natural experiments (and other messy kinds of ecological monitoring). Ecology and Evolution 5:5295-5304.

De Robertis, A.D., and I. Higginbotham. 2007. A post-processing technique to estimate the signal-to-noise ratio and remove echosounder background noise. ICES J. Mar. Sci. 64,1282–1291. http://dx.doi.org/10.1093/icesjms/fsm112.

De Robertis, A.D., D. McKelvey, and P. Ressler. 2010. Development and application of an empirical multifrequency method for backscatter classification. Can. J. Fish Aquat.Sci. 67, 1459–1474. http://dx.doi.org/10.1139/F10-075.

Dormann, Carsten & Elith, Jane & Bacher, Sven & Buchmann, Carsten & Carl, Gudrun & Carré, Gabriel & Diekötter, T. & García Márquez, Jaime & Gruber, Bernd & Lafourcade, Bruno & Leitão, Pedro & Münkemüller, Tamara & Mcclean, Colin & Osborne, Patrick & Reineking, Björn & Schröder, Boris & Skidmore, Andrew & Zurell, Damaris & Lautenbach, Sven. (2013). Collinearity: A review of methods to deal with it and a simulation study evaluating their performance. Ecography. 36. 27-46. 10.1111/j.1600-0587.2012.07348.x.

Egerton, J.P., D.G. Bolser, A. Grüss, and B.E. Erisman. 2021. Understanding patterns of fish backscatter, size and density around petroleum platforms of the US Gulf of Mexico using hydroacoustic data. Fisheries Research, 233, p.105752.

Fernandes, P.G. 2009. Classification trees for species identification of fish-school echotraces. – ICES Journal of Marine Science, 66: 1073–1080.

Foote, K.G., H.P. Knudsen, G. Vestnes, D.N. MacLennan, and E.J. Simmonds. Calibration of acoustic instruments for fish-density estimation: a practical guide. 1987. ICES Cooperative Research Report, 44.

Forstmeier, W. and H. Schielzeth. 2011. Cryptic multiple hypotheses testing in linear models: overestimated effect sizes and the winner's curse. Behavioral Ecology and Sociobiology 65:47-55.

Gallaway B.J., S. Raborn, K. McCain, T. Beyea, S. Default, A. Conrad., and K. Kim. 2020. Explosive removal of structures: fisheries impact assessment. New Orleans (LA): US Department of the Interior, Bureau of Ocean Energy Management. Contract No.: M16PC00005. Report No.: OCS Study BOEM 2020-038. 149 p.

Gallaway, B. J. 1981. An ecosystem analysis of oil and gas development on the Texas-Louisiana continental shelf. U.S. Fish and Wildlife Service. Office of Biological Services, Washington, D.C. FWS/OBS-81/27. Pp 89.

Gallaway, B. J. and Lewbel, G. S. 1982. Ecology of petroleum platforms in the northwestern Gulf of Mexico: a community profile. LGL Ecological Research Associates, Inc., Bryan TX (USA). FWS/OBS-82/27.

Gallaway, B.J., Raborn, S.W., McCain, K.A., Beyea, R.T., Dufault, S., Heyman, W., Putman, N.F. and Egerton, J. (2021), Absolute Abundance Estimates for Red Snapper, Greater Amberjack, and Other Federally Managed Fish on Offshore Petroleum Platforms in the Gulf of Mexico. North Am J Fish Manage, 41: 1665-1690. https://doi.org/10.1002/nafm.10678.

Gallaway, B.J., Szedlmayer, S., Gazey, W., 2009. A life history review for red snapper in the Gulf of Mexico with an evaluation of the importance of offshore petroleum platforms and other artificial reefs. Rev. Fish. Sci. 17, 48–67. http://dx.doi.org/10.080/10641260802160717.

Gastauer, S., B. Scoulding, and M. Parsons. 2017. Towards acoustic monitoring of a mixed demersal fishery based on commercial data: the case of the Northern Demersal Scalefish Fishery (Western Australia). Fisheries Research, 195, pp.91-104.

Gavin L. Simpson (2021). gratia: Graceful 'ggplot'-Based Graphics and Other Functions for GAMs Fitted Using 'mgcv'. R package version 0.6.0. https://CRAN.R-project.org/package=gratia

Gazey, W., and M.J. Staley,1986. Population estimation from mark-recapture experiments using a sequential bayes algorithm. Ecology. 67(4), 941-951. doi:10.2307/1939816.

Goodman, L. A. (1960). On the Exact Variance of Products. Journal of the American Statistical Association, 55, 708-713.

Gulf of Mexico Fisheries Management Council. 2019. State management program for recreational Red Snapper final draft amendment 50a to the fishery management plan for the reef fish resources of the Gulf of Mexico including programmatic environmental impact assessment. NOAA. Gulf of Mexico Fishery Management Council, National Oceanic and Atmospheric Administration. 236 pp.

Gulf States Marine Fisheries Commission. 2009. A Practical Handbook for Determining the Ages of Gulf of Mexico Fishes, July 2009. Pub num. 167. NOAA Award No. NA05NMF4070005.

Harrison XA, Donaldson L, Correa-Cano ME, Evans J, Fisher DN, Goodwin CED, Robinson BS, Hodgson DJ, Inger R. 2018. A brief introduction to mixed effects modelling and multi-model inference in ecology. PeerJ 6:e4794 https://doi.org/10.7717/peerj.4794

Hartig, F. (2022). DHARMa: Residual Diagnostics for Hierarchical (Multi-Level / Mixed) Regression Models. R package version 0.4.5. https://CRAN.R-project.org/package=DHARMa

Hurlbert, S. H. 1984. Pseudoreplication and the design ofecological field experiments. Ecol. Monogr. 54:187-211.

Karnauskas, M., J. F. Walter III, M. D. Campbell, A. G. Pollack, J. Marcus Drymon, and S. Powers. 2017. Red Snapper distribution on natural habitats and artificial structures in the Northern Gulf of Mexico. Marine and Coastal Fisheries: Dynamics, Management, and Ecosystem Science 9:50-67.

Kocovsky, P.M., L.G. Rudstam, D.L. Yule, D.M. Warner, T. Schaner, B. Pientka, J.W. Deller, H.A. Waterfield, L.D. Witzel, and P.J. Sullivan. 2013. Sensitivity of fish density estimates to standard analytical procedures applied to Great Lakes hydroacoustic data. Journal of Great Lakes Research, 39(4), pp.655-662.

Koenig, C.C., and C.D. Stallings. 2015. A new compact rotating video system for rapid survey of reef fish populations. Bulletin of Marine Science, 91(3), pp.365-373.

Korneliussen, R.J., Ona, E., 2002. An operational system for processing and visualizing multi-frequency acoustic data. ICES J. Mar. Sci. 59, 293–313. http://dx.doi.org/10.1006/jmsc.2001.1168.

Korneliussen, R.J., Y. Heggelund, I.K. Eliassen, and G.O. Johansen. 2009. Acoustic species identification of schooling fish. ICES J. Mar. Sci. 66, 1111–1118. http://dx.doi.org/10.1093/icesjms/fsp119.

Lee, Y. and J. A. Nelder. 2004. Conditional and marginal models: another view. Statistical Science. 19:219-238.

Lezama-Ochoa, A., M. Ballón, M. Woillez, D. Grados, X. Irigoien, and A. Bertrand. 2011. Spatial patterns and scale-dependent relationships between macrozooplankton and fish in the Bay of Biscay: an acoustic study. Marine Ecology Progress Series, 439, pp.151-168.

LGL Ecological Research Associates, Inc. (LGL). 2020. Estimation of total Red Snapper abundance in Louisiana and adjacent federal waters: proof of concept report for field sampling. LGL Ecological Research Associates, Inc. Bryan, TX. 80 p.

Louisiana Department of Wildlife and Fisheries. 2021. Artificial reefs [online database]. Louisiana Department of Wildlife and Fisheries, Baton Rouge, Louisiana. Available: http://www.wlf.louisiana.gov/page/artificial-reefs.

Love R.H. 1971. Measurements of fish target strength: a review, Fisheries Bulletin, 1971, vol. 69 (pp. 703-715).

MacLennan D.N., and E.J. Simmonds.Fisheries Acoustics, 1992. LondonChapman and Hall 325 pp.

Madureira, L.S., P.P. Ward, and A. Atkinson. 1993. Differences in backscattering strength determined at 120 and 38 kHz for three species of Antarctic macroplankton. Mar.Ecol.Prog. Ser. 93, 17-24. http://dx.doi.org/10.3354/meps093017.

Millar, R. B. and M. J. Anderson. 2004. Remedies for pseudoreplication. Fisheries Research 70:397-407.

Mosteiro, A., P.G. Fernandes, F. Armstrong, and S.P.R. Greenstreet. 2004. A dual frequency algorithm for the identification of sandeel school echotraces. ICES Document CM 2004/R:12. 13pp.

Munro, J.L. and D. Pauly. 1983. A simple method for comparing the growth of fishes and invertebrates. Fishybtes. The WorldFish Center 1(1):5-6.

National Oceanic and Atmospheric Administration Office of Coast Survey. 2021. Wrecks and Obstructions Database [online database]. NOAA Office of Coast Survey, Silver Spring, MD. Available: https://www.nauticalcharts.noaa.gov/data/wrecks-and-obstructions.html.

Ona, E., and R.B. Mitson. 1996. Acoustic sampling and signal processing near the seabed: the deadzone revisited. ICES J Mar Sci; 53, pp. 677-690.

Parker-Stetter, S.L., L.G. Rudstam, P.J. Sullivan, and D.M. Warner. 2009. Standard operating procedures for fisheries acoustic surveys in the Great Lakes, 2009. Great Lakes Fisheries Commission Special Publication, 2009-01.

Pedersen EJ, Miller DL, Simpson GL, Ross N. 2019. Hierarchical generalized additive models in ecology: an introduction with mgcv. PeerJ 7:e6876 https://doi.org/10.7717/peerj.6876

Potts, S. E. and K. A. Rose. 2018. Evaluation of GLM and GAM for estimating population indices from fishery independent surveys. Fisheries Research 208:167-178.

Reynolds, E.M., J.H. Cowan Jr, K.A. Lewis, and K.A. Simonsen. 2018. Method for estimating relative abundance and species composition around oil and gas platforms in the northern Gulf of Mexico, USA. Fisheries Research, 201, pp.44-55.

Ricker, W.E. 1975. Computation and interpretation of biological statistics of fish populations. Bulletin of the Fisheries Research Board of Canada 191: 382 p.

RStudio Team (2022). RStudio: Integrated Development Environment for R. RStudio, PBC, Boston, MA URL http://www.rstudio.com/.

Rudstam, L.G., S.L. Parker-Stetter,P.J. Sullivan, and D.M. Warner. 2009. Towards a standard operating procedure for fishery acoustic surveys in the Laurentian Great Lakes, North America. ICES Journal of Marine Science, 66(6), pp.1391-1397.

Ryan, T.E., R.A. Downie, R.J. Kloser, and G. Keith.2015. Reducing bias due to noise and attenuation in open-ocean echo integration data. ICES Journal of Marine Science, 72(8), pp.2482-2493.

Sawada K., M. Furusawa, and N.J. Williamson. 1993. Conditions for the precise measurement of fish target strength in situ, Journal of the Marine Acoustics Society of Japan, 1993, vol. 20 (pg. 73-79).

Schobernd Z.H., N.M. Bacheler, and P.B. Conn. 2014. Examining the utility of alternative video monitoring metrics for indexing reef fish abundance. Can J Fish Aquat Sci. 71(3):464-471.

Schultz AL, Malcolm HA, Bucher DJ, Smith SDA (2012) Effects of Reef Proximity on the Structure of Fish Assemblages of Unconsolidated Substrata. PLoS ONE 7(11): e49437. https://doi.org/10.1371/journal.pone.0049437

Scott, Molly & Smith, James & Lowry, Michael & Taylor, Matthew & Suthers, Iain. (2015). The influence of an offshore artificial reef on the abundance of fish in the surrounding pelagic environment. Marine and Freshwater Research. 66. 10.1071/MF14064.

SEDAR. 2018. SEDAR 52- Stock Assessment report Gulf of Mexico Red Snapper. SEDAR, North Charleston, SC. 434, p.

Segurado, P. & Araújo, Miguel & Kunin, William. (2006). Consequences of spatial autocorrelation for niche-based models. Journal of Applied Ecology. 43. 433 - 444. 10.1111/j.1365-2664.2006.01162.x.

Shipp, Robert L. and Bortone, Stephen A.(2009)'A Perspective of the Importance of Artificial Habitat on the Management of Red Snapper in the Gulf of Mexico',Reviews in Fisheries Science,17:1,41 – 47

Simonsen, K.A. 2013. Reef Fish Demographics on Louisiana Artificial Reefs: The Effects of Reef Size on Biomass Distribution and Foraging Dynamics. Louisiana State University, Baton Rouge (Ph.D. Dissertation).

Simpson GL (2018) Modelling Palaeoecological Time Series Using Generalised Additive Models. Front. Ecol. Evol. 6:149.doi: 10.3389/fevo.2018.00149

Stanley, D.R., and C.A. Wilson. 1997. Seasonal and spatial variation in the abundance and size distribution of fishes associated with a petroleum platform in the northern Gulf of Mexico. Canadian Journal of Fisheries and Aquatic Sciences, 54(5), pp.1166-1176.

Stanley, D.R., and C.A. Wilson. 2000. Variation in the density and species composition of fishes associated with three petroleum platforms using dual beam hydroacoustics. Fisheries Research, 47(2-3), pp.161-172.

Stanley, D.R., and Wilson, C.A. 1996. Abundance of fishes associated with a petroleum platform as measured with dual-beam hydroacoustics. ICES Journal of Marine Science, 53(2), pp.473-475.

Sterba, S. K. 2009. Alternative model-based and design-based frame-works for inference from samples to populations: From polarization to integration. Multivariate Behavioral Research, 44, 711–740. https://doi.org/10.1080/00273170903333574.

Streich, M. K., M. J. Ajemian, J.J. Wetz, J.D. Shively, J.B. Shipley, and G. W. Stunz. 2017. Effects of a new artificial reef complex on Red Snapper and the associated fish community: an evaluation using a before–after control–impact approach. Marine and Coastal Fisheries: Dynamics, Management, and Ecosystem Science 9:404-418.

Stroup, W. W. 2013. Generalized Linear Mixed Models: Modern Concepts, Methods and Applications. Taylor & Francis Group, LLC. Boca Raton, FL.

Stunz, G.W., W.F. Patterson III, S.P. Powers, J.H. Cowan Jr., J.R. Rooker, R.A. Aherns, K. Boswell, L. Carleton, M. Catalano, J.M. Dryon, J. Hoenig, R. Leaf, V. Lecours, S. Murawski, D. Portnoy, E. Saillant, L.S. Stokes, and R.J.D. Wells. 2021. Estimating the Absolute Abundance of Age-2+ Red Snapper (Lutjanus campechanus) in the U.S. Gulf of Mexico. Mississippi-Alabama Sea Grant Consortium, NOAA Sea Grant. 303 pages.

Stunz, G.W., W.F. Patterson III, S.P. Powers, J.H. Cowan Jr., J.R. Rooker, R.A. Aherns, K. Boswell, L. Carleton, M. Catalano, J.M. Dryon, J. Hoenig, R. Leaf, V. Lecours, S. Murawski, D. Portnoy, E. Saillant, L.S. Stokes, and R.J.D. Wells. 2021b. Estimating the Absolute Abundance of Age-2+ Red Snapper (Lutjanus

campechanus) in the U.S. Gulf of Mexico. Mississippi-Alabama Sea Grant Consortium, NOAA Sea Grant.408 pages.

Szedlmayer, S.T., Mudrak, P.A. and Jaxion-Harm, J., 2019. A comparison of two fishery-independent surveys of Red Snapper, Lutjanus campechanus, from 1999–2004 and 2011–2015. In Red Snapper biology in a changing world (pp. 249-274). CRC Press.

Thompson, S. K. 2002. Sampling. 2nd Ed. New York: Wiley.

Williams, B. K. and E. D. Brown. 2019. Sampling and analysis frameworks for inference in ecology. Methods Ecol Evol:1832–1842.

Wood, S.N. 2022. mgcv: Mixed GAM Computation Vehicle with Automatic Smoothness Estimation. R package version 1.8-39 https://CRAN.R-project.org/package=mgcv.

Zenone, A.M., D.E. Burkepile, and K.M. Boswell. 2017. A comparison of diver vs. acoustic methodologies for surveying fishes in a shallow water coral reef ecosystem. Fisheries Research, 189, pp.62-66.

APPENDIX 1. Sampling Site Detail

West Region (37 Sites)

siteNum	siteAuburnUCB	Latitude	Longitude	siteType	habitatType	pipeline	siteName	region	depthZone
1	n/a	29.40685	-92.89604	Discrete	Platform	n/a	EC-49-CGVALVE	West	Shallow
2	n/a	28.44399	-92.87869	Discrete	Platform	n/a	EC-265-D	West	Deep
3	n/a	28.75566	-92.80229	Discrete	Platform	n/a	EC-195-GP	West	Mid
12	n/a	28.25554	-92.51562	Discrete	Platform	n/a	VR-326-A	West	Deep
13	n/a	28.65235	-92.79150	Discrete	Artificial Reef	n/a	AR 1	West	Mid
14	n/a	28.45882	-92.66022	Discrete	Artificial Reef	n/a	AR 2	West	Deep
15	n/a	28.42707	-92.66252	Discrete	Artificial Reef	n/a	AR 3	West	Deep
16	n/a	28.42417	-92.66005	Discrete	Artificial Reef	n/a	AR 4	West	Deep
30	n/a	28.28902	-92.56978	Discrete	Pipeline Crossing	n/a	PC 4	West	Deep
32	n/a	28.42204	-92.96837	Discrete	Pipeline Crossing	n/a	PC 3	West	Deep
33	n/a	28.59660	-92.99000	Discrete	Pipeline Crossing	n/a	PC 2	West	Mid
34	n/a	29.37269	-93.04584	Discrete	Pipeline Crossing	n/a	PC 1	West	Shallow
41	A1	29.36852	-93.04605	UCB	UCB	pipeline	Mud 2	West	Shallow
42	A1	29.36847	-93.05136	UCB	UCB	n/a	Mud 1	West	Shallow
43	A3	29.37000	-92.93000	UCB	UCB	n/a	Mud 3	West	Shallow
44	A2	29.43000	-92.99000	UCB	UCB	n/a	Gravel 1	West	Shallow
45	A4	28.57000	-93.03000	UCB	UCB	n/a	Mud 4	West	Mid
46	A5	28.58975	-92.98872	UCB	UCB	pipeline	Mud 6	West	Mid
47	A5	28.58964	-92.99467	UCB	UCB	n/a	Mud 5	West	Mid
48	A6	28.61000	-92.95000	UCB	UCB	n/a	Shrimp Trawl 1	West	Mid
49	A7	28.61000	-92.91000	UCB	UCB	n/a	Shrimp Trawl 2	West	Mid
50	A8	28.61000	-92.87000	UCB	UCB	n/a	Shrimp Trawl 3	West	Mid
51	A9	28.59000	-92.77000	UCB	UCB	n/a	Gravel 2	West	Mid
52	A10	28.43052	-92.96958	UCB	UCB	pipeline	Mud 8	West	Deep
53	A10	28.43050	-92.97472	UCB	UCB	n/a	Mud 7	West	Deep
54	A12	28.43000	-92.71000	UCB	UCB	n/a	Mud 9	West	Deep
55	A11	28.43000	-92.85000	UCB	UCB	n/a	Gravel 3	West	Deep
56	A13	28.28994	-92.57473	UCB	UCB	pipeline	Mud 10	West	Deep
57	A13	28.28442	-92.57467	UCB	UCB	n/a	Mud 11	West	Deep
58	A14	28.31000	-92.49000	UCB	UCB	n/a	Gravel 4	West	Deep
59	A15	28.31000	-92.39000	UCB	UCB	n/a	Mud 12	West	Deep
92	n/a	27.88639	-93.30139	Discrete	Natural Bank	n/a	Bright 1	West	Shelf
93	n/a	27.88953	-93.27152	Discrete	Natural Bank	n/a	Bright 2	West	Shelf
94	n/a	27.91007	-93.30329	Discrete	Natural Bank	n/a	Bright 3	West	Shelf
95	n/a	28.34083	-92.45944	Discrete	Natural Bank	n/a	Sonnier 1	West	Deep
96	n/a	28.34108	-92.45068	Discrete	Natural Bank	n/a	Sonnier 2	West	Deep
97	n/a	28.32877	-92.46583	Discrete	Natural Bank	n/a	Sonnier 3	West	Deep

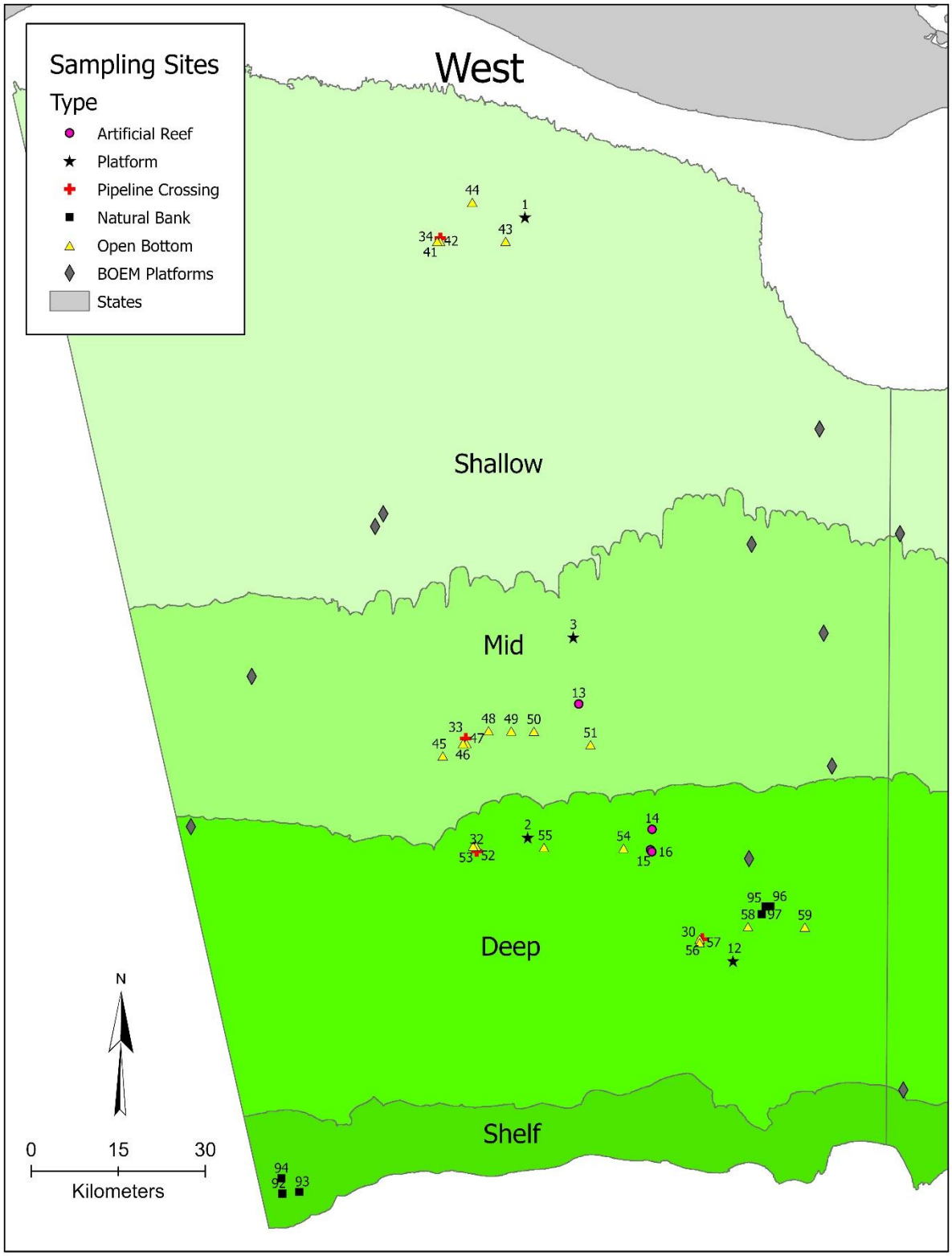
Sampling Sites
Type
Artificial Reef
Platform
Pipeline Crossing
Natural Bank
Open Bottom
BOEM Platforms
States
West
Shallow
Mid
Deep
Shelf
N
0
15
30
Kilometers
44
1
43
34
42
41
3
13
33
48
49
50
47
45
46
51
2
55
32
53
52
54
14
16
15
95
96
58
97
59
30
57
56
12
94
92
93

Central Region (33 Sites)

siteNum	siteAuburnUCB	Latitude	Longitude	siteType	habitatType	pipeline	siteName	region	depthZone
4	n/a	28.74786	-91.36797	Discrete	Platform	n/a	EI-189-B	Central	Shallow
5	n/a	28.42776	-91.47515	Discrete	Platform	n/a	EI-275-K	Central	Deep
6	n/a	28.24820	-91.74053	Discrete	Platform	n/a	EI-331-B	Central	Deep
7	n/a	28.58078	-91.52237	Discrete	Platform	n/a	EI-229-B	Central	Mid
17	n/a	28.64730	-91.93687	Discrete	Artificial Reef	n/a	AR 5	Central	Mid
18	n/a	28.41282	-91.60643	Discrete	Artificial Reef	n/a	AR 6	Central	Deep
19	n/a	28.41258	-91.60107	Discrete	Artificial Reef	n/a	AR 8	Central	Deep
20	n/a	28.41507	-91.60525	Discrete	Artificial Reef	n/a	AR 7	Central	Deep
21	n/a	28.25252	-91.75718	Discrete	Artificial Reef	n/a	AR 11	Central	Deep
22	n/a	28.25743	-91.75750	Discrete	Artificial Reef	n/a	AR 9	Central	Deep
23	n/a	28.25530	-91.75850	Discrete	Artificial Reef	n/a	AR 10	Central	Deep
31	n/a	28.70927	-91.35543	Discrete	Pipeline Crossing	n/a	PC 5	Central	Shallow
35	n/a	28.42269	-91.51777	Discrete	Pipeline Crossing	n/a	PC 7	Central	Deep
39	n/a	28.23575	-91.71112	Discrete	Pipeline Crossing	n/a	PC 8	Central	Deep
40	n/a	28.57276	-91.42801	Discrete	Pipeline Crossing	n/a	PC 6	Central	Mid
60	A16	28.79000	-91.43000	UCB	UCB	n/a	Mud 13	Central	Shallow
61	A17	28.70989	-91.35022	UCB	UCB	n/a	Mud 15	Central	Shallow
62	A17	28.71497	-91.35265	UCB	UCB	pipeline	Mud 14	Central	Shallow
63	A19	28.59000	-91.39000	UCB	UCB	n/a	Mud 16	Central	Mid
64	A18	28.57107	-91.42915	UCB	UCB	pipeline	Mud 17	Central	Mid
65	A18	28.56385	-91.42825	UCB	UCB	n/a	Mud 18	Central	Mid
66	A23	28.42979	-91.50974	UCB	UCB	pipeline	Mud 20	Central	Deep
67	A23	28.43503	-91.51070	UCB	UCB	n/a	Mud 19	Central	Deep
68	A22	28.41000	-91.57000	UCB	UCB	n/a	Mud 21	Central	Deep
69	A20	28.31000	-91.77000	UCB	UCB	n/a	Mud 22	Central	Deep
70	A21	28.22859	-91.71249	UCB	UCB	pipeline	Mud 23	Central	Deep
71	A21	28.22423	-91.70682	UCB	UCB	n/a	Mud 24	Central	Deep
98	n/a	28.08250	-92.00056	Discrete	Natural Bank	n/a	Alderdice 1	Central	Deep
99	n/a	28.07865	-91.99240	Discrete	Natural Bank	n/a	Alderdice 2	Central	Deep
100	n/a	28.08334	-92.01537	Discrete	Natural Bank	n/a	Alderdice 3	Central	Deep
101	n/a	28.08667	-91.00722	Discrete	Natural Bank	n/a	Ewing 1	Central	Deep
102	n/a	28.10340	-91.00416	Discrete	Natural Bank	n/a	Ewing 2	Central	Deep
103	n/a	28.10254	-91.03560	Discrete	Natural Bank	n/a	Ewing 3	Central	Deep

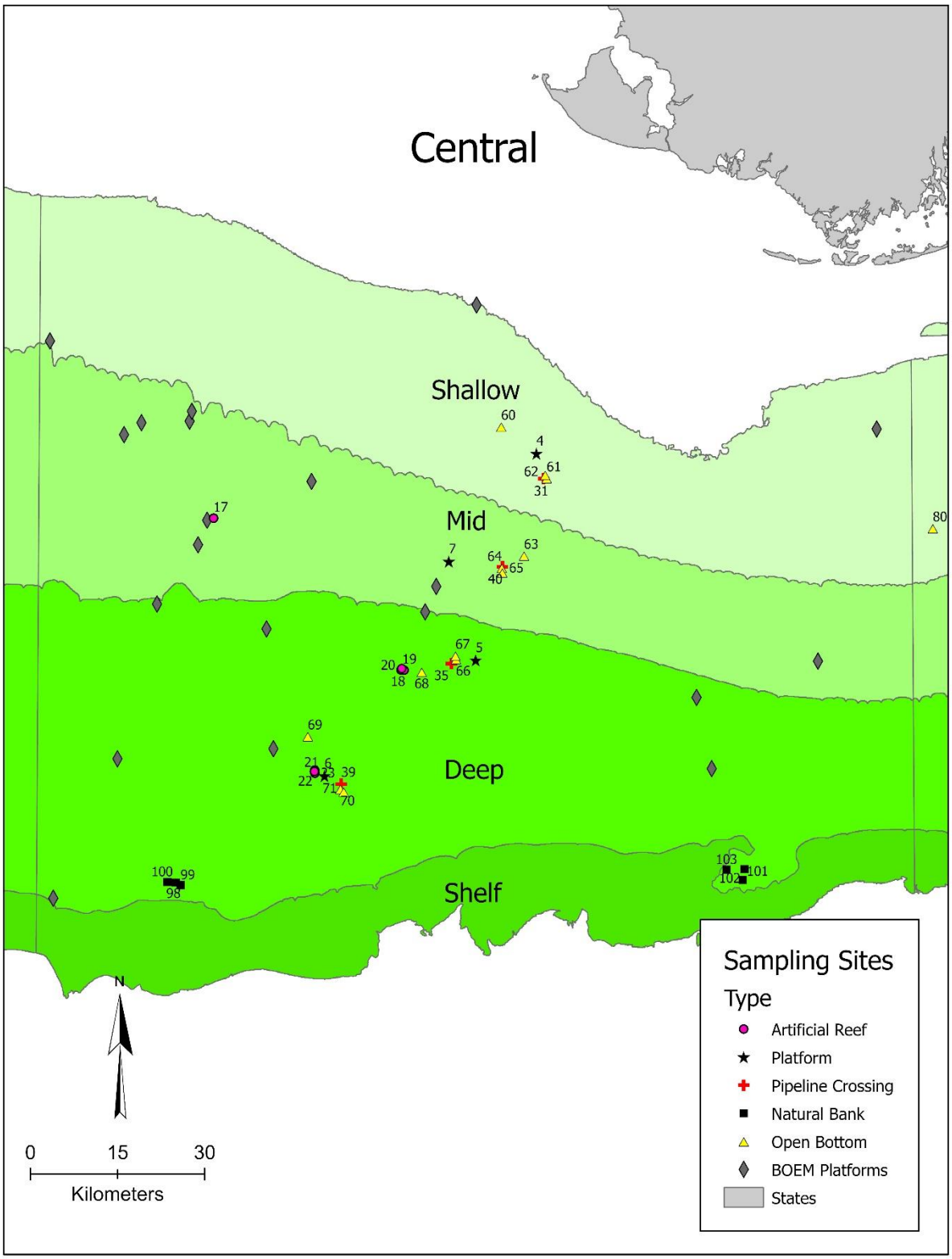
Central
Shallow
Mid
Deep
Shelf
60
4
62
61
31
17
80
7
64
63
65
40
67
5
20
19
18
68
35
66
69
21
6
3
39
22
71
70
100
99
98
103
102
101
N
0
15
30
Kilometers
Sampling Sites
Type
Artificial Reef
Platform
Pipeline Crossing
Natural Bank
Open Bottom
BOEM Platforms
States

East Region (36 Sites)

siteNum	siteAuburnUCB	Latitude	Longitude	siteType	habitatType	pipeline	siteName	region	depthZone
8	n/a	28.61810	-90.24219	Discrete	Platform	n/a	ST-152-P	East	Mid
9	n/a	28.63713	-90.19350	Discrete	Pipeline Crossing	n/a	PC13	East	Deep
10	n/a	28.36609	-90.20184	Discrete	Platform	n/a	ST-232-A	East	Deep
11	n/a	28.93815	-90.17356	Discrete	Platform	n/a	ST-41-B PROD	East	Shallow
24	n/a	28.61702	-90.25667	Discrete	Artificial Reef	n/a	AR 12	East	Mid
25	n/a	28.61958	-90.24327	Discrete	Artificial Reef	n/a	AR 13	East	Mid
26	n/a	28.61938	-90.24320	Discrete	Artificial Reef	n/a	AR 14	East	Mid
27	n/a	28.61545	-90.14325	Discrete	Artificial Reef	n/a	AR 15	East	Deep
28	n/a	28.61947	-90.13940	Discrete	Artificial Reef	n/a	AR 16	East	Deep
29	n/a	28.61514	-90.24793	Discrete	Pipeline Crossing	n/a	PC 10	East	Mid
36	n/a	28.64200	-89.55600	Discrete	Pipeline Crossing	n/a	PC 9	East	Shallow
37	n/a	28.32029	-90.19826	Discrete	Pipeline Crossing	n/a	PC 12	East	Deep
38	n/a	28.57910	-90.19439	Discrete	Pipeline Crossing	n/a	PC 11	East	Deep
72	A28	28.89000	-90.37000	UCB	UCB	n/a	Gravel 5	East	Shallow
73	A30	28.85175	-90.19036	UCB	UCB	pipeline	Mud 27	East	Shallow
74	A30	28.85050	-90.19618	UCB	UCB	n/a	Mud 26	East	Shallow
75	A29	28.83000	-90.23000	UCB	UCB	n/a	Mud 25	East	Shallow
76	A33	28.67000	-90.21000	UCB	UCB	n/a	Mud 30	East	Mid
77	A27	28.75000	-90.41000	UCB	UCB	n/a	Shrimp Trawl 7	East	Shallow
78	A26	28.73000	-90.45000	UCB	UCB	n/a	Shrimp Trawl 6	East	Shallow
79	A25	28.67000	-90.57000	UCB	UCB	n/a	Shrimp Trawl 5	East	Shallow
80	A24	28.63000	-90.67000	UCB	UCB	n/a	Shrimp Trawl 4	East	Shallow
81	A31	28.63000	-90.37000	UCB	UCB	n/a	Gravel 6	East	Mid
82	A32	28.61173	-90.24709	UCB	UCB	pipeline	Mud 29	East	Mid
83	A32	28.60415	-90.25125	UCB	UCB	n/a	Mud 28	East	Mid
84	A35	28.59000	-90.13000	UCB	UCB	n/a	Mud 33	East	Deep
85	A34	28.57049	-90.19453	UCB	UCB	pipeline	Mud 31	East	Deep
86	A34	28.57044	-90.19008	UCB	UCB	n/a	Mud 32	East	Deep
87	A39	28.35000	-90.15000	UCB	UCB	n/a	Mud 36	East	Deep
88	A38	28.33106	-90.19818	UCB	UCB	pipeline	Mud 34	East	Deep
89	A38	28.33063	-90.19019	UCB	UCB	n/a	Mud 35	East	Deep
90	A37	28.84423	-89.33650	UCB	UCB	n/a	Bottom Longline 2	East	Deep
91	A36	28.83445	-89.46740	UCB	UCB	n/a	Bottom Longline 1	East	Deep
104	n/a	28.64750	-89.56472	Discrete	Natural Bank	n/a	Sackett 1	East	Shelf
105	n/a	28.64300	-89.55300	Discrete	Natural Bank	n/a	Sackett 2	East	Shelf
106	n/a	28.62300	-89.54800	Discrete	Natural Bank	n/a	Sackett 3	East	Shelf

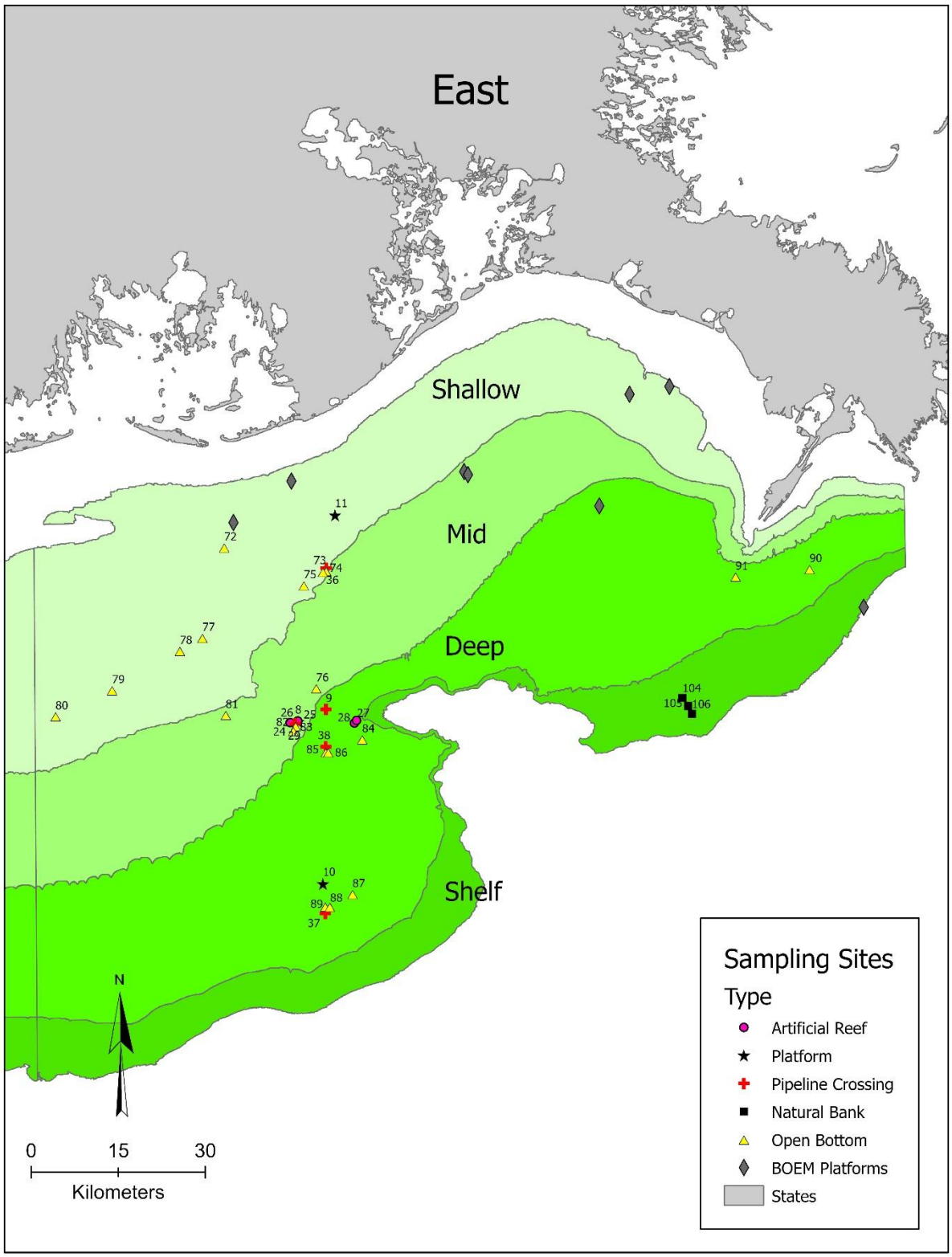
East
Shallow
Mid
Deep
Shelf
N
0
15
30
Kilometers
Sampling Sites
Type
Artificial Reef
Platform
Pipeline Crossing
Natural Bank
Open Bottom
BOEM Platforms
States

APPENDIX 2. Float Plan Template

LGL Ecological Research Associates, Inc.

Float Plan

Project: TX -624 - Estimation of Red Snapper LDWF

Date	Port	Departure Time	Estimated Return Time	Captain	Cell #	Vessel	Sat Communication
5/29/2020	Galveston, TX	5:30	21:00	Scott Hickman		F/V Catch Share	

LGL Staff	Cell #	Garmin Sat Communication	Crew Members	Cell #
Kyle McCain			Darrell Wiley	
			Tristen Dobson	

Sites	Latitude	Longitude	Zone	Task 1	Task 2	Estimated Arrival Time	Estimated Departure Time
3	28.634438	-92.771399	West Mid	Hook/Line	Sonde	9:00	10:45
13	28.65235	-92.7915	West Mid	Hook/Line	Sonde	11:15	13:00
33	28.596853	-92.99014	West Mid	Hook/Line	Sonde	13:30	17:15

Safety Contacts	Phone Number	Check Out Time	Communication Method	Check In Time	Communication Method
Office	979-846-7000				
Alana Sunmerlin					
Benny Gallway					

LDWF Contacts	Phone Number	Coast Guard Contact	Phone Number
Andy Fischer		Heartland 8th District	504-589-6225
Jason Froeba			

APPENDIX 3. Letter of Authorization

UNITED STATES DEPARTMENT OF COMMERCE
National Oceanic and Atmospheric Administration
NATIONAL MARINE FISHERIES SERVICE
Southeast Regional Office
263 13th Avenue South
St. Petersburg, Florida 33701-5505
https://www.fisheries.noaa.gov/region/southeast

02/18/2020

F/SER24: DL

Benny Gallaway, Ph.D.
LGL Ecological Research Associates, Inc.
4103 South Texas Avenue, Suite 211
Bryan, Texas 77802

Dear Dr. Gallaway:

This Letter of Acknowledgment (LOA) recognizes the activities outlined in your December 12, 2019, e-mail as scientific research in accordance with the definitions and guidance at 50 CFR Sections 600.10 and 600.745(a). As such, the activities are not subject to fishing regulations at 50 CFR Part 622 or essential fish habitat requirements at 50 CFR Sections 600.805 *et seq.* developed in accordance with the Magnuson-Stevens Fishery Conservation and Management Act.

NOAA Fisheries understands that LGL Ecological Research Associates has received funding from the Louisiana Department of Wildlife and Fisheries through a project entitled *Estimation of Total Red Snapper Abundance in Louisiana and Adjacent Federal Waters*. The research activities will occur at 106 site locations in the vicinity of offshore oil and gas structures, artificial reefs, pipeline crossings, and pipelines in the central and western Gulf of Mexico in water depths of 10-150 meters, and distances of 10-100 nautical miles offshore.

The project will focus primarily on red snapper but may also collect other federally managed species that are found in association with structures. The research will consist of:

- Hook and line capture and sacrifice of red snapper for age and growth research including otolith removal (Maximum of 3 hours fishing time or 75 fish per site);
- Hook and line capture of red snapper; dart tagging for mark/recapture study (up to 100 fish per site at each of 2 selected sites to be double-tagged). Tagged fish will be released at depth using a cage-release method developed during previous research;
- Trammel net sampling for species composition at open water sites.
    - Maximum of 10-30 minute soak time.
    - Estimate of 100-1,000 red snapper caught and sacrificed (donated to charity after processing).
    - Estimated 200-2,000 fish of other (various) species caught and sacrificed or returned to ocean as quickly as possible (kept fish donated to charity).
    - Most catch is intended to be retained. However, researchers will endeavor to reduce mortality of released catch by using short soak times and by releasing individuals as quickly as is practicable.

- Longline or chevron fish traps may be used in lieu of trammel net sampling at open water sites. These alternative gear types would be used if trammel net sampling is found to be ineffective. Catch estimates mirror those listed above for trammel nets.
- Collection of environmental data (temperature, turbidity, salinity, etc.) using a data sonde.
- Hydroacoustic survey transects using a split beam echosounder with submerged transducers.
- Deployment of submersible rotating video (SRV) cameras, which may include a baited SRV camera and a towable camera sled.

This LOA is valid through December 31, 2020. The fishing vessels identified in the appendix, while chartered by and controlled by your group, and operating in accordance with the scientific research plan, are considered research vessels as defined by 50 CFR 600.10. This list of approved vessels may be amended during the course of the LOA. Requests for such amendments must be provided at least 30 days in advance of a sampling trip.

A copy of this LOA and the approved research plan should be on board the vessels while conducting your scientific research activities. This LOA is separate and distinct from any permit or consultation required by the Marine Mammal Protection Act, Endangered Species Act, National Marine Sanctuaries Act, or any other applicable law. If such a permit or consultation is required, it should be obtained prior to embarking on the activity. We wish you success with this important research project and would appreciate a copy of your findings. Please send a copy of any cruise report or other publications resulting from the scientific research activity to me and to the Director, Southeast Fisheries Science Center, 75 Virginia Beach Drive, Miami, Florida 33149-1003. Should you have any questions or concerns please contact Daniel Luers at 727-551-5719.

Sincerely,

CRABTREE.ROY.E.DR.1365849559 Digitally signed by CRABTREE.ROY.E.DR.1365849559 Date: 2020.02.18 13:02:46 -05'00'

Roy E. Crabtree, Ph.D.
Regional Administrator

Enclosure
cc: F/SEFSC, F/EN3

APPENDIX 4. Field Sampling Completion Schedule

All Sites Were Successfully Sampled Despite COVID and Bad Hurricane Season

Site_num	SiteChara	Sample_type	Mark Recapture	Zone_ID	Hydroacoustic survey date	SRV survey date	Open Bottom Sampling Date	Hook/Line Sampling Date	Mark Date	Recapture Date
1	Platform	Hook and Line		West Shallow	5/19/2020	5/19/2020	X	5/19/2020	X	X
34	Pipeline Crossing	Hook and Line		West Shallow	5/18/2020	5/18/2020	X	5/19/2020	X	X
41	Open Bottom	Longline		West Shallow	5/18/2020	5/19/2020	5/19/2020	X	X	X
42	Open Bottom	Longline		West Shallow	5/18/2020	5/19/2020	5/19/2020	X	X	X
43	Open Bottom	Longline		West Shallow	5/19/2020	5/19/2020	5/19/2020	X	X	X
44	Open Bottom	Longline		West Shallow	5/19/2020	5/19/2020	5/19/2020	X	X	X
3	Platform	Hook and Line	MR	West Mid	5/29/2020	5/29/2020	X	5/29/2020	5/29/2020	6/14/2020
13	Artificial Reef	Hook and Line	MR	West Mid	5/29/2020	5/29/2020	X	5/29/2020	5/29/2020	6/14/2020
33	Pipeline Crossing	Hook and Line		West Mid	5/29/2020	5/29/2020	X	5/29/2020	X	X
45	Open Bottom	Longline		West Mid	5/29/2020	5/30/2020	5/30/2020	X	X	X
46	Open Bottom	Longline		West Mid	5/29/2020	5/30/2020	5/30/2020	X	X	X
47	Open Bottom	Longline		West Mid	5/29/2020	5/30/2020	5/30/2020	X	X	X
48	Open Bottom	Longline		West Mid	5/30/2020	5/30/2020	5/30/2020	X	X	X
49	Open Bottom	Longline		West Mid	5/30/2020	5/30/2020	5/30/2020	X	X	X
50	Open Bottom	Longline		West Mid	5/30/2020	5/31/2020	5/31/2020	X	X	X
51	Open Bottom	Longline		West Mid	5/30/2020	5/31/2020	5/31/2020	X	X	X
2	Platform	Hook and Line		West Deep	6/16/2020	6/16/2020	X	6/16/2020	X	X
12	Platform	Hook and Line		West Deep	6/17/2020	6/17/2020	X	6/17/2020	X	X
14	Artificial Reef	Hook and Line		West Deep	6/16/2020	6/16/2020	X	6/16/2020	X	X
15	Artificial Reef	Hook and Line		West Deep	6/16/2020	6/16/2020	X	6/17/2020	X	X
16	Artificial Reef	Hook and Line		West Deep	6/16/2020	6/16/2020	X	6/17/2020	X	X
30	Pipeline Crossing	Hook and Line		West Deep	6/17/2020	6/17/2020	X	6/17/2020	X	X
32	Pipeline Crossing	Hook and Line		West Deep	6/16/2020	6/16/2020	X	6/16/2020	X	X
95	Sonnier bank	Hook and Line		West Deep	6/17/2020	6/17/2020	X	6/18/2020	X	X
96	Sonnier bank	Hook and Line		West Deep	6/17/2020	6/17/2020	X	6/18/2020	X	X
97	Sonnier bank	Hook and Line		West Deep	6/17/2020	6/17/2020	X	6/18/2020	X	X
52	Open Bottom	Longline		West Deep	6/20/2020	6/21/2020	6/21/2020	X	X	X
53	Open Bottom	Longline		West Deep	6/20/2020	6/21/2020	6/21/2020	X	X	X
54	Open Bottom	Longline		West Deep	6/20/2020	6/20/2020	6/20/2020	X	X	X
55	Open Bottom	Longline		West Deep	6/19/2020	6/20/2020	6/20/2020	X	X	X
56	Open Bottom	Longline		West Deep	6/19/2020	6/20/2020	6/20/2020	X	X	X
57	Open Bottom	Longline		West Deep	6/19/2020	6/20/2020	6/20/2020	X	X	X
58	Open Bottom	Longline		West Deep	6/19/2020	6/20/2020	6/20/2020	X	X	X
59	Open Bottom	Longline		West Deep	6/19/2020	6/20/2020	6/20/2020	X	X	X

All Sites Were Successfully Sampled Despite COVID and Bad Hurricane Season

Site_num	SiteChara	Sample_type	Mark Recapture	Zone_ID	Hydroacoustic survey date	SRV survey date	Open Bottom Sampling Date	Hook/Line Sampling Date	Mark Date	Recapture Date
92	Bright bank	Hook and Line		West Shelf	8/3/2020	8/3/2020	X	7/16/2020	X	X
93	Bright bank	Hook and Line		West Shelf	8/3/2020	8/3/2020	X	7/16/2020	X	X
94	Bright bank	Hook and Line		West Shelf	8/3/2020	8/3/2020	X	7/16/2020	X	X
11	Platform	Hook and Line		East Shallow	9/5/2020	9/5/2020	X	9/6/2020	X	X
36	Pipeline Crossing	Hook and Line		East Shallow	9/5/2020	9/5/2020	X	9/6/2020	X	X
72	Open Bottom	Longline		East Shallow	7/8/2020	7/9/2020	7/9/2020	X	X	X
73	Open Bottom	Longline		East Shallow	7/8/2020	7/10/2020	7/10/2020	X	X	X
74	Open Bottom	Longline		East Shallow	7/8/2020	7/10/2020	7/10/2020	X	X	X
75	Open Bottom	Longline		East Shallow	7/8/2020	7/10/2020	7/10/2020	X	X	X
77	Open Bottom	Longline		East Shallow	7/9/2020	7/9/2020	7/9/2020	X	X	X
78	Open Bottom	Longline		East Shallow	7/1/2020	7/2/2020	7/2/2020	X	X	X
79	Open Bottom	Longline		East Shallow	6/30/2020	7/2/2020	7/2/2020	X	X	X
80	Open Bottom	Longline		East Shallow	6/30/2020	7/2/2020	7/2/2020	X	X	X
8	Platform	Hook and Line	MR	East Mid	9/4/2020	9/4/2020	X	9/4/2020	5/21/2020	6/17/2020
24	Artificial Reef	Hook and Line		East Mid	9/4/2020	9/4/2020	X	9/6/2020	X	X
25	Artificial Reef	Hook and Line		East Mid	9/4/2020	9/4/2020	X	9/5/2020	X	X
26	Artificial Reef	Hook and Line	MR	East Mid	9/4/2020	9/4/2020	X	9/5/2020	5/21/2020	6/18/2020
29	Pipeline Crossing	Hook and Line		East Mid	9/4/2020	9/4/2020	X	9/6/2020	X	X
76	Open Bottom	Longline		East Mid	7/3/2020	7/9/2020	7/9/2020	X	X	X
81	Open Bottom	Longline		East Mid	7/1/2020	7/8/2020	7/8/2020	X	X	X
82	Open Bottom	Longline		East Mid	7/4/2020	7/9/2020	7/9/2020	X	X	X
83	Open Bottom	Longline		East Mid	7/4/2020	7/9/2020	7/9/2020	X	X	X
9	Platform	Hook and Line		East Deep	9/4/2020	9/4/2020	X	9/6/2020	X	X
10	Platform	Hook and Line		East Deep	9/3/2020	9/3/2020	X	9/3/2020	X	X
27	Artificial Reef	Hook and Line		East Deep	9/3/2020	9/3/2020	X	9/4/2020	X	X
28	Artificial Reef	Hook and Line		East Deep	9/3/2020	9/3/2020	X	9/4/2020	X	X
37	Pipeline Crossing	Hook and Line		East Deep	9/3/2020	9/3/2020	X	9/3/2020	X	X
38	Pipeline Crossing	Hook and Line		East Deep	9/3/2020	9/3/2020	X	9/3/2020	X	X
84	Open Bottom	Longline		East Deep	7/4/2020	7/9/2020	7/9/2020	X	X	X
85	Open Bottom	Longline		East Deep	7/3/2020	7/9/2020	7/9/2020	X	X	X
86	Open Bottom	Longline		East Deep	7/3/2020	7/9/2020	7/9/2020	X	X	X

All Sites Were Successfully Sampled Despite COVID and Bad Hurricane Season

Site_num	SiteChara	Sample_type	Mark Recapture	Zone_ID	Hydroacoustic survey date	SRV survey date	Open Bottom Sampling Date	Hook/Line Sampling Date	Mark Date	Recapture Date
87	Open Bottom	Longline		East Deep	7/3/2020	7/8/2020	7/8/2020	X	X	X
88	Open Bottom	Longline		East Deep	7/3/2020	7/8/2020	7/8/2020	X	X	X
89	Open Bottom	Longline		East Deep	7/3/2020	7/8/2020	7/8/2020	X	X	X
90	Open Bottom	Longline		East Deep	7/2/2020	7/3/2020	7/3/2020	X	X	X
91	Open Bottom	Longline		East Deep	7/2/2020	7/3/2020	7/3/2020	X	X	X
104	Sackett bank	Hook and Line		East Shelf	9/2/2020	9/2/2020	X	8/16/2020	X	X
105	Sackett bank	Hook and Line		East Shelf	9/2/2020	9/2/2020	X	8/16/2020	X	X
106	Sackett bank	Hook and Line		East Shelf	9/2/2020	9/2/2020	X	8/16/2020	X	X
4	Platform	Hook and Line		Central Shallow	7/2/2020	7/2/2020	X	7/2/2020	X	X
31	Pipeline Crossing	Hook and Line		Central Shallow	7/2/2020	7/2/2020	X	7/2/2020	X	X
60	Open Bottom	Longline		Central Shallow	7/29/2020	8/4/2020	8/4/2020	X	X	X
61	Open Bottom	Longline		Central Shallow	7/30/2020	8/4/2020	8/4/2020	X	X	X
62	Open Bottom	Longline		Central Shallow	7/30/2020	8/4/2020	8/4/2020	X	X	X
7	Platform	Hook and Line	MR	Central Mid	7/2/2020	7/2/2020	X	7/3/2020	5/28/2020	6/16/2020
17	Artificial Reef	Hook and Line	MR	Central Mid	7/2/2020	7/2/2020	X	7/3/2020	5/28/2020	6/16/2020
40	Pipeline Crossing	Hook and Line		Central Mid	7/2/2020	7/2/2020	X	7/2/2020	X	X
63	Open Bottom	Longline		Central Mid	7/30/2020	8/4/2020	8/4/2020	X	X	X
64	Open Bottom	Longline		Central Mid	7/30/2020	8/4/2020	8/4/2020	X	X	X
65	Open Bottom	Longline		Central Mid	7/30/2020	8/4/2020	8/4/2020	X	X	X
5	Platform	Hook and Line		Central Deep	7/10/2020	7/10/2020	X	7/10/2020	X	X
6	Platform	Hook and Line		Central Deep	7/9/2020	7/9/2020	X	7/9/2020	X	X
18	Artificial Reef	Hook and Line		Central Deep	7/9/2020	7/9/2020	X	7/10/2020	X	X
19	Artificial Reef	Hook and Line		Central Deep	7/9/2020	7/9/2020	X	7/10/2020	X	X
20	Artificial Reef	Hook and Line		Central Deep	7/9/2020	7/9/2020	X	7/10/2020	X	X
21	Artificial Reef	Hook and Line		Central Deep	7/8/2020	7/8/2020	X	7/9/2020	X	X
22	Artificial Reef	Hook and Line		Central Deep	7/8/2020	7/8/2020	X	7/9/2020	X	X
23	Artificial Reef	Hook and Line		Central Deep	7/8/2020	7/8/2020	X	7/9/2020	X	X
35	Pipeline Crossing	Hook and Line		Central Deep	7/9/2020	7/9/2020	X	7/10/2020	X	X
39	Pipeline Crossing	Hook and Line		Central Deep	7/9/2020	7/9/2020	X	7/11/2020	X	X
66	Open Bottom	Longline		Central Deep	7/31/2020	8/4/2020	8/4/2020	X	X	X
67	Open Bottom	Longline		Central Deep	7/31/2020	8/4/2020	8/4/2020	X	X	X
68	Open Bottom	Longline		Central Deep	7/31/2020	8/4/2020	8/4/2020	X	X	X
69	Open Bottom	Longline		Central Deep	7/31/2020	8/5/2020	8/5/2020	X	X	X
70	Open Bottom	Longline		Central Deep	7/31/2020	8/5/2020	8/5/2020	X	X	X

All Sites Were Successfully Sampled Despite COVID and Bad Hurricane Season

Site_num	SiteChara	Sample_type	Mark Recapture	Zone_ID	Hydroacoustic survey date	SRV survey date	Open Bottom Sampling Date	Hook/Line Sampling Date	Mark Date	Recapture Date
71	Open Bottom	Longline		Central Deep	7/31/2020	8/5/2020	8/5/2020	X	X	X
98	Alderdice bank	Hook and Line		Central Deep	7/15/2020	7/15/2020	X	7/11/2020	X	X
99	Alderdice bank	Hook and Line		Central Deep	7/15/2020	7/15/2020	X	7/11/2020	X	X
100	Alderdice bank	Hook and Line		Central Deep	7/15/2020	7/15/2020	X	7/11/2020	X	X
101	Ewing bank	Hook and Line		Central Deep	7/16/2020	7/16/2020	X	7/14/2020	X	X
102	Ewing bank	Hook and Line		Central Deep	7/16/2020	7/16/2020	X	7/14/2020	X	X
103	Ewing bank	Hook and Line		Central Deep	7/15/2020	7/15/2020	X	7/14/2020	X	X

APPENDIX 5. Sample Analyses Completion Schedule

All Samples Have Been Analyzed

Site_num	Auburn_Area_ID	SiteChara	Sample_type	Mark Recapture	Zone_ID	Hydroacoustic Data Workup	SRV Workup	TV Workup	Aged
1		Platform	Hook and Line		West Shallow	12/21/2020	8/17/2020	X	10/7/2020
34		Pipeline Crossing	Hook and Line		West Shallow	12/21/2020	8/17/2020	X	No Catch
41	A1	Open Bottom	Longline		West Shallow	12/8/2020	X	8/31/2020	No Catch
42		Open Bottom	Longline		West Shallow	12/8/2020			No Catch
43	A3	Open Bottom	Longline		West Shallow	12/8/2020	X	9/8/2020	No Catch
44	A2	Open Bottom	Longline		West Shallow	12/8/2020	X	9/8/2020	No Catch
3		Platform	Hook and Line	MR	West Mid	12/21/2020	8/18/2020	X	10/8/2020
13		Artificial Reef	Hook and Line	MR	West Mid	12/21/2020	10/1/2020	X	10/12/2008
33		Pipeline Crossing	Hook and Line		West Mid	12/21/2020	10/8/2020	X	10/13/2020
45	A4	Open Bottom	Longline		West Mid	12/8/2020	X	8/31/2020	10/13/2020
46	A5	Open Bottom	Longline		West Mid	12/8/2020	X	9/8/2020	No Catch
47		Open Bottom	Longline		West Mid	12/8/2020			10/13/2020
48	A6	Open Bottom	Longline		West Mid	12/8/2020	X	9/9/2020	No Catch
49	A7	Open Bottom	Longline		West Mid	12/8/2020	X	9/9/2020	10/13/2020
50	A8	Open Bottom	Longline		West Mid	12/8/2020	X	9/9/2020	10/13/2020
51	A9	Open Bottom	Longline		West Mid	12/9/2020	X	9/10/2020	10/13/2020
2		Platform	Hook and Line		West Deep	12/21/2020	10/5/2020	X	10/15/2020
12		Platform	Hook and Line		West Deep	12/21/2020	10/5/2020	X	10/20/2020
14		Artificial Reef	Hook and Line		West Deep	12/21/2020	10/7/2020	X	10/21/2020
15		Artificial Reef	Hook and Line		West Deep	12/21/2020	9/23/2020	X	10/21/2020
16		Artificial Reef	Hook and Line		West Deep	1/4/2021	9/25/2020	X	10/22/2020
30		Pipeline Crossing	Hook and Line		West Deep	1/4/2021	10/7/2020	X	10/30/2020
32		Pipeline Crossing	Hook and Line		West Deep	1/4/2021	10/8/2020	X	10/28/2020
95		Sonnier bank	Hook and Line		West Deep	1/12/2021	10/14/2020	X	10/23/2020
96		Sonnier bank	Hook and Line		West Deep	1/12/2021	10/20/2020	X	10/26/2020
97		Sonnier bank	Hook and Line		West Deep	1/12/2021	10/15/2020	X	10/28/2020

All Samples Have Been Analyzed

Site_num	Auburn_Area_ID	SiteChara	Sample_type	Mark Recapture	Zone_ID	Hydroacoustic Data Workup	SRV Workup	TV Workup	Aged
52	A10	Open Bottom	Longline		West Deep	12/9/2020	X	9/10/2020	11/2/2020
53		Open Bottom	Longline		West Deep	12/9/2020			No Catch
54	A12	Open Bottom	Longline		West Deep	12/9/2020	X	9/11/2020	11/2/2020
55	A11	Open Bottom	Longline		West Deep	12/9/2020	X	9/11/2020	11/2/2020
56	A13	Open Bottom	Longline		West Deep	12/9/2020	X	9/14/2020	11/2/2020
57		Open Bottom	Longline		West Deep	12/9/2020			11/3/2020
58	A14	Open Bottom	Longline		West Deep	12/11/2020	X	9/14/2020	11/3/2020
59	A15	Open Bottom	Longline		West Deep	12/11/2020	X	9/16/2020	11/3/2020
92		Bright bank	Hook and Line		West Shelf	1/21/2021	11/3/2020	X	No Catch
93		Bright bank	Hook and Line		West Shelf	1/21/2021	12/3/2020	X	11/3/2020
94		Bright bank	Hook and Line		West Shelf	1/21/2021	12/7/2020	X	11/19/2020
4		Platform	Hook and Line		Central Shallow	1/12/2021	10/14/2020	X	11/19/2020
31		Pipeline Crossing	Hook and Line		Central Shallow	1/12/2021	10/13/2020	X	No Catch
60	A16	Open Bottom	Longline		Central Shallow	12/11/2020	X	12/2/2020	No Catch
61	A17	Open Bottom	Longline		Central Shallow	12/11/2020	X	12/1/2020	No Catch
62		Open Bottom	Longline		Central Shallow	12/11/2020	X		No Catch
7		Platform	Hook and Line	MR	Central Mid	1/4/2021	10/21/2020	X	11/20/2020
17		Artificial Reef	Hook and Line	MR	Central Mid	1/4/2021	10/13/2020	X	11/23/2020
40		Pipeline Crossing	Hook and Line		Central Mid	1/12/2021	10/14/2020	X	11/23/2020
63	A19	Open Bottom	Longline		Central Mid	12/11/2020	X	12/3/2020	No Catch
64	A18	Open Bottom	Longline		Central Mid	12/11/2020	X	9/28/2020	11/24/2020
65		Open Bottom	Longline		Central Mid	12/11/2020			11/24/2020
5		Platform	Hook and Line		Central Deep	1/4/2021	11/4/2020	X	No Catch
6		Platform	Hook and Line		Central Deep	1/4/2021	12/16/2020	X	11/24/2020
18		Artificial Reef	Hook and Line		Central Deep	1/4/2021	11/5/2020	X	11/24/2020
19		Artificial Reef	Hook and Line		Central Deep	1/4/2021	11/5/2020	X	11/24/2020
20		Artificial Reef	Hook and Line		Central Deep	1/4/2021	11/9/2020	X	11/24/2020
21		Artificial Reef	Hook and Line		Central Deep	1/4/2021	11/16/2020	X	11/24/2020
22		Artificial Reef	Hook and Line		Central Deep	1/4/2021	11/17/2020	X	11/24/2020
23		Artificial Reef	Hook and Line		Central Deep	1/4/2021	11/18/2020	X	11/24/2020
35		Pipeline Crossing	Hook and Line		Central Deep	1/4/2021	11/19/2020	X	12/1/2020
39		Pipeline Crossing	Hook and Line		Central Deep	1/4/2021	11/23/2020	X	No Catch

All Samples Have Been Analyzed

Site_num	Auburn_Area_ID	SiteChara	Sample_type	Mark Recapture	Zone_ID	Hydroacoustic Data Workup	SRV Workup	TV Workup	Aged
66	A23	Open Bottom	Longline		Central Deep	12/16/2020	X	1/6/2021	12/2/2020
67		Open Bottom	Longline		Central Deep	12/16/2020			12/2/2020
68	A22	Open Bottom	Longline		Central Deep	12/11/2020	X	1/7/2021	12/2/2020
69	A20	Open Bottom	Longline		Central Deep	12/11/2020	X	1/7/2021	No Catch
70	A21	Open Bottom	Longline		Central Deep	12/11/2020	X	1/7/2021	No Catch
71		Open Bottom	Longline		Central Deep	12/11/2020			No Catch
98		Alderdice bank	Hook and Line		Central Deep	1/12/2021	12/10/2020	X	12/8/2020
99		Alderdice bank	Hook and Line		Central Deep	1/12/2021	12/11/2020	X	12/8/2020
100		Alderdice bank	Hook and Line		Central Deep	1/12/2021	12/14/2020	X	12/14/2020
101		Ewing bank	Hook and Line		Central Deep	1/12/2021	12/15/2020	X	12/14/2020
102		Ewing bank	Hook and Line		Central Deep	1/12/2021	1/18/2021	X	12/14/2020
103		Ewing bank	Hook and Line		Central Deep	1/12/2021	1/20/2021	X	12/14/2020
11		Platform	Hook and Line		East Shallow	1/15/2021	11/25/2020	X	12/14/2020
36		Pipeline Crossing	Hook and Line		East Shallow	1/21/2021	12/14/2020	X	12/14/2020
72	A28	Open Bottom	Longline		East Shallow	12/16/2020	X	1/7/2021	No Catch
73	A30	Open Bottom	Longline		East Shallow	12/16/2020	X	1/8/2021	12/14/2020
74		Open Bottom	Longline		East Shallow	12/16/2020			No Catch
75	A29	Open Bottom	Longline		East Shallow	12/16/2020	X	1/8/2021	No Catch
77	A27	Open Bottom	Longline		East Shallow	12/16/2020	X	1/8/2021	No Catch
78	A26	Open Bottom	Longline		East Shallow	12/16/2020	X	1/12/2021	No Catch
79	A25	Open Bottom	Longline		East Shallow	12/16/2020	X	1/12/2021	No Catch
80	A24	Open Bottom	Longline		East Shallow	12/16/2020	X	9/23/2020	No Catch
8		Platform	Hook and Line	MR	East Mid	1/15/2021	12/28/2020	X	2/9/2021
24		Artificial Reef	Hook and Line		East Mid	1/15/2021	12/21/2020	X	2/26/2021
25		Artificial Reef	Hook and Line		East Mid	1/15/2021	12/21/2020	X	2/5/2021
26		Artificial Reef	Hook and Line	MR	East Mid	1/15/2021	12/22/2020	X	2/8/2021
29		Pipeline Crossing	Hook and Line		East Mid	1/15/2021	12/22/2020	X	2/1/2021
76	A33	Open Bottom	Longline		East Mid	12/16/2020	X	1/8/2021	2/2/2021
81	A31	Open Bottom	Longline		East Mid	12/16/2020	X	9/23/2020	No Catch
82	A32	Open Bottom	Longline		East Mid	12/16/2020	X	9/29/2020	1/5/2021
83		Open Bottom	Longline		East Mid	12/16/2020			1/5/2021
9		Pipeline Crossing	Hook and Line		East Deep	1/15/2021	1/6/2021	X	2/3/2021
10		Platform	Hook and Line		East Deep	1/15/2021	1/7/2021	X	2/9/2021
27		Artificial Reef	Hook and Line		East Deep	1/15/2021	1/8/2021	X	2/26/2021
28		Artificial Reef	Hook and Line		East Deep	1/15/2021	1/12/2021	X	2/25/2021
37		Pipeline Crossing	Hook and Line		East Deep	1/21/2021	1/12/2021	X	2/11/2021
38		Pipeline Crossing	Hook and Line		East Deep	1/21/2021	1/13/2021	X	2/5/2021

All Samples Have Been Analyzed

Site_num	Auburn_Area_ID	SiteChara	Sample_type	Mark Recapture	Zone_ID	Hydroacoustic Data Workup	SRV Workup	TV Workup	Aged
84	A35	Open Bottom	Longline		East Deep	12/18/2020	X	9/30/2020	2/4/2021
85	A34	Open Bottom	Longline		East Deep	12/18/2020	X	10/5/2020	2/4/2021
86		Open Bottom	Longline		East Deep	12/18/2020			2/1/2021
87	A39	Open Bottom	Longline		East Deep	12/18/2020	X	10/8/2020	2/9/2021
88	A38	Open Bottom	Longline		East Deep	12/18/2020	X	10/8/2020	2/2/2021
89		Open Bottom	Longline		East Deep	12/18/2020			2/2/2021
90	A37	Open Bottom	Longline		East Deep	12/18/2020	X	10/13/2020	2/1/2021
91	A36	Open Bottom	Longline		East Deep	12/18/2020	X	10/13/2020	2/26/2021
104		Sackett bank	Hook and Line		East Shelf	1/21/2021	1/19/2021	X	1/19/2021
105		Sackett bank	Hook and Line		East Shelf	1/21/2021	1/15/2021	X	1/19/2021
106		Sackett bank	Hook and Line		East Shelf	1/21/2021	1/21/2021	X	1/19/2021

APPENDIX 6.

Statistical Diagnostics for the Model Used to Predict the Proportion of Fish Densities that were Red Snapper

Model Fit and Diagnostics

Plotting the observed versus predicted values from the GAMM for *PropRS* (Figure A6.1) indicated no substantial bias with the fitted line approximating that of equality (i.e., intercept=0 and slope=1). The ratio of data points to model parameters (N/k) was 3.4, which borders on the model possibly being too complex, but was still above the minimum threshold of 3.0 (Forstmeier and Schielzeth 2010, Crawley 2013). Models were further assessed for fit, overdispersion, and zero-inflation with scaled (quantile) simulated residuals (number of simulations = 1,000) via the DHARMa Package Version 0.4.5, which extends this tool to models parameterized with the mgcv Package (Hartig 2022). A QQ plot of these residuals indicated no substantial deviation from the expected distribution (Figure A6.2), nor were there any apparent problems with overdispersion (Figure A6.3) or zero-inflation (Figure A6.4). The output statistics produced by mgcv Package Version 1.8-38 (Wood 2021) show the random intercept term for *Sites* (Figure A6.5) accounted for most of the variation and appeared to meet the assumption of normality based on the QQ-plot in Figure A6.6 created with the gratia Package Version 0.7.0 (Simpson 2022).

Finally, concurvity (akin to collinearity for linear regression) among smooth terms was checked with indices quantifying this issue available in the mgcv Package (Figure A6.7). Two matrices are produced, the first of which reflects the extent to which each smooth term can be approximated by the rest of the model, and the second shows pairwise concurvity between each term. Three sets of indices--“worst”, “observed”, and “estimate”— are reported for each matrix. Interpretation of these indices is somewhat tedious. Even Wood (2021) is vague on how to interpret these indices, and the literature is sparce on definitive thresholds. An internet search yielded a general rule-of-thumb that when worst values are >0.8 in the overall matrix, then the pairwise matrix should be examined more closely. Wood (2021) does say that the worst index is overly pessimistic and that the observed index is potentially optimistic. The estimate index is said to be somewhere in between. From Figure A6.7, we see that this worst index threshold of being >0.8 was breached for most of the terms in the overall matrix. However, while the pairwise matrix still shows problematic concurvity for most terms with the random effect of *Site*, the estimate indices are less concerning.

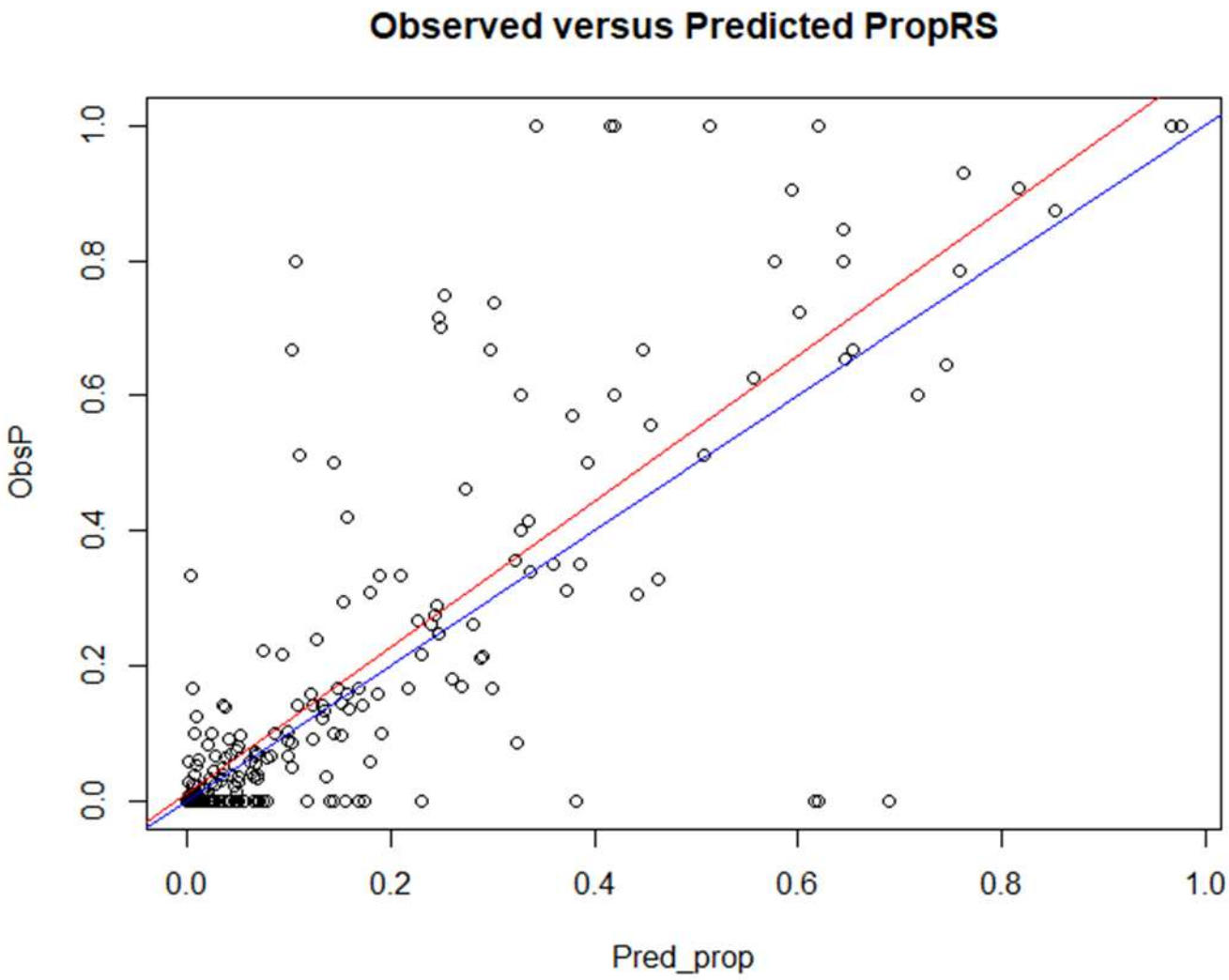

Figure A6.1. Observed versus fitted values. Equality is indicated by the blue line and the fitted trend by the red line.

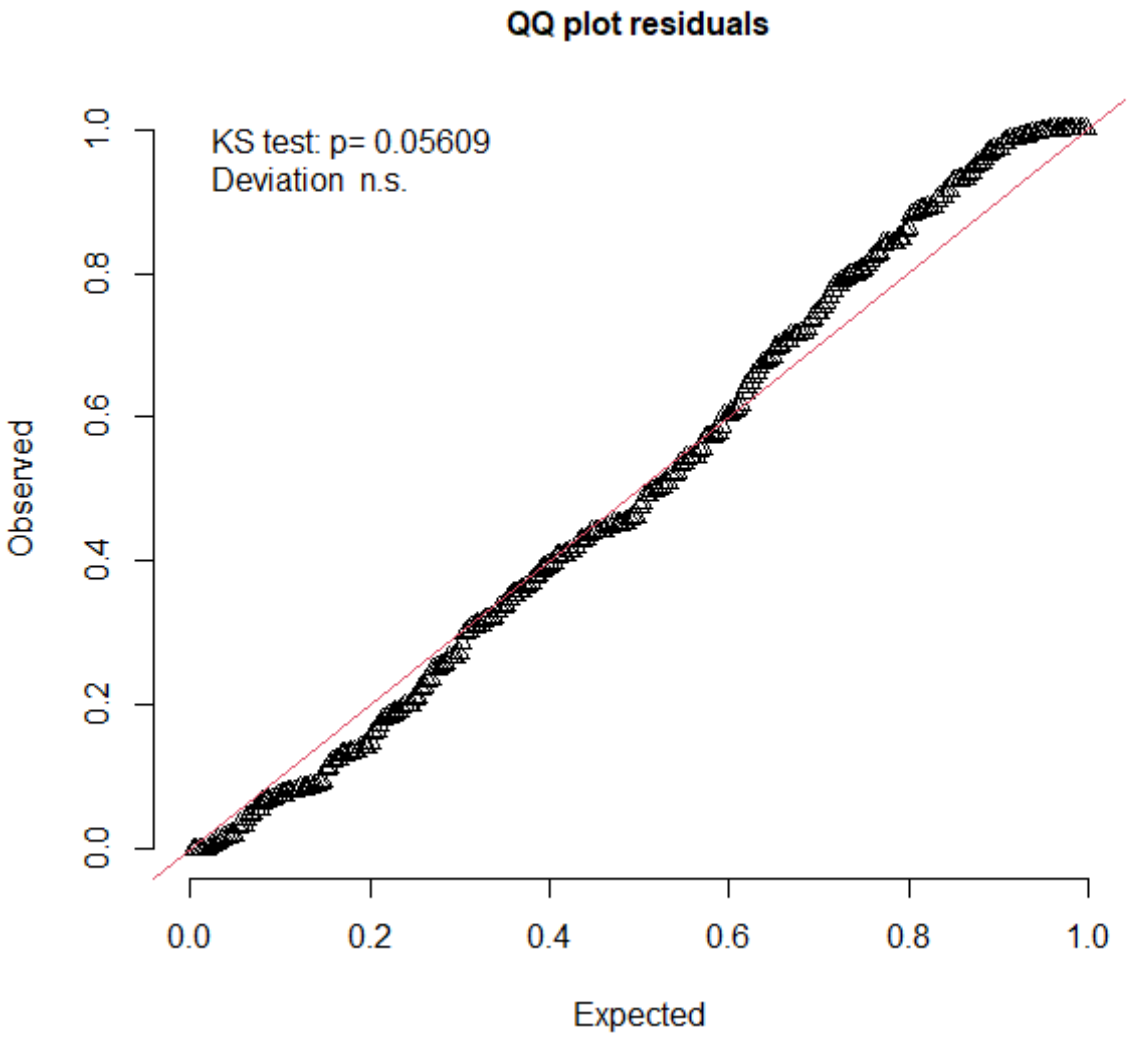

Figure A6.2. QQ-plot of observed residuals versus simulated DHARMa residuals to detect overall deviations.

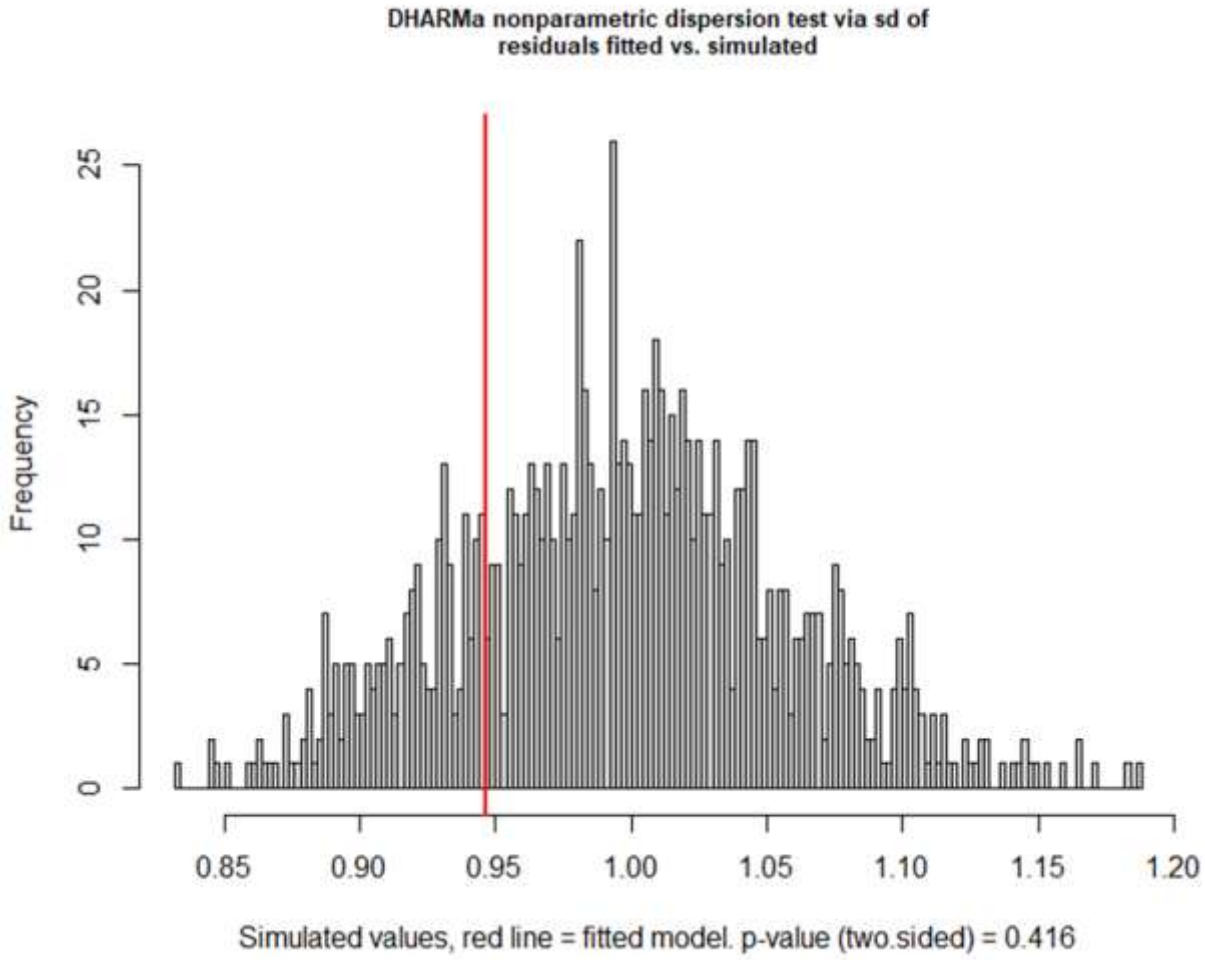

Figure A6.3. Non-parametric test comparing the variance of simulated DHARMa residuals (gray bars) to the observed residuals (red bar). A low p-value indicates a problem with underdispersion/overdispersion.

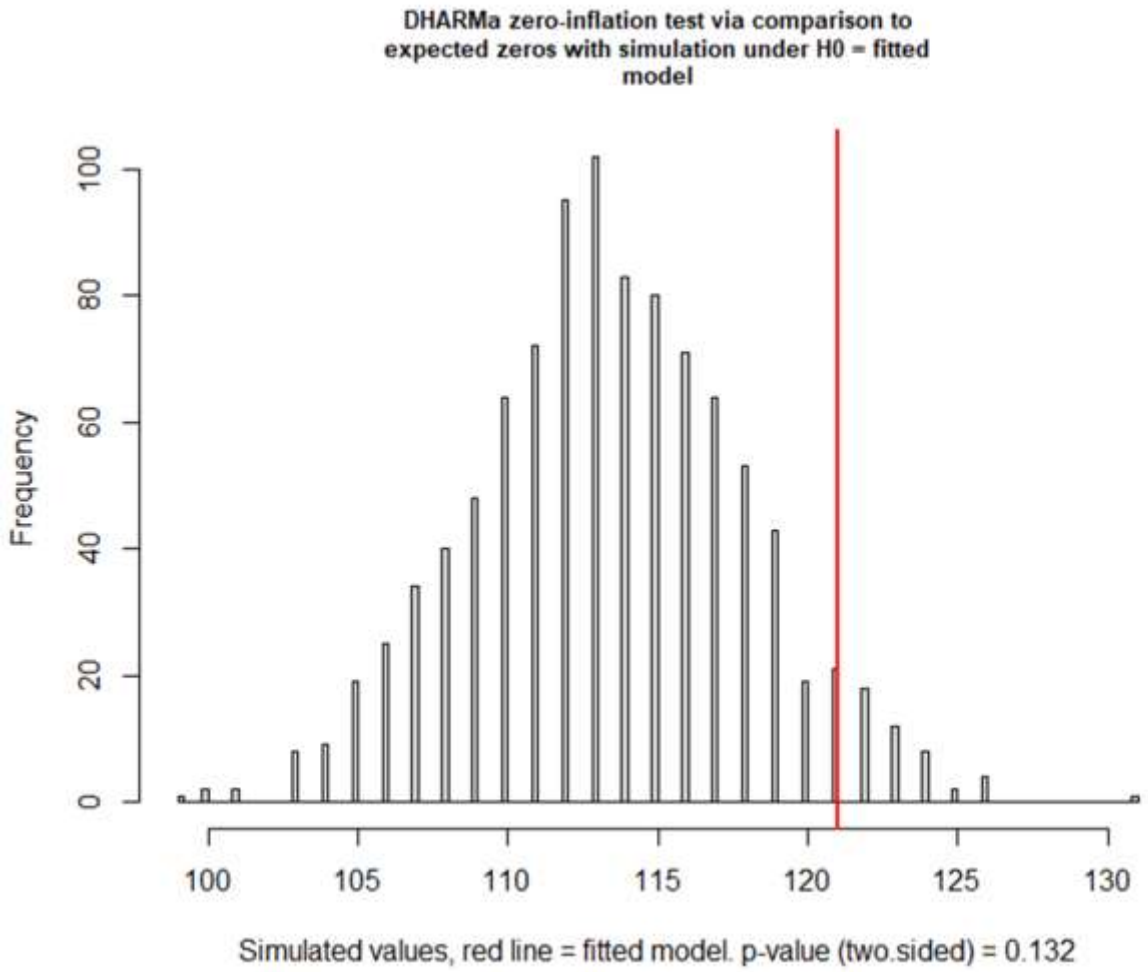

Figure A6.4. Distribution of expected zeros (gray bars) in the data compared to the observed zeros (red bar). A low p-value means that more or less zeros were observed in the data than expected.

A

component	variance	std_dev	lower_ci	upper_ci
<chr>	<dbl>	<dbl>	<dbl>	<dbl>
s(DO)	0.895	0.946	0.412	2.17
s(Sal)	0.808	0.899	0.439	1.84
s(M_FromBot):HabTypeArtificialReef	0.209	0.457	0.170	1.23
s(M_FromBot):HabTypeNaturalBank	0.0773	0.278	0.0997	0.776
s(M_FromBot):HabTypeOpenBottom	0.363	0.602	0.187	1.94
s(M_FromBot):HabTypePlatform	0.230	0.479	0.182	1.26
s(Site)	3.13	1.77	1.44	2.18

B

```
Approximate significance of smooth terms:
                                    edf Ref.df   Chi.sq  p-value
s(DO)                             3.579      4  1543.26 0.002721 **
s(Sal)                            3.900      4 18138.32  < 2e-16 ***
s(M_FromBot):HabTypeArtificialReef  2.410      4   483.94  < 2e-16 ***
s(M_FromBot):HabTypeNaturalBank     1.857      4   307.79 0.000175 ***
s(M_FromBot):HabTypeOpenBottom      2.626      4    39.16 0.089752 .
s(M_FromBot):HabTypePlatform        3.552      4  5978.86  < 2e-16 ***
s(Site)                           56.361     70  1513.92  < 2e-16 ***
---
Signif. codes:  0 '***' 0.001 '**' 0.01 '*' 0.05 '.' 0.1 ' ' 1

R-sq.(adj) =  0.782   Deviance explained = 87.5%
-REML = 752.36  Scale est. = 1         n = 283
```

C

```
Family: binomial
Link function: logit

Formula:
RS/Total ~ Region + DZ + HabType + s(DO, bs = "tp", k = 5,
    m = 1) + s(Sal, k = 5, m = 1) + s(M_FromBot, by = HabType,
    bs = "tp", k = 5, m = 1) + s(Site, bs = "re")

Parametric Terms:
         df Chi.sq  p-value
Region    2  0.206    0.902
DZ        2  0.818    0.664
HabType   3 30.388 1.14e-06
```

Figure A6.5. GAMM output statistics. Panel **A** shows the smoothing parameters expressed as variance components and their 95% confidence intervals on the standard deviation scale. Panels **B** gives the approximated p-values for smooth and parametric terms, respectively. Furthermore, Panel B shows the effective degrees of freedom (edf) for each smooth after penalization, the deviance explained, the dispersion parameter ("Scale est."), as well as sample size n. Panel **C** indicates the assumed distribution for the response and the corresponding link function, the model specification, and p-values for parametric terms.

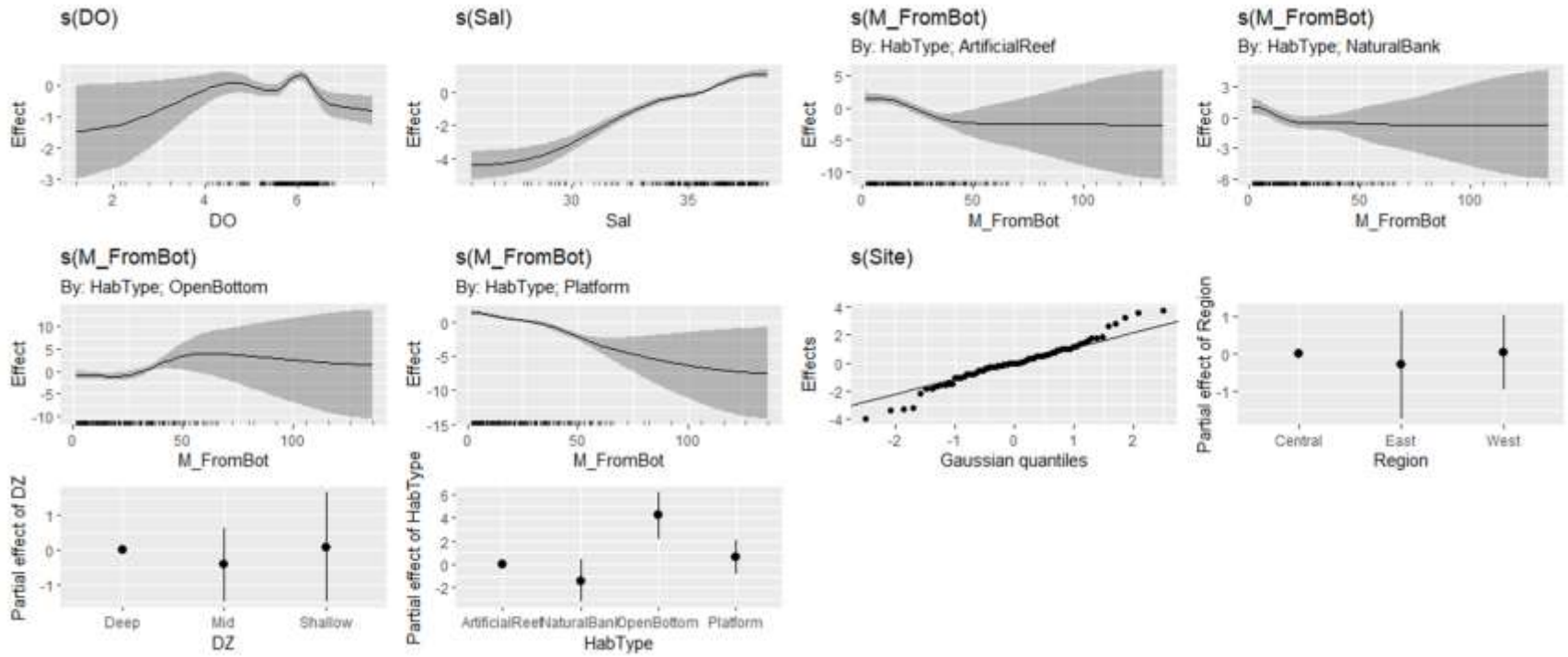

Figure A6.6. Plots of partial effects of fixed model terms with 95% credible intervals. A QQ plot is shown for the random effect of *Site* to assess the normality assumption.

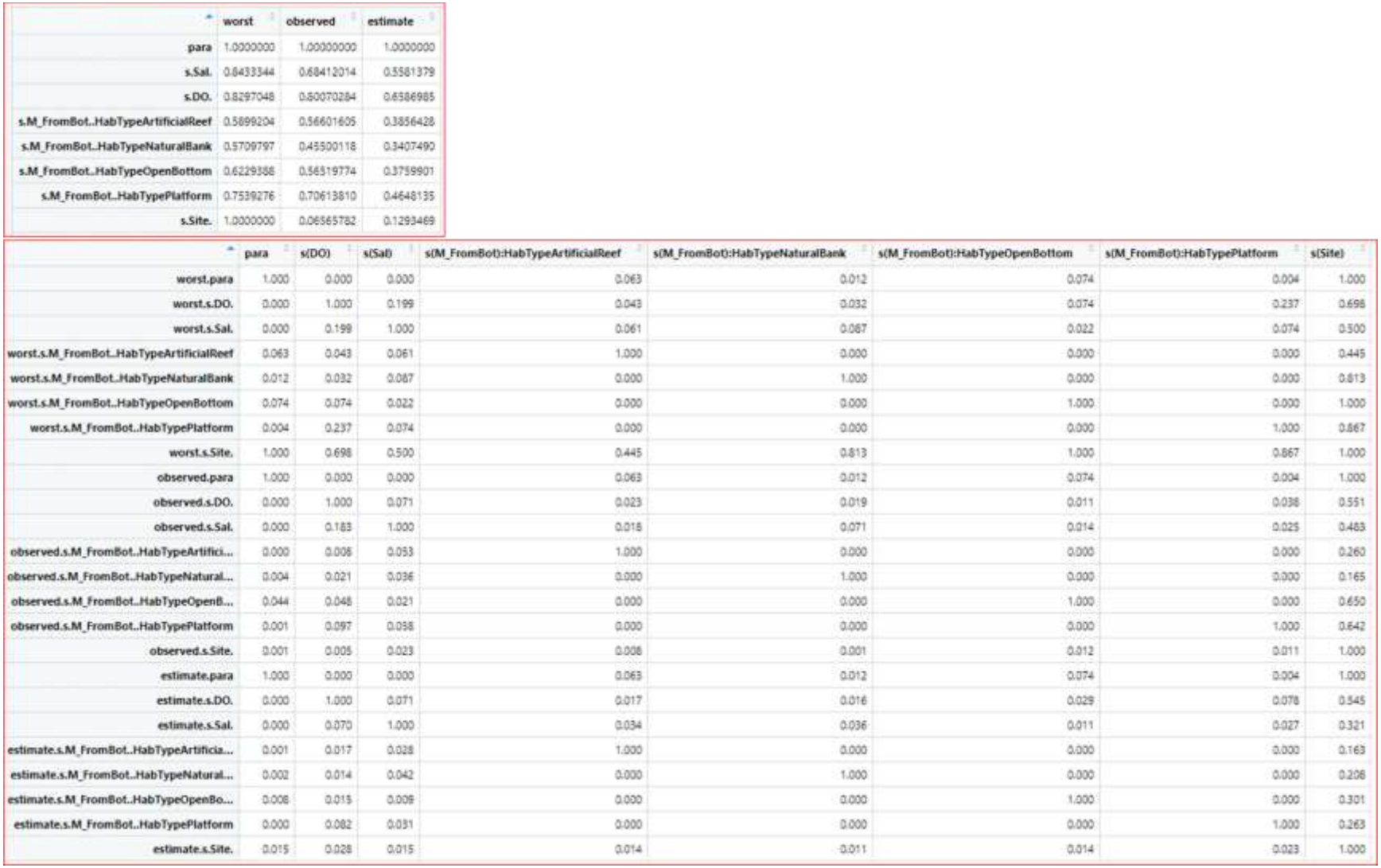

	worst	observed	estimate
para	1.0000000	1.00000000	1.0000000
s.Sal.	0.8433344	0.68412014	0.5581379
s.DO.	0.8297048	0.80070284	0.6586985
s.M_FromBot..HabTypeArtificialReef	0.5899204	0.56601605	0.3856428
s.M_FromBot..HabTypeNaturalBank	0.5709797	0.45500118	0.3407490
s.M_FromBot..HabTypeOpenBottom	0.6229388	0.56519774	0.3759901
s.M_FromBot..HabTypePlatform	0.7539276	0.70613810	0.4648135
s.Site.	1.0000000	0.06565782	0.1293469

	para	s(DO)	s(Sal)	s(M_FromBot):HabTypeArtificialReef	s(M_FromBot):HabTypeNaturalBank	s(M_FromBot):HabTypeOpenBottom	s(M_FromBot):HabTypePlatform	s(Site)
worst.para	1.000	0.000	0.000	0.063	0.012	0.074	0.004	1.000
worst.s.DO.	0.000	1.000	0.199	0.043	0.032	0.074	0.237	0.698
worst.s.Sal.	0.000	0.199	1.000	0.061	0.067	0.022	0.074	0.500
worst.s.M_FromBot..HabTypeArtificialReef	0.063	0.043	0.061	1.000	0.000	0.000	0.000	0.445
worst.s.M_FromBot..HabTypeNaturalBank	0.012	0.032	0.067	0.000	1.000	0.000	0.000	0.813
worst.s.M_FromBot..HabTypeOpenBottom	0.074	0.074	0.022	0.000	0.000	1.000	0.000	1.000
worst.s.M_FromBot..HabTypePlatform	0.004	0.237	0.074	0.000	0.000	0.000	1.000	0.867
worst.s.Site.	1.000	0.698	0.500	0.445	0.813	1.000	0.867	1.000
observed.para	1.000	0.000	0.000	0.063	0.012	0.074	0.004	1.000
observed.s.DO.	0.000	1.000	0.071	0.023	0.019	0.011	0.038	0.551
observed.s.Sal.	0.000	0.183	1.000	0.018	0.071	0.014	0.025	0.483
observed.s.M_FromBot..HabTypeArtifici...	0.000	0.008	0.053	1.000	0.000	0.000	0.000	0.260
observed.s.M_FromBot..HabTypeNatural...	0.004	0.021	0.036	0.000	1.000	0.000	0.000	0.165
observed.s.M_FromBot..HabTypeOpenB...	0.044	0.048	0.021	0.000	0.000	1.000	0.000	0.650
observed.s.M_FromBot..HabTypePlatform	0.001	0.097	0.038	0.000	0.000	0.000	1.000	0.642
observed.s.Site.	0.001	0.005	0.023	0.008	0.001	0.012	0.011	1.000
estimate.para	1.000	0.000	0.000	0.063	0.012	0.074	0.004	1.000
estimate.s.DO.	0.000	1.000	0.071	0.017	0.016	0.029	0.078	0.545
estimate.s.Sal.	0.000	0.070	1.000	0.034	0.036	0.011	0.027	0.321
estimate.s.M_FromBot..HabTypeArtificia...	0.001	0.017	0.028	1.000	0.000	0.000	0.000	0.163
estimate.s.M_FromBot..HabTypeNatural...	0.002	0.014	0.042	0.000	1.000	0.000	0.000	0.206
estimate.s.M_FromBot..HabTypeOpenBo...	0.008	0.015	0.009	0.000	0.000	1.000	0.000	0.301
estimate.s.M_FromBot..HabTypePlatform	0.000	0.082	0.031	0.000	0.000	0.000	1.000	0.263
estimate.s.Site.	0.015	0.028	0.015	0.014	0.011	0.014	0.023	1.000

Figure A6.7. Concurvity assessment. The top panel reflects the extent to which each smooth term can be approximated by the rest of the model. The bottom panel shows pairwise concurvity between each term. Three sets of indices are reported for each: “worst”, “observed”, “estimate”. Terms with worst values >0.8 in the top panel should be checked closer in the pairwise panel below according to Wood (2021). The “estimate” values measure the extent to which a smooth can be explained by one or more other terms.

APPENDIX 7.

Statistical Diagnostics for the Model Used to Predict Total Fish Densities

Model Fit and Diagnostics

Plotting the observed versus predicted values from the GAMM for *TFD* (Figure A7.1) indicated no substantial bias with the fitted line approximating that of equality (i.e., intercept=0 and slope=1). The ratio of data points to model parameters (N/k) was 4.7, which was above the minimum threshold of 3.0 (Forstmeier and Schielzeth 2010, Crawley 2013). Models were further assessed for fit, overdispersion, and zero-inflation with scaled (quantile) simulated residuals (number of simulations = 1,000) via the DHARMa Package Version 0.4.5, which extends this tool to models parameterized with the mgcv Package (Hartig 2022). A QQ plot of these residuals indicated no deviation from the expected distribution (Figure A7.2), nor were there any apparent problems with overdispersion (Figure A7.3) or zero-inflation (Figure A7.4). The output statistics produced by mgcv Package Version 1.8-38 (Wood 2021) show the random intercept term for *Sites* (Figure A7.5) accounted for most of the variation and appeared to meet the assumption of normality based on the QQ-plot in Figure A7.6 created with the gratia Package Version 0.7.0 (Simpson 2022).

Finally, concurvity (akin to collinearity for linear regression) among smooth terms was checked with indices quantifying this issue available in the mgcv Package (Figure A7.7). Two matrices are produced, the first of which reflects the extent to which each smooth term can be approximated by the rest of the model, and the second shows pairwise concurvity between each term. Three sets of indices--“worst”, “observed”, and “estimate”– are reported for each matrix. Interpretation of these indices is somewhat tedious. Even Wood (2021) is vague on how to interpret these indices, and the literature is sparce on definitive thresholds. An internet search yielded a general rule-of-thumb that when worst values are >0.8 in the overall matrix, then the pairwise matrix should be examined more closely. Wood (2021) does say that the worst index is overly pessimistic and that the observed index is potentially optimistic. The estimate index is said to be somewhere in between. From Figure A7.7, we see that this worst index threshold of being >0.8 was breached for the *Salinity* and *DO* smooth terms in the overall matrix. However, none of the indices showed cause for alarm in the pairwise matrix.

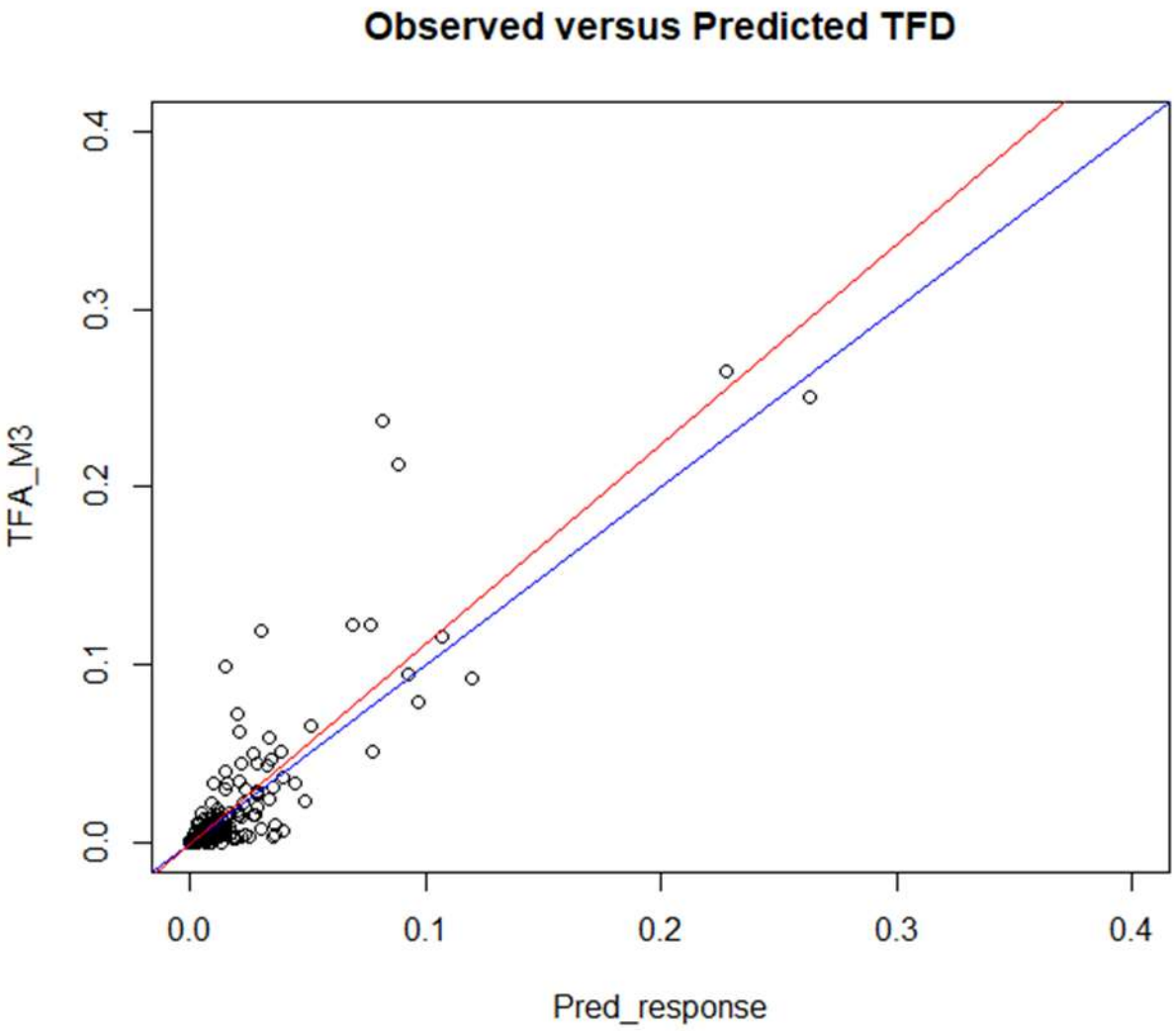

Figure A7.1. Observed versus fitted values. Equality is indicated by the blue line and the fitted trend by the red line.

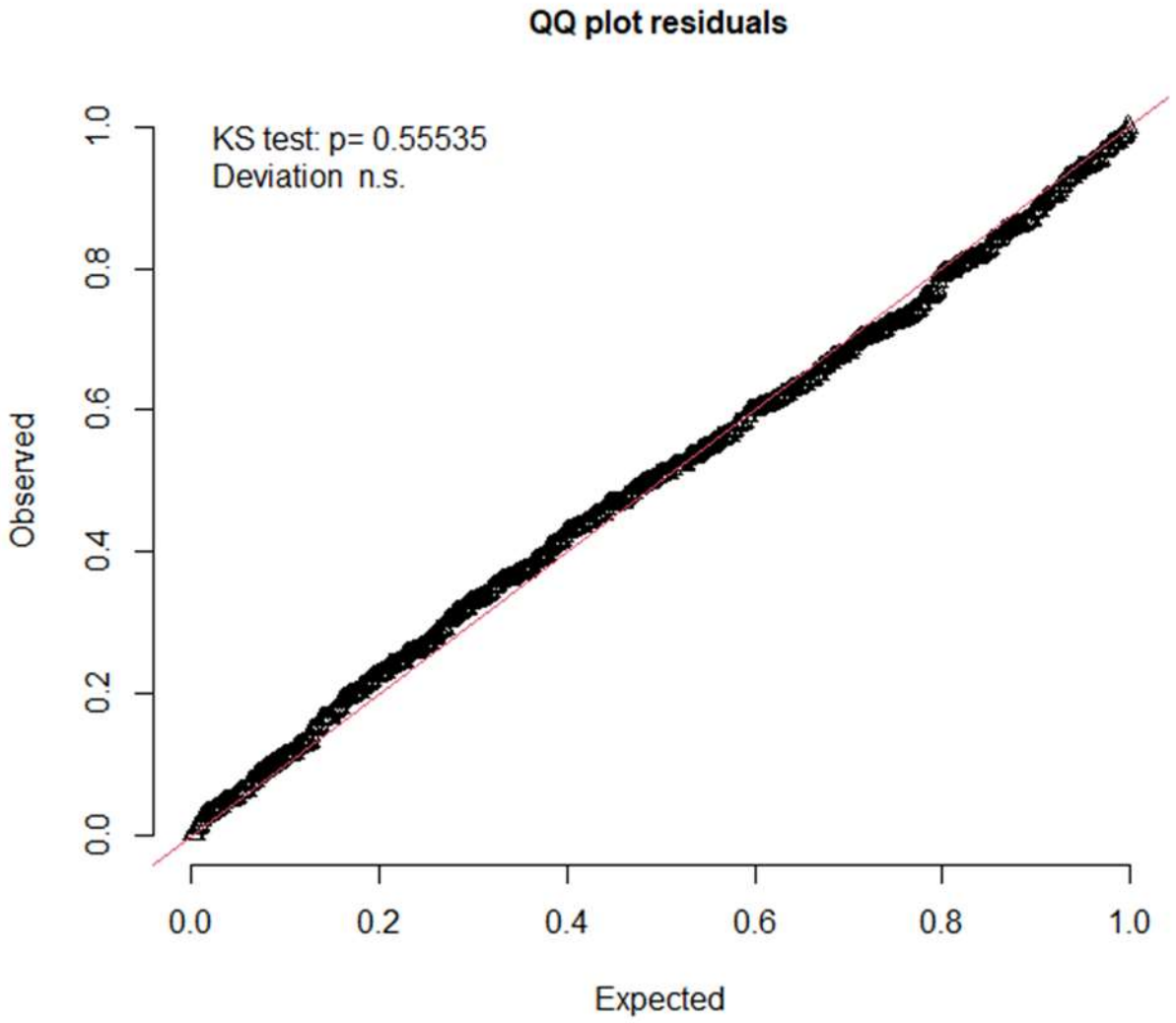

Figure A7.2. QQ-plot of observed residuals versus simulated DHARMa residuals to detect overall deviations.

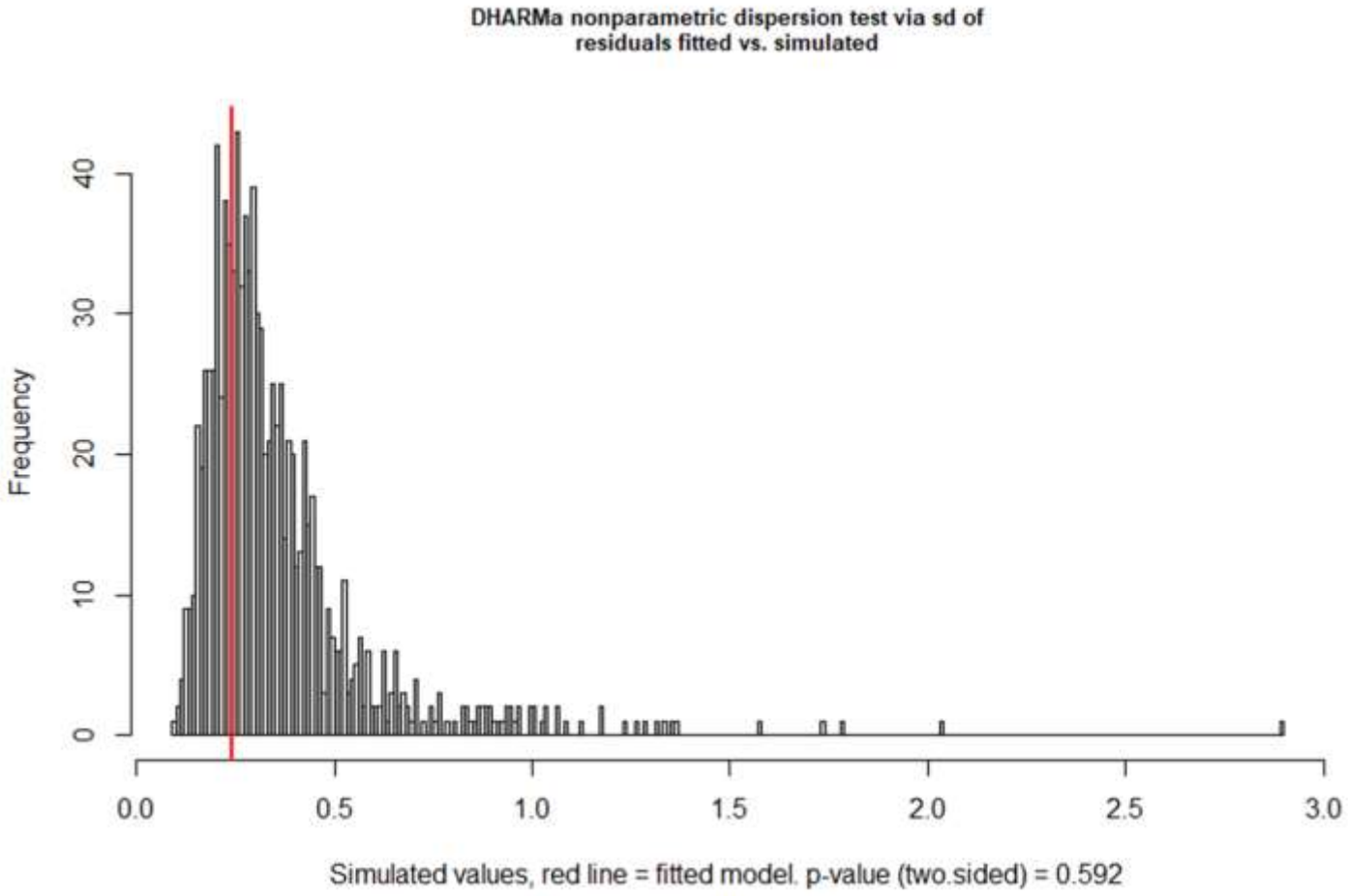

Figure A7.3. Non-parametric test comparing the variance of simulated DHARMa residuals (gray bars) to the observed residuals (red bar). A low p-value indicates a problem with underdispersion/overdispersion.

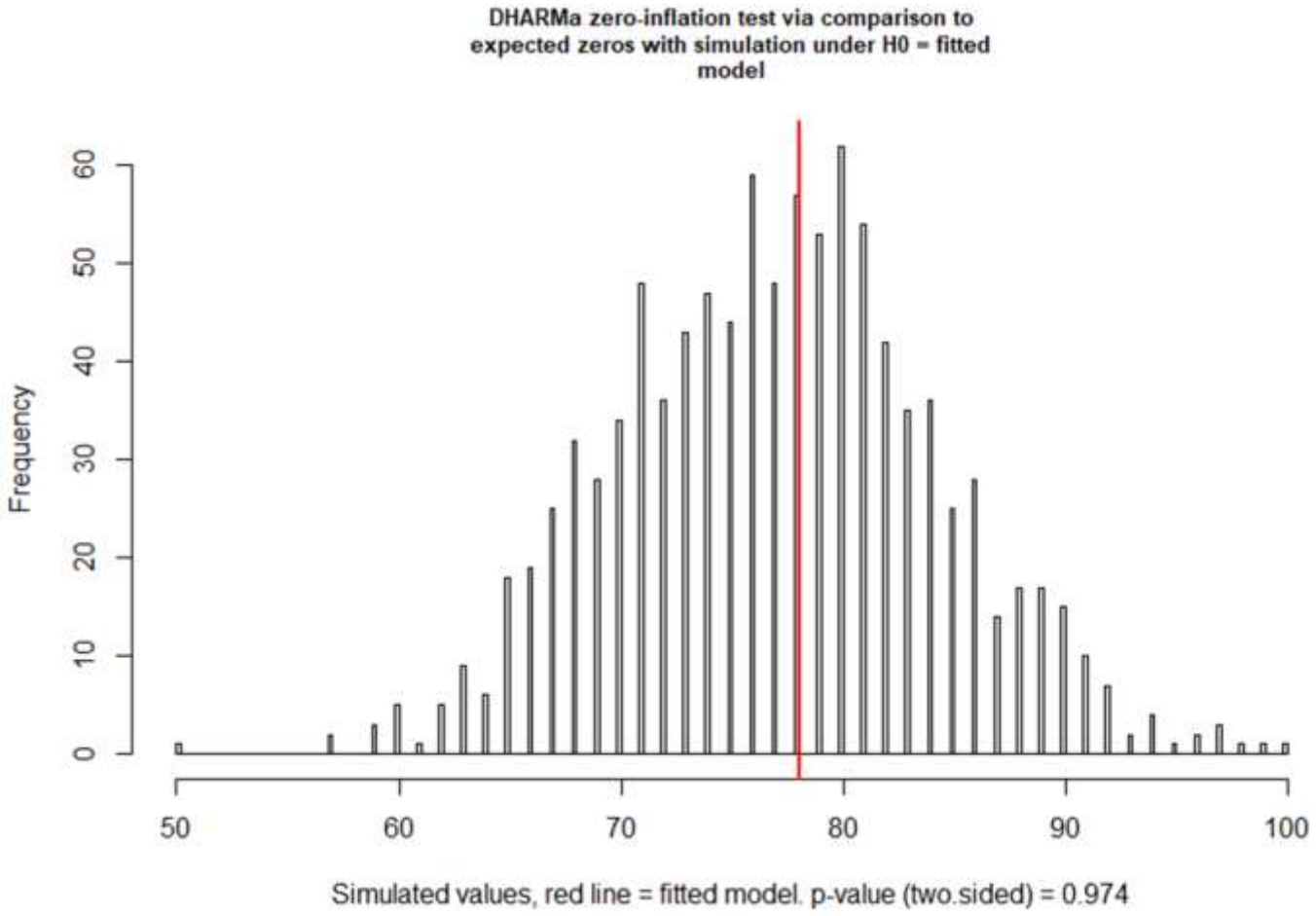

Figure A7.4. Distribution of expected zeros (gray bars) in the data compared to the observed zeros (red bar). A low p-value means that more or less zeros were observed in the data than expected.

A

component	variance	std_dev	lower_ci	upper_ci
<chr>	<dbl>	<dbl>	<dbl>	<dbl>
s(Sal)	0.197	0.444	0.188	1.05
s(DO)	0.459	0.678	0.296	1.55
s(M_FromBot):HabTypeArtificialReef	0.265	0.515	0.176	1.51
s(M_FromBot):HabTypeNaturalBank	0.144	0.380	0.175	0.825
s(M_FromBot):HabTypeOpenBottom	0.190	0.436	0.176	1.08
s(M_FromBot):HabTypePlatform	0.00889	0.0943	0.0360	0.247
s(Site)	1.58	1.26	1.02	1.54
scale	0.320	0.565	0.535	0.598

B

```
Approximate significance of smooth terms:
                                    edf Ref.df      F  p-value
s(Sal)                            3.415      4 26.307 1.35e-05 ***
s(DO)                             3.143      4 48.938 4.94e-07 ***
s(M_FromBot):HabTypeArtificialReef 3.442      4 26.852  < 2e-16 ***
s(M_FromBot):HabTypeNaturalBank   3.410      4 36.133  < 2e-16 ***
s(M_FromBot):HabTypeOpenBottom    3.131      4 25.127  < 2e-16 ***
s(M_FromBot):HabTypePlatform      2.531      4 17.096 0.000866 ***
s(Site)                          80.155    105  3.836  < 2e-16 ***
---
Signif. codes:  0 '***' 0.001 '**' 0.01 '*' 0.05 '.' 0.1 ' ' 1

R-sq.(adj) =   0.71   Deviance explained = 83.3%
-REML = -2795.7  Scale est. = 0.31951   n = 533
```

C

```
Family: Tweedie(p=1.789)
Link function: log

Formula:
TFA_M3 ~ Region + DZ + HabType + s(Sal, k = 5, m = 1) + s(DO,
    k = 5, m = 1) + s(M_FromBot, by = HabType, bs = "tp",
    k = 5, m = 1) + s(Site, bs = "re")

Parametric Terms:
         df       F p-value
Region    2   6.147 0.00233
DZ        2   3.727 0.02484
HabType   3 128.493 < 2e-16
```

Figure A7.5. GAMM output statistics. Panel **A** shows the smoothing parameters expressed as variance components and their 95% confidence intervals on the standard deviation scale. Panels **B** gives the approximated p-values for smooth and parametric terms, respectively. Furthermore, Panel B shows the effective degrees of freedom (edf) for each smooth after penalization, the deviance explained, the dispersion parameter ("Scale est."), as well as sample size n. Panel **C** indicates the assumed distribution for the response and the corresponding link function, the model specification, and p-values for parametric terms.

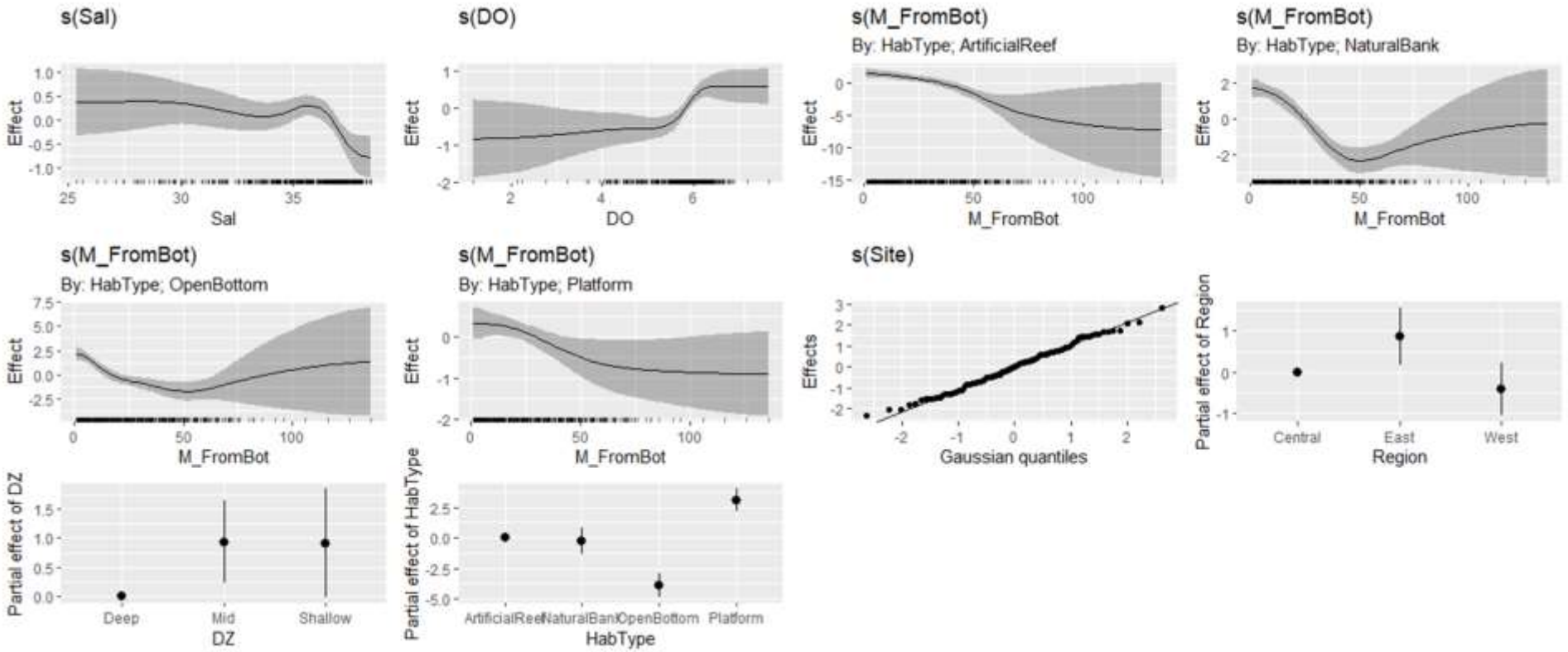

Figure A7.6. Plots of partial effects of fixed model terms with 95% credible intervals. A QQ plot is shown for the random effect of *Site* to assess the normality assumption.

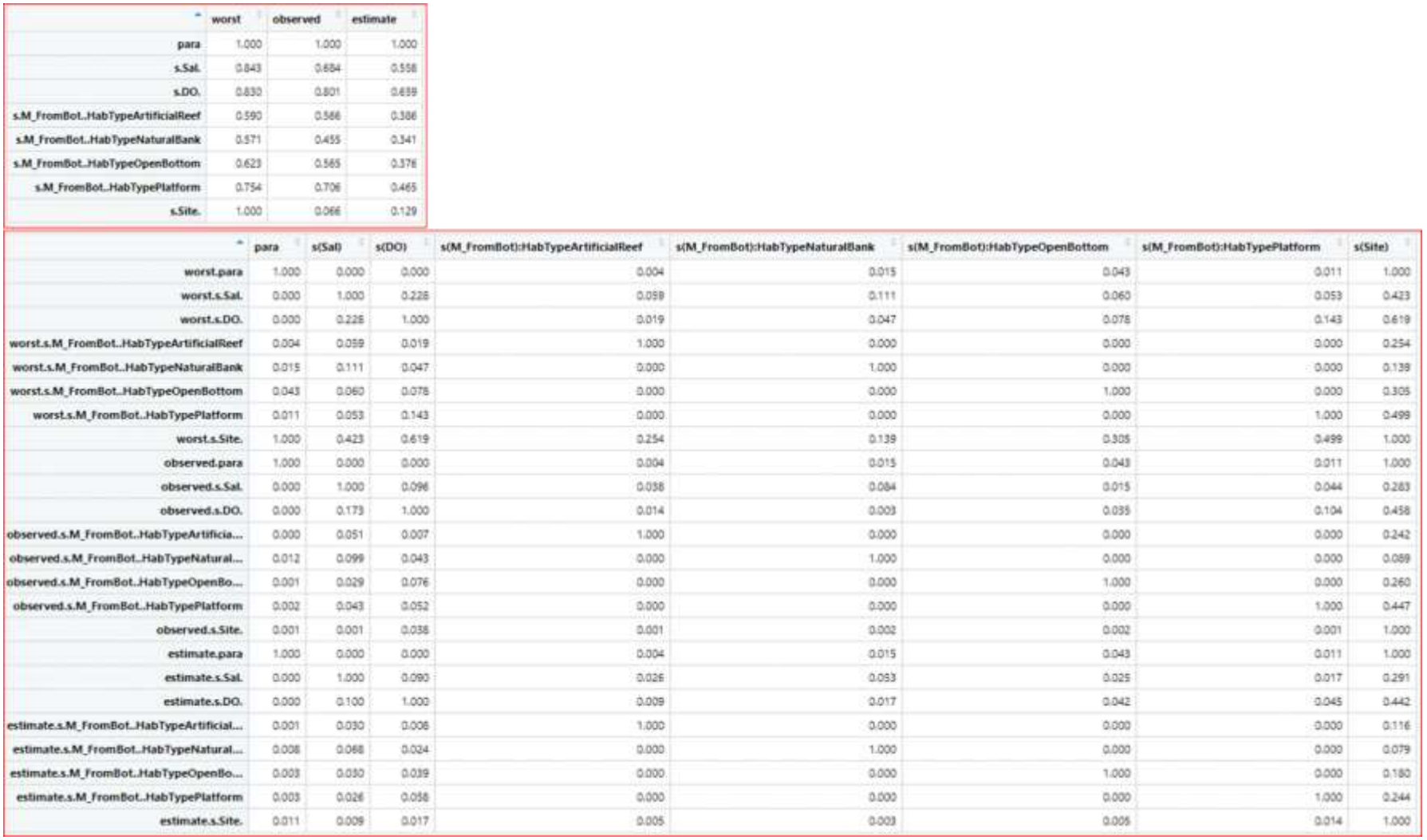

	worst	observed	estimate
para	1.000	1.000	1.000
s.Sal.	0.843	0.684	0.558
s.DO.	0.830	0.801	0.639
s.M_FromBot..HabTypeArtificialReef	0.590	0.566	0.386
s.M_FromBot..HabTypeNaturalBank	0.571	0.455	0.341
s.M_FromBot..HabTypeOpenBottom	0.623	0.565	0.378
s.M_FromBot..HabTypePlatform	0.754	0.706	0.465
s.Site.	1.000	0.066	0.129

	para	s(Sal)	s(DO)	s(M_FromBot):HabTypeArtificialReef	s(M_FromBot):HabTypeNaturalBank	s(M_FromBot):HabTypeOpenBottom	s(M_FromBot):HabTypePlatform	s(Site)
worst.para	1.000	0.000	0.000	0.004	0.015	0.043	0.011	1.000
worst.s.Sal.	0.000	1.000	0.228	0.059	0.111	0.060	0.053	0.423
worst.s.DO.	0.000	0.228	1.000	0.019	0.047	0.078	0.143	0.619
worst.s.M_FromBot..HabTypeArtificialReef	0.004	0.059	0.019	1.000	0.000	0.000	0.000	0.254
worst.s.M_FromBot..HabTypeNaturalBank	0.015	0.111	0.047	0.000	1.000	0.000	0.000	0.139
worst.s.M_FromBot..HabTypeOpenBottom	0.043	0.060	0.078	0.000	0.000	1.000	0.000	0.305
worst.s.M_FromBot..HabTypePlatform	0.011	0.053	0.143	0.000	0.000	0.000	1.000	0.499
worst.s.Site.	1.000	0.423	0.619	0.254	0.139	0.305	0.499	1.000
observed.para	1.000	0.000	0.000	0.004	0.015	0.043	0.011	1.000
observed.s.Sal.	0.000	1.000	0.096	0.038	0.084	0.015	0.044	0.283
observed.s.DO.	0.000	0.173	1.000	0.014	0.003	0.035	0.104	0.458
observed.s.M_FromBot..HabTypeArtificia...	0.000	0.051	0.007	1.000	0.000	0.000	0.000	0.242
observed.s.M_FromBot..HabTypeNatural...	0.012	0.099	0.043	0.000	1.000	0.000	0.000	0.089
observed.s.M_FromBot..HabTypeOpenBo...	0.001	0.029	0.076	0.000	0.000	1.000	0.000	0.260
observed.s.M_FromBot..HabTypePlatform	0.002	0.043	0.052	0.000	0.000	0.000	1.000	0.447
observed.s.Site.	0.001	0.001	0.038	0.001	0.002	0.002	0.001	1.000
estimate.para	1.000	0.000	0.000	0.004	0.015	0.043	0.011	1.000
estimate.s.Sal.	0.000	1.000	0.090	0.026	0.053	0.025	0.017	0.291
estimate.s.DO.	0.000	0.100	1.000	0.009	0.017	0.042	0.045	0.442
estimate.s.M_FromBot..HabTypeArtificial...	0.001	0.030	0.006	1.000	0.000	0.000	0.000	0.116
estimate.s.M_FromBot..HabTypeNatural...	0.008	0.068	0.024	0.000	1.000	0.000	0.000	0.079
estimate.s.M_FromBot..HabTypeOpenBo...	0.003	0.030	0.039	0.000	0.000	1.000	0.000	0.180
estimate.s.M_FromBot..HabTypePlatform	0.003	0.026	0.058	0.000	0.000	0.000	1.000	0.244
estimate.s.Site.	0.011	0.009	0.017	0.005	0.003	0.005	0.014	1.000

Figure A7.7. Concurvity assessment. The top panel reflects the extent to which each smooth term can be approximated by the rest of the model. The bottom panel shows pairwise concurvity between each term. Three sets of indices are reported for each: “worst”, “observed”, “estimate”. Terms with worst values >0.8 in the top panel should be checked closer in the pairwise panel below according to Wood (2021). The “estimate” values measure the extent to which a smooth can be explained by one or more other terms.